On the propagation of cosmic rays in the galaxy

Dickinson, Geoffrey J.

On the propagation of cosmic rays in the Galaxy

A thesis submitted to the University of Durham

for the Degree of Doctor of Philosophy

by

Geoffrey J. Dickinson, B.Sc.

May 1975

To my parents

ABSTRACT

An important problem in the study of cosmic rays, under the assumption of a Galactic origin for energies $\lesssim 10^{14}$ eV, is their propagation in the Galaxy. The experimental observations of the cosmic rays, i.e. the energy spectrum, anisotropy, composition, γ-rays and long term variations, are reviewed. Parameters of the interstellar medium relevant to the propagation of cosmic rays are discussed. Theories about Galactic cosmic ray sources and cosmic ray acceleration are also discussed.

Calculations are presented which indicate the improbability of the compound diffusion model as a reasonable theory for the galactic propagation of cosmic rays. The effect of turbulence in the interstellar medium on the rate of separation of neighbouring magnetic field lines is investigated. It is concluded that cosmic ray propagation is better described by an isotropic three dimensional diffusion than by a compound diffusion.

Plasma effects of the cosmic rays with respect to the generation of Alfvén waves are discussed. Cosmic ray generated Alfvén waves are able to confine cosmic rays with energies $\lesssim 100$ GeV in the Galaxy.

Model calculations are presented for the propagation of cosmic rays with energy 10^9–10^{13} eV in the Galaxy using idealised parameters for the cosmic rays and interstellar medium and random discrete sources at a frequency corresponding to supernova explosions.

The most encouraging model suggests that cosmic rays with
energy $\lesssim 10$ GeV are confined to spiral arms by self genera-
ted waves, cosmic rays with energy > 10 GeV and $\lesssim 300$ GeV
are confined within a "leaky box" of Galactic dimensions
by self generated waves and cosmic rays with energy
$\gtrsim 300$ GeV are confined to the spiral arms by interstellar
turbulence.

PREFACE

The work presented in this thesis was carried out
during the period 1972-75, while the author was a research
student under the supervision of Dr. J. L. Osborne in the
Physics Department of the University of Durham. The cal-
culations carried out by the author represent a numerical
treatment of the problem of the propagation of cosmic rays
in the Galaxy. The theoretical models developed by the
author are extensions of models previously published by
other physicists.

The results of the one dimensional diffusion calcula-
tion presented in Chapter 5 have been published in the
Journal of Physics (Dickinson, G. J. and Osborne, J. L.,
1974. J.Phys.A: Math. Nucl. Gen., $\underline{7}$, 728). The results
of the calculation presented in Chapter 7 have been
reported at the NATO Advanced Study Institute, "Origin
of Cosmic Rays", held at Durham in August 1974. (Origin
of Cosmic Rays, ed. Osborne, J.L. and Wolfendale, A. W.,
De Reidel, 1975).

Contents

Chapter 1 Introduction

All of man's knowledge about the universe as a whole is gained from the radiations which are incident on the earth. Until the last 50 years almost all our information has come from the 'optical channel'. Despite the successes of optical astronomy, particularly over the last hundred years, the narrowness of the optical channel in the electromagnetic spectrum severely limits the amount of information available from it. A revolution in astronomical research was brought about in the 1950's by the advent of radio astronomy. Now in the 1970's, with man's improved technology, almost the full range of the electromagnetic spectrum may be studied using orbiting satellites. X-ray and γ-ray astronomy are now in the same position as radio astronomy 20 years ago.

Apart from the study of the electromagnetic radiations man's only other source of information about the nature of the universe outside our own planet is the cosmic radiation which was discovered over 60 years ago. The first observations of the penetrating cosmic radiation were made by physicists such as C. T. R. Wilson, Elster and Geitel who showed that despite their careful precautions to prevent known radiations from reaching samples of air in their ionisation chambers, a significant residual conductivity was due to radiation from outside the chamber. This residual conductivity was at first believed to be due to radioactive materials in the Earth. In 1912 Hess transported his apparatus to great altitudes in a balloon and found that,
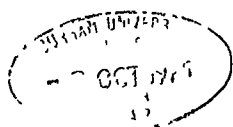
after a decrease from sea level to 700 m, the ionisation
increased with altitude. The increase was obviously due to
radiation coming in from outer space. The cosmic radiation
was first believed to be γ-radiation. Bothe and Kolhörster
(1929) interpreted the variation of cosmic ray intensity
with geomagnetic latitude as the consequence of charged
cosmic ray particles. Johnson and Street (1933) discovered
that the cosmic ray intensity coming from the east was less
than that from the west, proving that the majority of cosmic
rays are positively charged.

There are two main reasons for interest in the cosmic
radiation:

(i) to learn about nuclear physics from the interactions of
     cosmic ray particles in the atmosphere

(ii) to consider the astrophysical significance of the cosmic
     radiation

It is the second reason which is the concern of this thesis.

Since their discovery, physicists have tried to find
out where the cosmic rays originate in the hope that the
cosmic rays will provide information about the physical
processes which occur in the universe, such processes as
stellar or galactic evolution or even possibly the big bang
itself. There are two schools of thought regarding the
origin of the cosmic radiation.

The first proposes a galactic origin for the cosmic
radiation in objects such as supernovae explosions (Ginzburg
and Syrovatskii, 1964). There are two models for galactic
confinement, confinement in the galactic disk and confinement

within a galactic halo. The energy density of the cosmic rays in the neighbourhood of the sun is $\sim 10^{-12}$ erg cm^{-3}. This value is often taken to be the average galactic energy density. The observed amount of material the cosmic rays pass through in the Galaxy, ~ 5g cm^{-2}, suggests an age for the cosmic rays of $\sim 3 \times 10^6$ years for the galactic disk model and $\sim 3 \times 10^8$ years for the halo model. The amount of energy required from the sources to maintain an energy density of $\sim 10^{-12}$ erg cm^{-3} is $\sim 10^{40-41}$ erg s^{-1} for both models, the extra volume in the halo case being compensated for by the longer lifetime. A typical supernova explosion is expected to release 10^{50-51} ergs. If the rate of supernovae in the Galaxy, calculated from observations of supernovae remnants, is one per 26 years (Tamman, 1970) then the energy requirement for maintaining the cosmic ray flux could be met by galactic sources. The validity of the halo model has been questioned on two counts. Firstly, there is no observational evidence for a radio halo and secondly measurements of the Be^{10} isotope in the cosmic rays indicate a cosmic ray lifetime of a few million years. There is no direct evidence for the acceleration of cosmic ray nuclei in supernovae and the very low observed anisotropy coupled with a fairly short lifetime in the galactic disk provides a difficult problem for any Galactic theory for the origin of the cosmic rays to overcome.

The requirements for the second, an extragalactic origin for the cosmic rays (Brecher and Burbidge, 1972), may be summarised as follows:

a) Evidence is required that the cosmic rays exist outside
    the Galaxy with an energy density equal to that inside
    the Galaxy. There is no such evidence at the present
    time.

b) It must be shown that there exist powerful extragalac-
    tic cosmic ray sources.

c) The escape of cosmic rays from sources must be considered.
    Evidence exists that the electron component is able to
    escape from possible extragalactic sources.

d) The energy density requirement for a truly universal
    cosmic ray flux, is that about 0.5% of all the rest
    energy in the universe is converted to relativistic
    particles. The modified extragalactic theory suggests
    that the region of universal energy density may be
    restricted to volumes where there are clusters of
    galaxies. This would lower the total energy require-
    ment to a more reasonable level.

e) Evidence is required that cosmic rays are able to
    propagate to the Galaxy without being destroyed or
    giving rise to components which are not observed.

f) The cosmic rays must be able to enter the Galaxy.
    Parker (1973) has suggested that if the Galactic
    Magnetic field configuration is closed the cosmic
    rays may experience difficulty in entering the Galaxy.

Both schools of thought are agreed that the cosmic ray
electrons are of galactic origin; they would not survive
the long journey through intergalactic space, and that the
very high energy cosmic rays i.e. $\gtrsim 10^{17}$ eV must be mainly
extragalactic from a consideration of their isotropy. The

area of greatest controversy is the nuclear component with energy $\lesssim 10^{17}$ eV.

This thesis assumes that the bulk of the cosmic rays $\lesssim 10^{17}$ eV are galactic in origin and investigates the propagation of the cosmic rays in the Galactic disk, with a view to reconciling the short lifetime of the cosmic rays in the Galaxy, ~few x 10^6 yrs possibly decreasing with energy, with the isotropy of the cosmic radiation. It is necessary to have a good understanding of the propagation before the composition and energy spectrum of the cosmic rays immediately after acceleration can be well known and conclusions regarding stellar evolution may be drawn.

With these aims in mind Chapter 2 reviews the relevant observations of the cosmic ray flux. Chapter 3 reviews briefly the properties of the interstellar medium which are important to a discussion of the propagation. In Chapter 4 possible galactic sources, acceleration mechanisms and some of the older propagation models are considered. In Chapter 5 the compound diffusion model is criticised and a model of one dimensional diffusion along magnetic field lines is developed. Chapter 6 discusses the fine scale structure of the magnetic field in the Galaxy in the light of recent theoretical ideas regarding turbulence in the interstellar medium. The effects of cosmic ray particles generating and being confined by hydromagnetic waves are discussed in Chapter 7 and these ideas are developed and applied to several idealised confinement regions in Chapter 8. The status of all the present day propagation models is reviewed in the concluding chapter.

References

Bothe, W. and Kolhörster, W., 1929   Z.Phys. 56, 751

Brecher, K. and Burbidge, G. R., 1972   Astrophys. J., 174, 253

Ginzburg, V. L. and Syrovatskii, S. I., 1964   "The Origin of
    Cosmic Rays", Pergamon Press

Hess, V. F., 1912   Physik. Zeitschr., 13, 1804

Johnson, J. H. and Street, J. C., 1933   J.Frank.Inst., 25,
    239 and Phys. Rev. 43, 381

Parker, E. N., 1973   Astrophys. Space Sci. 24, 279

Tamman, G. A., 1970   Astron. Astrophys. 8, 458

Chapter 2   Properties of Cosmic Rays

2.1 The Primary Energy Spectrum

2.1.1 Methods of Measurement

The energy spectra of the primary cosmic ray particles
may be expressed in a variety of ways, the choice being
usually determined by the method of measurement. The
numbers of particles above a given threshold rigidity
(pc/Ze) may be determined by studies at different latitudes,
using the Earth's magnetic field as a momentum analyser.
Insatellite or balloon experiments, individual nuclei of
comparatively low energy may be identified enabling spectra
to be given in terms of the number of nuclei in a given
energy range per nucleus, or, more commonly, energy per
nucleon. Indirect studies of single muons at low levels
in the atmosphere give no information about the mass com-
position of the primary cosmic rays but yield the number of
primary nucleons with energy per nucleon in a given range.
At the highest energies information on the energy spectra
is obtained in terms of primary energy per nucleus from
measurements of extensive air showers.

Wolfendale (1973) has made a survey of the data avail-
able at the present and the result is shown in figure 2.1.

2.1.2 Energies below 10^{12} eV/nucleon

The energy regions may be considered in turn starting
with the lowest energies.

At energies below 10^9 eV satellite measurements are
possible and precise measurements can be made, particularly
for particles with comparatively low masses. At energies
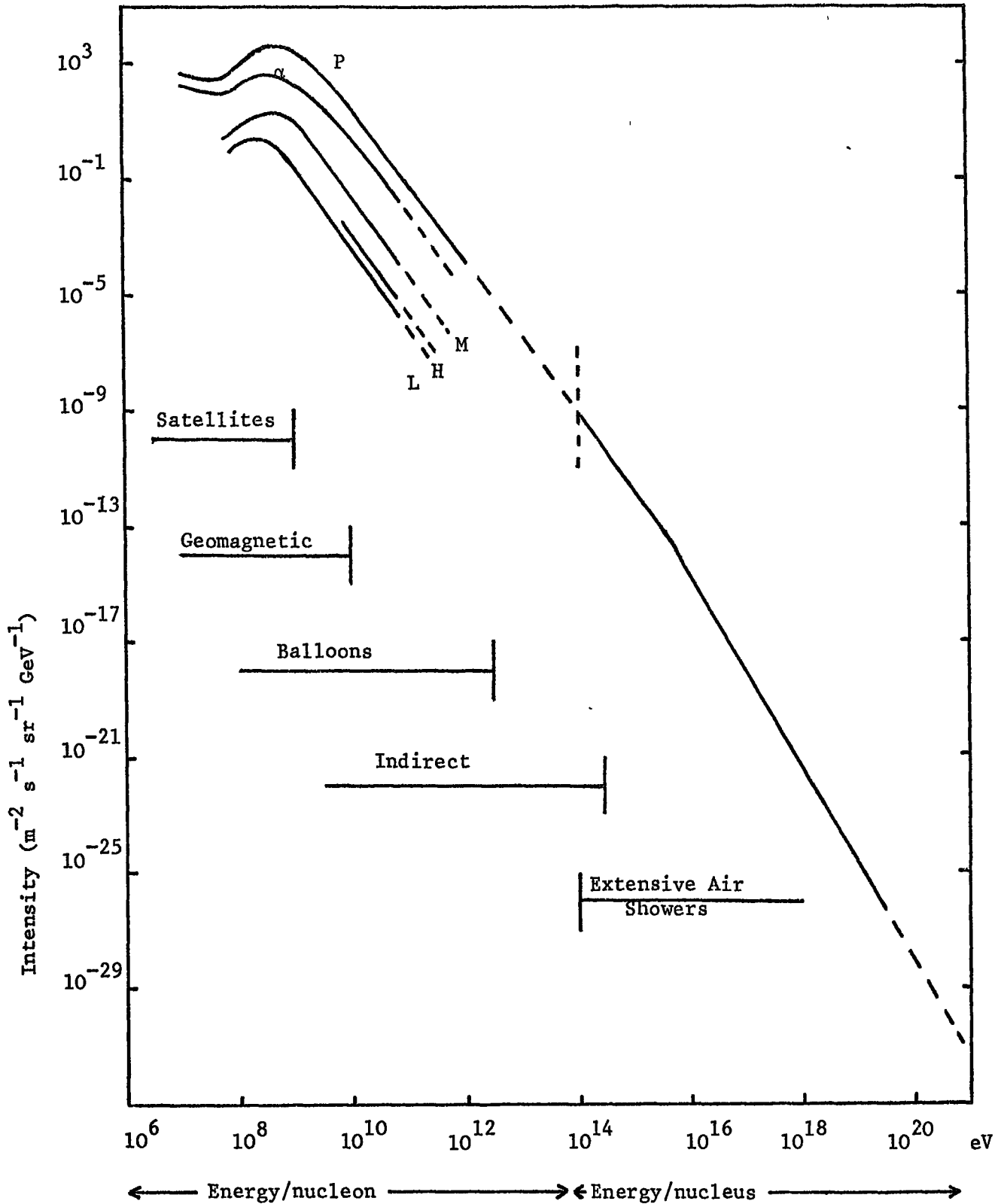
Figure 2.1: Summary of measurements on the primary spectrum of protons and nuclei in the cosmic radiation corrected for geomagnetic effects. The groupings are as follows. L:$3 \leqslant Z \leqslant 5$; M:$6 \leqslant Z \leqslant 9$; H:$10 \leqslant Z$. From Wolfendale (1973).

above 10^9 eV balloon borne detectors have been used, however
the statistical accuracy soon becomes poor for particles
with z>2.

The spectrum for protons in the energy range below
10^{12} eV is shown in figure 2.2 (10^7 - 10^{10} eV) and figure
2.3 (10^9 - 10^{12} eV).

In the region below a few times 10^9 eV the inter-
planetary magnetic field reduces the primary cosmic ray
intensity below its value in interstellar space. Figure 2.2
shows the results of observations of protons in 1966 and
1968, below 2 GeV as compiled by Lezniak and Webber (1971)
and above 2 GeV as compiled by Gloeckler and Jokipii (1967).
The data for the proton spectrum shown in figure 2.3 come
from the measurements of Ormes and Webber (1965), Ryan et al
(1972), Anand et al (1968) and Smith et al (1973).

The slope of the differential spectrum for protons
appears to be nearly constant above 10^{10} eV at 2.7 $\pm$ 0.1.
At 10^{10} eV there appears to be a steepening in the primary
proton spectrum. Holmes (1974) interprets this break in
the spectrum as due to the energy at which confinement of
the cosmic rays by self-generated magnetohydrodynamic waves
breaks down in the galactic plane. However, it has not
yet been proved that this break in the primary spectrum
does not represent the highest energy affected by the inter-
planetary magnetic field. Burger and Swanenburg (1971)
have calculated the effect of the interplanetary magnetic
field on the galactic cosmic ray spectrum.
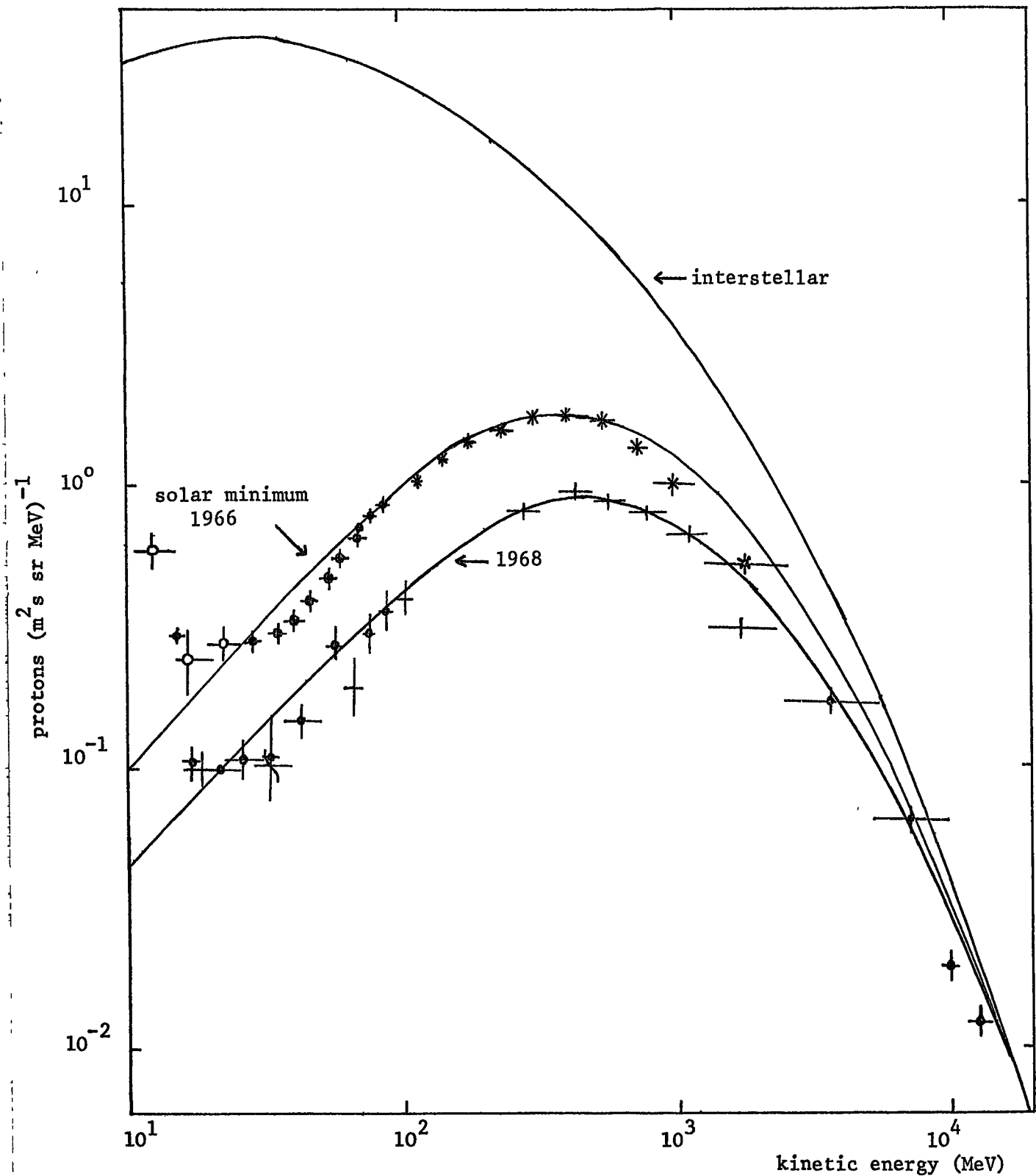
Figure 2.2: Proton observations in 1966 and 1968, below 2 GeV as compiled by Lezniak and Webber (1971) and above 2 GeV as compiled by Gloeckler and Jokipii (1967). The curves through the data points show the calculated spectra (Burger and Swanenburg 1971).
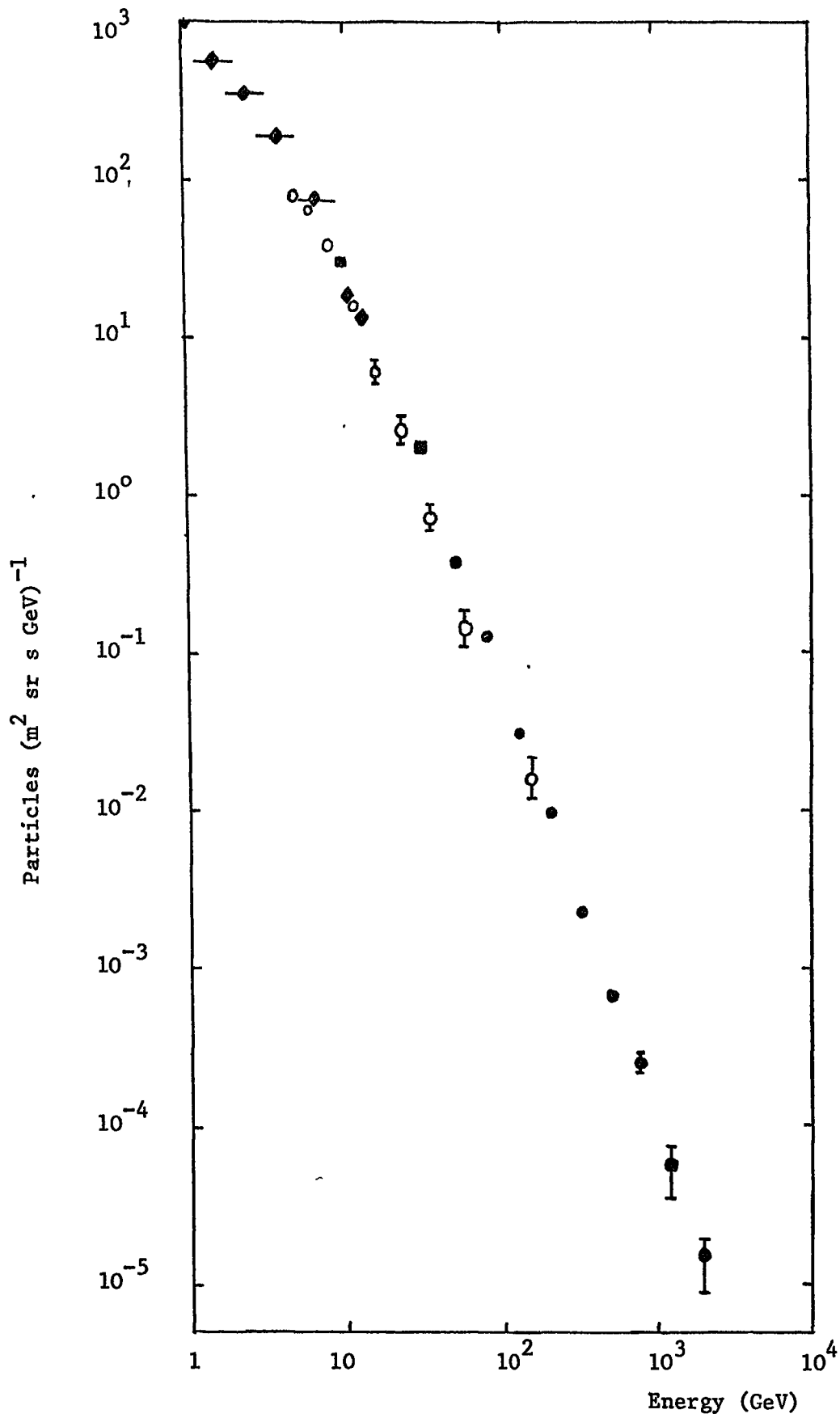
Figure 2.3: The cosmic ray proton spectrum at energies between 10^9 eV and 10^{12} eV

◆ Ormes and Webber (1965) ; ● Ryan et al (1972)

▩ Anand et al (1968)   ; ○ Smith et al (1973)

Using an interstellar energy spectrum for electrons deduced from Galactic non-thermal radio data Burger and Swanenburg calculate an interplanetary cosmic ray diffusion coefficient to fit the modulation of the electron energy spectrum. They then calculate an interstellar proton spectrum which is the equilibrium for an injection spectrum following in particle density versus rigidity the same shape as the interstellar electron spectrum. Using the same parameters for propagation in the interplanetary magnetic field the modulated proton spectra for 1966 and 1968 were calculated and the results of this calculation are shown as the curves in figure 2.2. The fit to the observations is quite good indicating that the break in the cosmic ray primary spectrum at $\sim$10 GeV could be due to the solar modulation effects.

2.1.3   <u>Energies between 10^{12} eV and 10^{14} eV</u>

At energies $>10^{12}$ eV there is almost no direct information about particles with $z>1$ although a few individual particles have been detected in balloon borne nuclear emulsions.

Direct measurements on protons by Ryan et al (1972) extend to about 3×10^{12} eV. The only other direct measurements above 10^{12} eV are those of Grigorov et al (1971). Using apparatus carried by the PROTON 1, 2 and 3 satellites Grigorov et al found that the proton spectrum steepened from an integral spectral index, $\gamma+1$, of -1.7 to -2.5 at 10^{12} eV. The "all particle" spectrum measured in these experiments showed no such steepening. Data from the PROTON 4

satellite have been used to make a confirmatory measurement. The PROTON 4 results also show a "cutoff" in the "all particle" spectrum just above 10^{15} eV, but this could arise due to the limited volume of their calorimeter.

Ramana Murthy and Subramanian (1972) have attempted to derive a precise nucleon flux from the sea-level muon data assuming the spectral index, γ, to be - 2.67 and by adopting the scaling parameters determined at machine energies. (To convert to energy per nucleus their flux estimates are multiplied by 1.55). Work along similar lines by Elbert et al (1973) indicates that there is still considerable uncertainty in this method of derivation of the primary cosmic ray spectrum. The nucleon flux estimates of Elbert et al are about two times lower than those of Ramana Murthy and Subramanian, the discrepancy appearing to lie partly in a different choice of scaling parameters and partly in different mean free paths for proton and pion interactions.

Measurements of the primary energy spectrum in this energy range are summarised in figure 2.4. For a more complete discussion of the spectrum between 10^{12} and 10^{14} eV the reader is referred to a review by Watson (1974).

2.1.4   Energies above 10^{14} eV

All of the information about the spectrum of primary cosmic rays with energies $> 10^{14}$ eV/nucleus is based on the rather indirect technique of studying the properties of extensive air showers, which are created by the successive interactions of the progeny of the primary cosmic rays in the atmosphere.
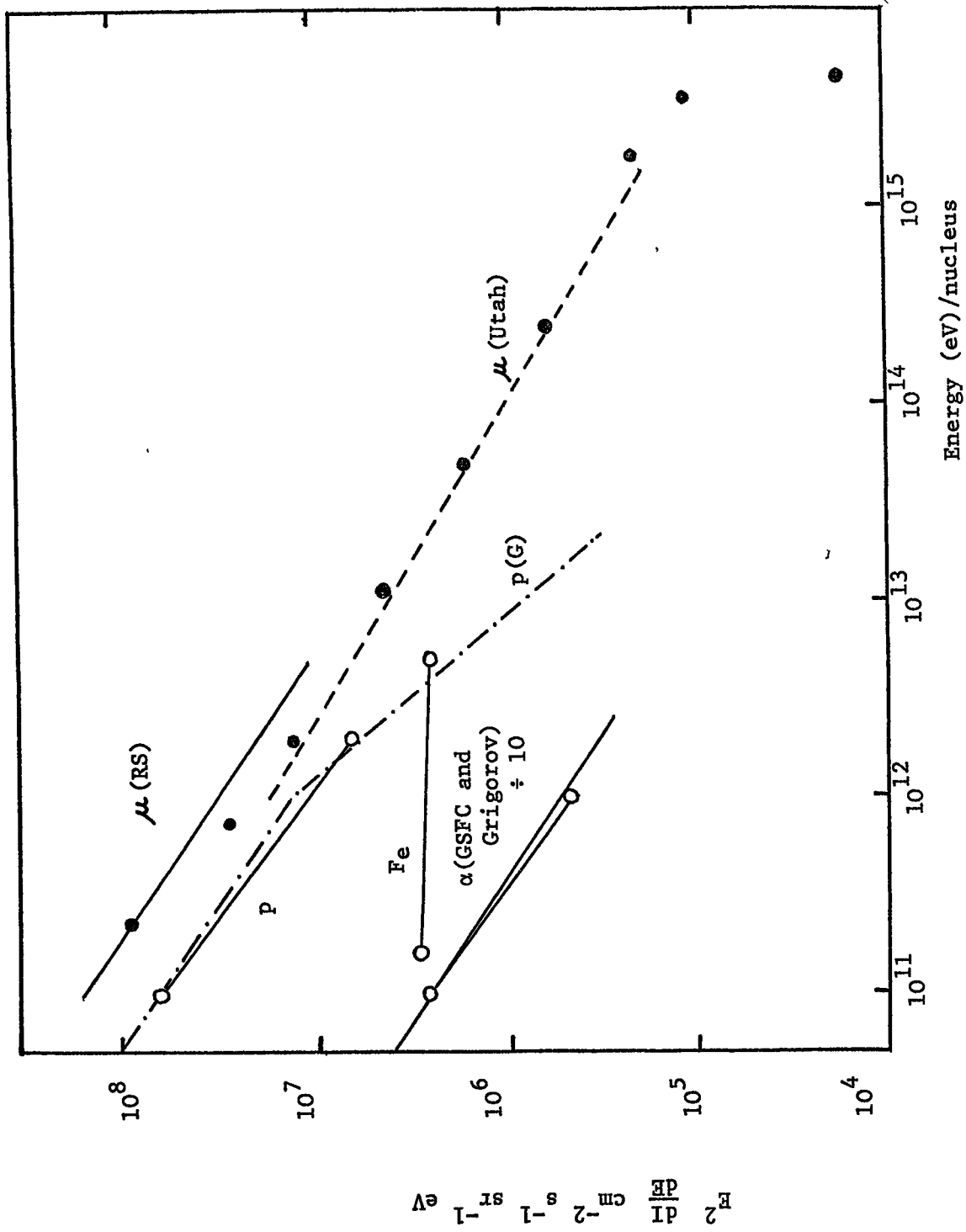
Figure 2.4: Energy Spectrum measurements, from direct and indirect methods, 10^{11} eV to 10^{15} eV. (Watson, 1974).

Perhaps the most interesting feature in the energy spectrum above 10^{14} eV is the change of slope at about 3×10^{15} eV where the exponent, γ, changes from a value of $\simeq -2.6$ to $\simeq -3.2$. This energy range is not discussed at any length in this thesis and for more complete discussions of the spectrum at energies greater than 10^{14} eV the reader is referred to review articles by Watson (1974) and Kempa et al (1974).

2.2 Anisotropy in the Cosmic Ray Flux observed at the Earth

An anisotropy in the primary cosmic ray flux with respect to galactic coordinates would appear to an observer on the earth as a regular variation of the intensity of the secondary particles, due to the primary cosmic rays, with a period of one sidereal day. The observed anisotropy is defined as:

$$\delta = \frac{(I_{max} - I_{min})}{(I_{max} + I_{min})}$$

In practice a first harmonic sinusoidal variation of intensity with sidereal time is fitted to the data and I_{max} and I_{min} are the maximum and minimum secondary particle intensities from this fit.

Table 2.1 contains a summary of experiments measuring the cosmic ray anisotropy. The experiments shown in table 2.1 are those which reported an anisotropy greater than two standard deviations from zero or those reporting the lowest upper limits to the anisotropy. Fig. 2.5 shows the results of these experiments plotted as a function of

Table 2.1

Experiments Measuring Cosmic Ray Anisotropy

Reference	Type of Measurement (Elevation)	Period of obs	Location	Latitude	Primary Energy (eV)	1st Harmonic	
						Amp %	T_{max} LST
Murakami et al (1973)	Muons underground 54 MWE	1968–72	Takeyama		10^{11}	0.037±0.016	22±2 hrs
Elliot et al (1970)	Muons underground 60 MWE	1960–68	London	51.5°N	$10^{11}-10^{12}$	0.020±0.005	18 hrs
Sherman (1953)	Muons underground 846 MWE	April 1951 – March 1952	Michigan	42°N	$\sim10^{13}$	≲0.2	
Cachon (1962)	E.A.S. 2860 m	1 year	Pic du Midi	43°N	2×10^{13}	<0.1	
Kolomeets et al (1970)	Crossed Telescopes	1964–67	Kazakh		$10^{13}-10^{14}$	≲0.1	17.6–23.5 hrs
Delvaille et al (1962)	E.A.S. 260 m	1958–59	Ithaca	43°N	5×10^{15}	0.41±0.17	13.8 hrs
Gombosi et al (1974)	E.A.S. 2925 m	1968–72	Mussala	42°N	6×10^{13}	0.13±0.05	Between 24 & 8 hrs
Daudin et al (1956)	E.A.S. 2860 m	1951–54	Pic du Midi	43°N	3×10^{14} 6×10^{14} 2×10^{15}	0.09±0.015 0.12±0.04 0.17±0.06	20.3±0.5 hrs 19.8±1.5 hrs 21.4±1.3 hrs
Lapikens et al (1971)	E.A.S.	1966–70	Haverah Park	54°N	10^{17}	≲1.2	
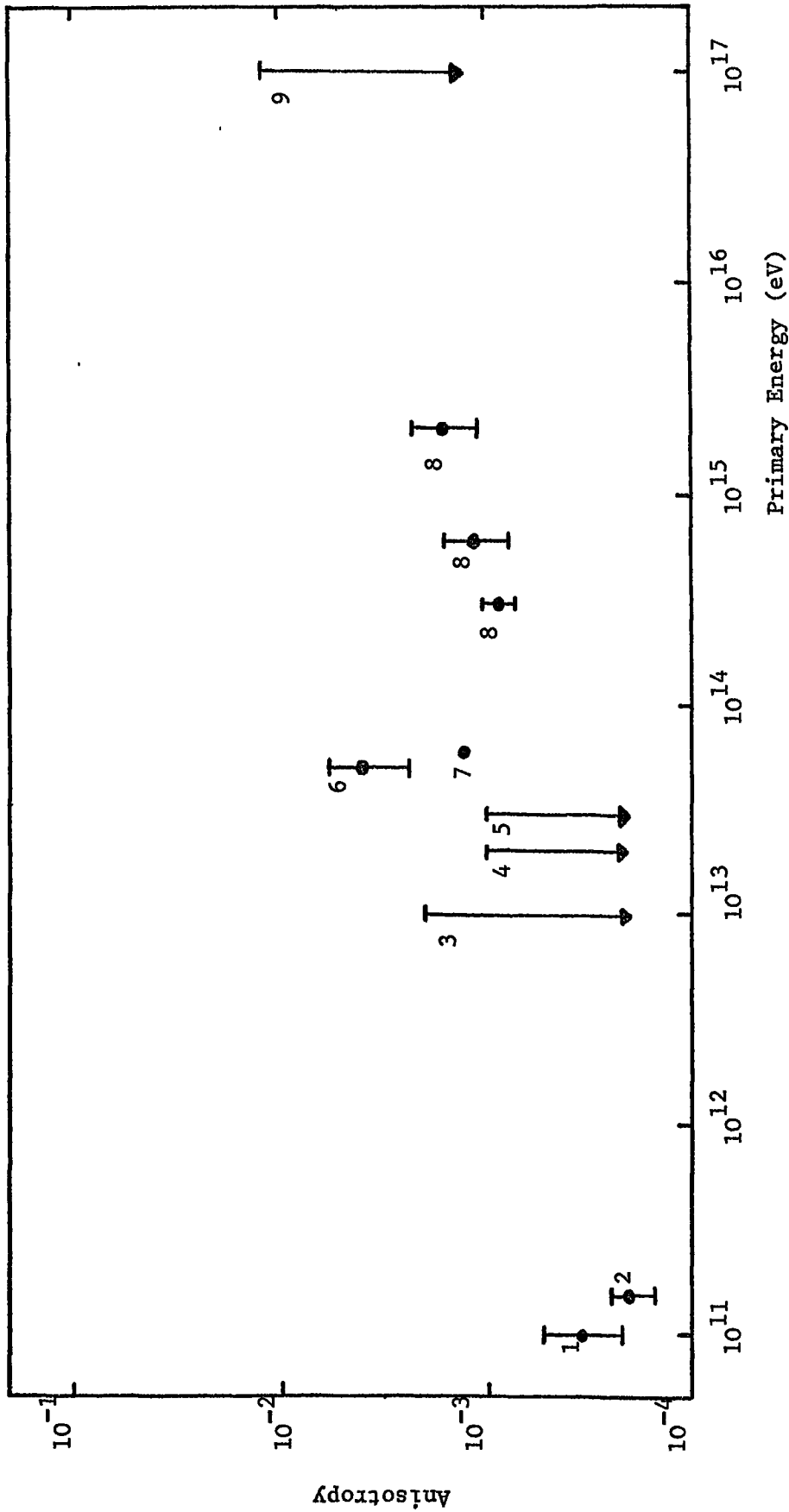
Figure 2.5: Experimental measurements of cosmic ray anisotropy as a function of energy.

1: Murakami et al (1973), 2: Elliot et al (1970), 3: Sherman et al (1953),

4: Cachon (1962), 5: Kolomeets et al (1970), 6: Delvaille et al (1962), 7: Gombosi et al

(1974), 8: Daudin et al (1956), 9: Lapikens et al (1971).

energy, the error bars and upper limits indicating one standard deviation. The experiments measuring anisotropy at the lowest energies detect muons underground whereas those at energies greater than 10^{13} eV use observations of extensive air showers.

The relatively large anisotropy reported by Delvaille et al (1962) is at variance with the results of Cachon (1962) and Kolomeets et al (1970) in the same energy range, and has not been confirmed by the more recent observations of Gombosi et al (1974).

The two lowest energy points, those of Elliot et al (1970) and Murakami et al (1973), apparently give the most stringent limit to the anisotropy. The result of Elliot et al (1970) is obtained from the variation in intensity of muons which penetrate a depth of 6×10^{3} g cm^{-2} of rock. In figure 2, it has been plotted at a median primary energy of 1.5×10^{11} eV which is obtained using recent accelerator data on multiplicities of secondary particles produced in proton-nucleus interactions.

Primary particles of this energy may be influenced by the interplanetary magnetic field which will tend to reduce any galactic anisotropy. If a model of the interplanetary field is chosen the effect on the anisotropy as a function of energy can be calculated. Barnden and McCracken (1973) have made calculations for 2-sector and 4-sector models of the interplanetary field and conclude that a detector at 6×10^{3} g cm^{-2} would record an anisotropy typically 2.5 times smaller than the true galactic anisotropy. There

may, however, be enough uncertainty in the response function
of the detector to primary energy and in the form of the
interplanetary magnetic field that $2x10^{-4}$ represents the
actual   galactic anisotropy at $1.5x10^{11}$ eV.
The Murakami et al (1973) result comes from a similar type
of muon measurement at a smaller depth underground. The
same uncertainties due to the interplanetary field apply
to the Murakami et al result as apply to the Elliot et al
result.

A measurement of the anisotropy at two or three times
higher primary energy would be sure of avoiding any diluting
effect of the interplanetary magnetic field.

We conclude that in the region of primary energy between
10^{11} eV and 10^{14} eV the upper limit to the galactic aniso-
tropy lies between 10^{-4} and 10^{-3}.

2.3 Variation of the Cosmic Ray Flux in the Galaxy

An indication of the distribution of cosmic rays in
the galaxy can be found from the distribution of galactic
γ-radiation. The energy spectrum of the γ-radiation in
the Galactic plane above 10 MeV is consistent with a mainly
π^{o}-decay origin for the γ-radiation, the π^{o} mesons being
derived from cosmic ray-interstellar gas nucleus interactions,
with perhaps 30% of the γ-radiation[*] in the Galactic centre
direction coming from a process, possibly the Inverse
Compton Effect, with a steeper exponent (Stecker et al
1974). Figure 2.6   shows the results of observations
of γ-radiation in the Galactic plane as a function of
galactic longitude, as measured by the OSO III and SAS II
satellites.

[*] with energy >100 Mev
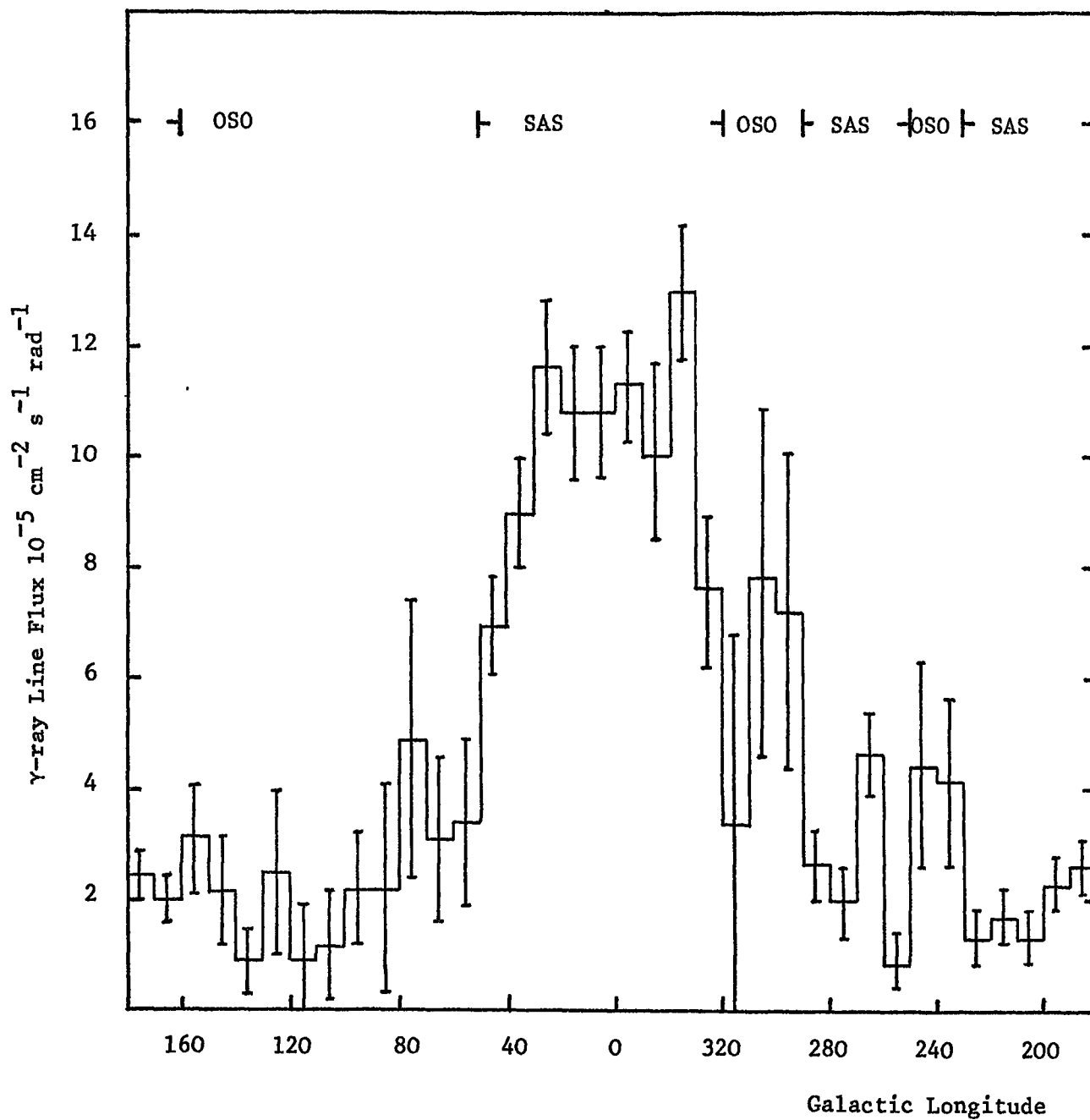
Figure 2.6: Flux of γ-rays around the Galactic Plane, from SAS II and OSO IlI experiments.

To see how the cosmic ray flux varies through the galaxy an estimate of the emissivity of the γ-radiation as a function of galactic radius must be made. The emissivity (w) of the γ-radiation is a function of the number density of cosmic rays, (n_{CR}), with energies between 1 and 10 GeV and the density of interstellar gas, (n_H).

$$w \propto n_{CR} \, n_H$$

Strong (1974) has made an analysis of the γ-radiation data to obtain the best estimate of the radial variation of the γ-radiation emissivity in the Galaxy and the uncertainties in the resulting emissivity distribution. The result of this calculation is shown in figure 2.7. Strong shows that there is evidence for the emissivity being higher in a region 3 to 8 kpc from the galactic centre than elsewhere. This increace in emissivity could be due to:

(i)   an increase in the cosmic ray flux in the region

(ii) an increase in the interstellar gas density

(iii)a mixture of (i) and (ii)

Studies of the 21 cm neutral hydrogen emission show that the density of neutral hydrogen in the 3 to 8 kpc region is of the same order as, or slightly lower than, the density in the region of the sun. However, recent measurements by Stecker and Solomon (1974) indicate that there may be large clouds of molecular hydrogen in this region of the galaxy which could increase the density of the gas seen by the cosmic rays.

If the increased γ-radiation emissivity is due to an increase in the cosmic ray density one or more of the
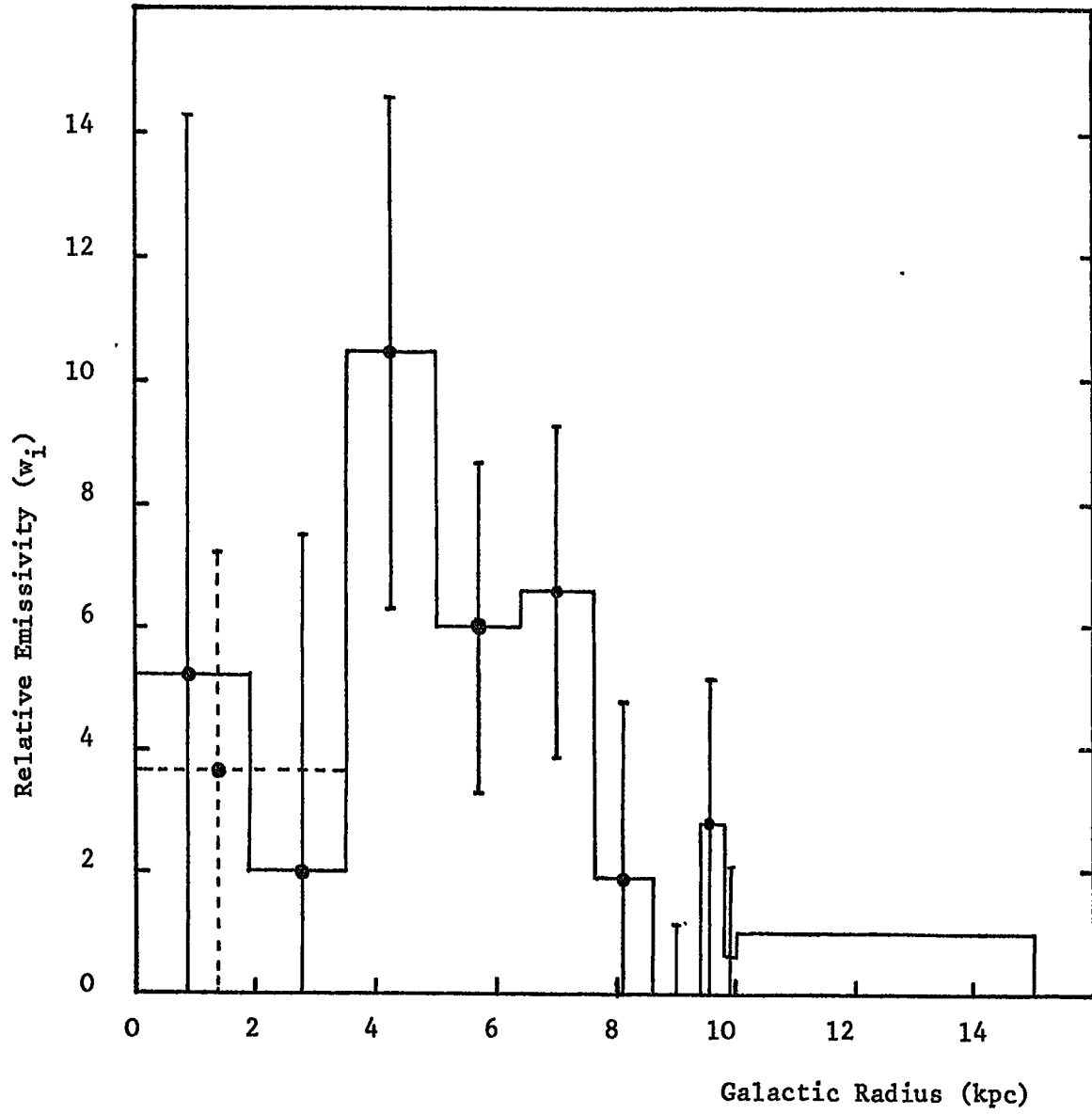
Figure 2.7: The relative γ-ray emissivity as a function of Galactic Radius (Strong, 1974).

following could be true:

a)   there is an increase in the number density of cosmic ray sources towards the galactic centre

b)   there is an increase in the containment time of the particles in this region

c)   there is a large scale acceleration mechanism operative towards the galactic centre

Models predicting the γ-ray emissivity based on all these possibilities are discussed in a recent paper by Dodds et al (1974).

In conclusion, the experimental data are not at present able to distinguish between the models for γ-radiation production, so no definite statement can be made regarding the variation of the cosmic ray flux in the galaxy. However an enhancement of the flux of cosmic rays towards the galactic centre cannot be ruled out.

2.4   The Chemical Composition of the Cosmic Ray Flux

Observations of the chemical composition of cosmic rays can provide information on the propagation parameters of cosmic rays in the galaxy, such as the lifetime in the galaxy and the amount of matter traversed, and about the nature of the cosmic ray sources. Two types of measurement of the chemical composition can be made. Integral measurements observe the composition over limited or unlimited energy ranges, whilst differential measurements are able to specify individual particle energy more accurately allowing the dependence of the chemical composition with energy to be studied. Many useful results have been obtained from the

integral measurements, but during the last three years
results, showing that the chemical composition does change
with energy, have been published by workers using apparatus
capable of differential measurements.

The two types of observation and the conclusions
resulting from them are discussed separately.

2.4.1 Integral Measurements

Most of the early measurements of the cosmic ray com-
position were carried out using stacks of nuclear emulsion
flown high in the atmosphere on balloons. Allowing for
interactions between the incoming cosmic rays and nuclei
in the atmosphere above the detector, the relative abund-
ances of the different cosmic ray species could be obtained.
More recently, scintillation counters, Cerenkov detectors
and spark chambers have been used in both balloon and
satellite experiments.

A recent measurement of the relative abundances of
cosmic rays above 5 GeV/nucleon normalised to carbon, is
presented in table 2.2 (Smith et al 1973).

To ascertain the nature of the cosmic ray sources
from the observed composition, allowance must be made for
any change in the composition brought about by nuclear
interactions in the interstellar medium. When a heavy
nucleus collides with a nucleus in the interstellar medium
it breaks up into a number of pions and lighter nuclei
which are called "spallation products". Observations of
these spallation products can also tell us how much inter-
stellar material the cosmic rays traverse during their

Table 2.2

The relative abundances of cosmic rays above 5 GeV/nucleon, normalised to carbon (from Smith et al 1973).

Element	Abundance
H·	24000 ± 2800
He	4200 ± 100
Li	18.1 ± 1.8
Be	4.2 ± 0.8
B	23.5 ± 1.3
C	100
N	24.8 ± 1.3
O	94.0 ± 2.3
F	2.1 ± 0.7
Ne	18.9 ± 1.3
Na	0.8 ± 0.5
Mg	23.6 ± 1.4
Al	1.8 ± 0.5
Si	19.6 ± 1.3
P-Cr	18.1 ± 1.4
Fe	12.0 ± 1.1

lifetime in the Galaxy. Fortunately some of these spalla-
tion products can be readily identified.

Figure 2.8 shows the observed abundances of cosmic rays
plotted with those of the solar photosphere and meteorites.
The light elements Li, Be and B are rapidly consumed in
stellar interiors, consequently their abundance in stellar
objects is very low as shown in figure 2.8. However, the
abundance of these light elements in the cosmic radiation
shows no such depletion. If it is reasonable to assume
that the source abundance of these light elements is very
small, then they must be created by spallation reactions
in the interstellar medium. The Li, Be and B are spallation
products of reactions between C N and O cosmic ray nuclei
and interstellar H, He and D nuclei. Measurements above
1 GeV/nucleon yield a L/M ratio

$$\frac{Li + Be + B}{C + N + O} = 0.25$$

(O'Dell et al 1962, Durgaprasad et al 1970, von Rosenvinge
et al 1969).

Using available cross-sections for various spallation
reactions and allowing for the effects of decay in dilated
time of the radioactive nuclides formed, Shapiro and Silber-
berg (1968) calculated the average amount of matter traversed
by cosmic rays required to create the observed abundance of
the light elements. Using a "slab" approximation, in which
all cosmic rays traverse the same amount of matter, the
"slab" thickness they obtained was

$$\lambda = 4.0 \, ^{+1.0}_{-0.5} \, g \, cm^{-2}$$
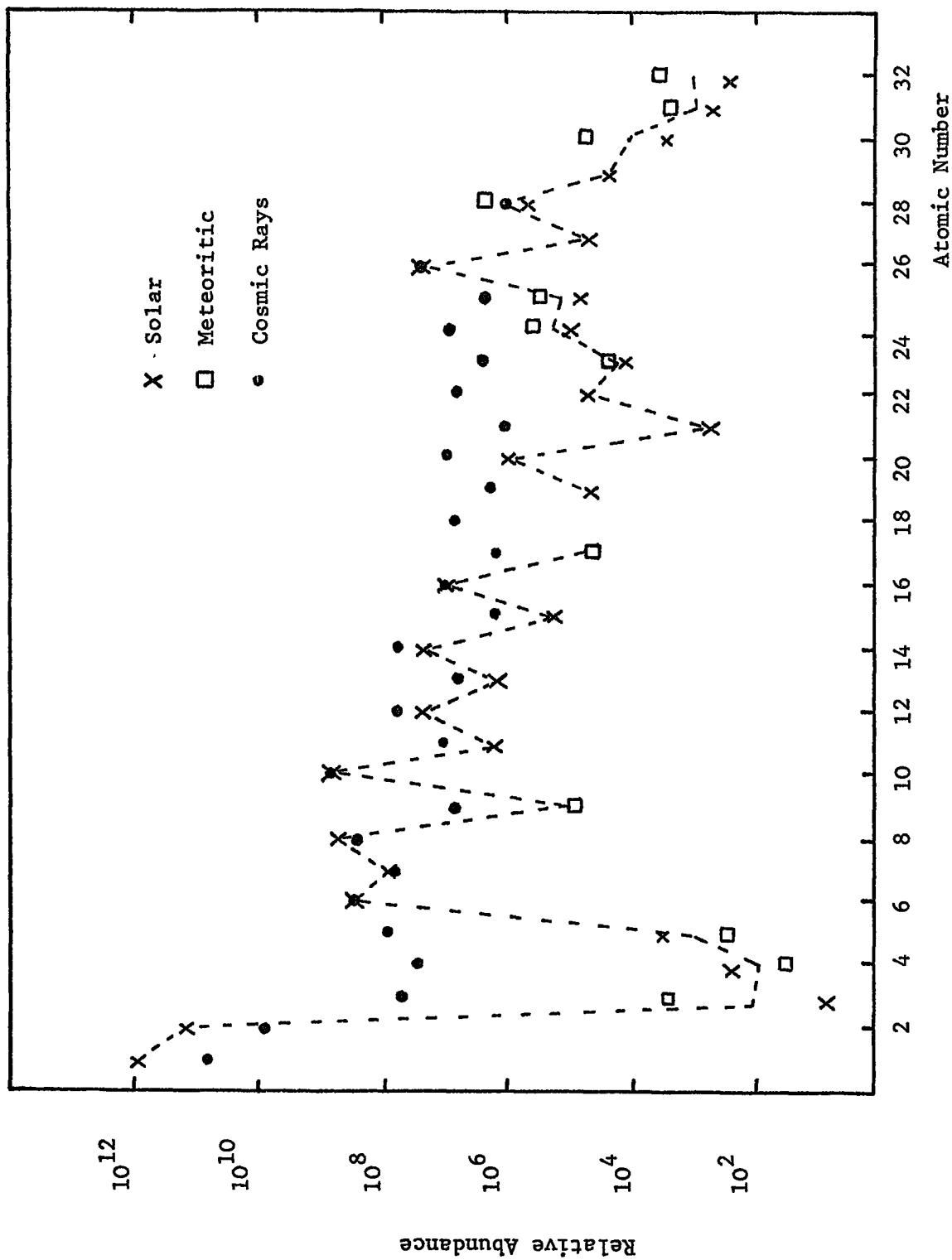
Figure 2.8: The observed abundances of cosmic rays plotted with those of the solar photosphere and of meteorites. Cosmic ray fluxes are adjusted so that the Carbon value coincides with that for solar carbon (Shapiro, 1971).

Another estimate of the mean path length may be obtained from the abundance of He^3 which has a low stellar abundance. He^3 is a product of the break up of He^4 nuclei and measurement of the Helium isotopes between 100 and 400 MeV/nucleon gives

$$\frac{He^3}{He^3 + He^4} = 0.1 \pm 0.02$$

(Hildebrand et al 1963). Using this information Ramaty and Lingenfelter (1969) obtained a mean path length of 4.0 g cm^{-2} agreeing with the results derived from the light nuclei despite the difference in energy domain. Rasmussen (1974) reports that Dwyer and Meyer have recently measured the He^3/He^4 ratio at energies between 1.5 and 5 GeV/nucleon. Preliminary analysis of their data gives the result $He^3/He^4 =$ 0.13 $\pm$ 0.07.

The assumption that all cosmic rays traverse the same amount of matter is an over simplification. A wide range of path lengths is necessary in order to obtain a good fit to the observed abundances of the secondaries of Fe. A recent example of such a path length distribution is

$$\frac{dN}{d\lambda} = \left[1 - \exp(-2.8\lambda^2) \right] \exp(-0.23\lambda)$$

Where N is the fractional flux intensity of particles having a path length λ (g cm^{-2}) (Shapiro and Silberberg 1974).

Figure 2.9 shows the result of a calculation using an exponential path length distribution, made by taking a trial source composition and propagating it forward until the composition resembles the observed composition. From figure
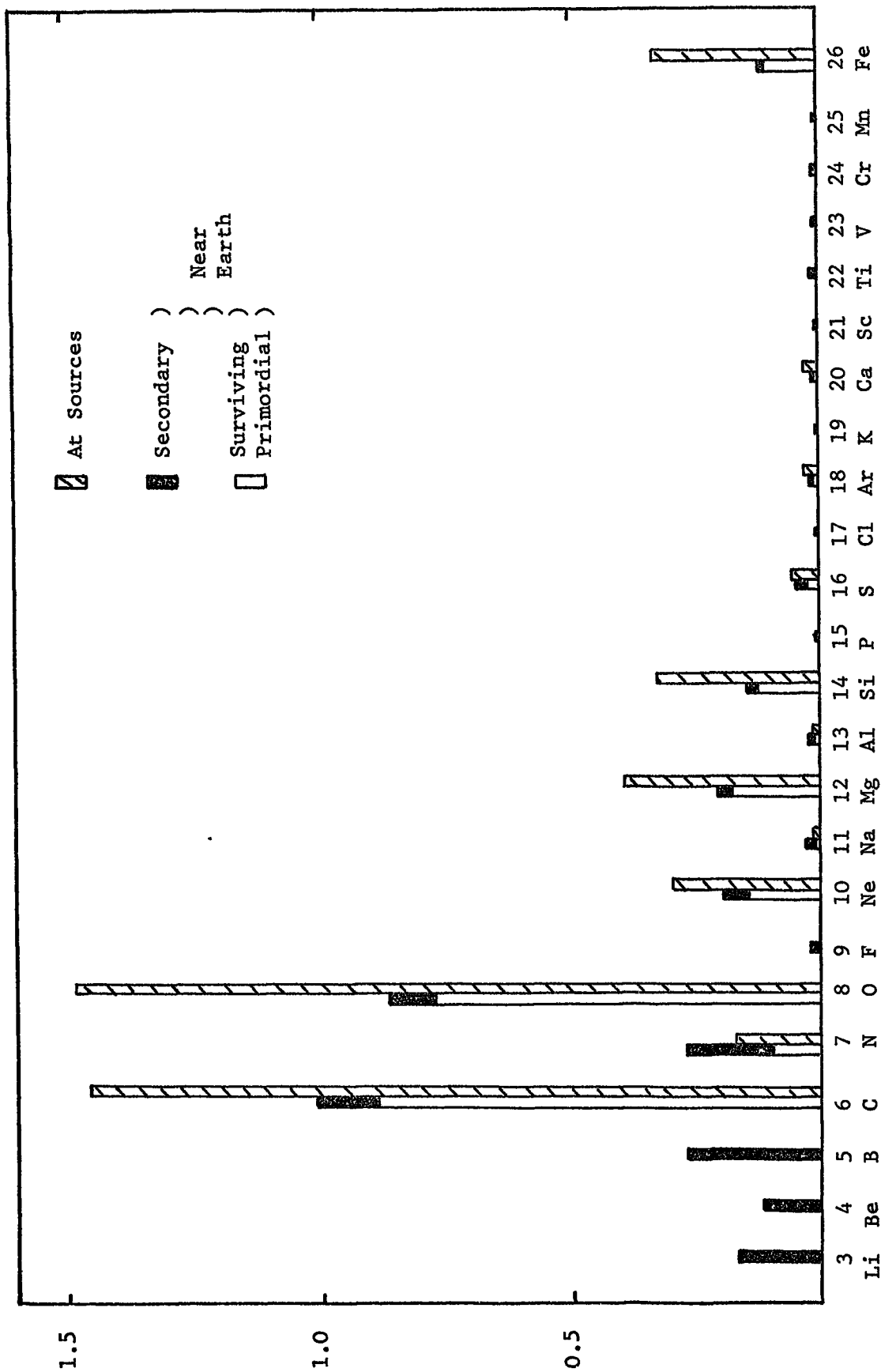
Figure 2.9: Cosmic ray composition at the sources and near the Earth. The Flux of arriving Carbon is normalised to unity. The white portions represent the residual primordial fluxes reaching the Earth and the dark portions represent Spallation products. (Shapiro, 1971)

2.9 it can be seen that the spallation reactions cause substantial changes in the composition. It should be noted however that in a calculation of this nature only the source abundances of C, N, O, Ne, Mg, Si and Fe are determined with a precision of better than 20%.

By making assumptions about the region of propagation of the cosmic rays it is possible to estimate their mean age. For example, a particle confined to the galactic disk (of average density ~ 1 atom cm^{-3}) requires a lifetime of 3×10^6 years in order to traverse 4 g cm^{-2} of matter. Estimates of this nature can be compared with that obtained from the abundance of Be^{10}, which acts as a "radioactive clock". If the light elements in the cosmic rays are separated into their respective isotopes, the amount of Be^{10} present is found to be less than that predicted from a propagation model which satisfies the other isotopic abundances. The discrepancy is attributed to the radioactive decay of Be^{10}, which has a half life of 1.5×10^6 years (Yiou and Raisbeck 1972). Webber et al (1973a) conclude that the deficiency of Be^{10} in the energy range 100-200 MeV/nucleon implies a mean cosmic ray lifetime of

$$\tau = (3.4 \; {}^{+3.4}_{-1.3}) \; \times \; 10^6 \; \text{years}$$

2.4.2 Differential Measurements

The first evidence of a variation in the cosmic ray composition with energy came from Juliusson and Meyer (1972), who observed that the ratio of all the secondary nuclei (i.e. those which originate mainly from spallation reactions) to

the primary nuclei (i.e. those originating in the cosmic ray sources) decreased with increasing energy above 20 GeV/ nucleon. This measurement was subsequently confirmed and extended by several other groups. An example of this energy dependence is shown in figure 2.10 where the ratio (Li + Be + B + N)/(C + O) is plotted as a function of energy.

Above a few GeV/nucleon the cross-sections for spalla- tion do not vary appreciably with energy (Shapiro and Silberberg 1970, Kaufman et al 1973). This implies that the higher energy particles of each species must have passed through less material after acceleration than those of lower energy. Cesarsky and Audouze (1974) have obtained an expression for the mean path length of the cosmic rays in the galaxy as a function of energy from an analysis of the available data. They find that the mean path length decreases slowly up to 30 GeV/nucleon, and more sharply above 30 GeV/nucleon reaching a value of $\sim$1 g cm^{-2} at 100 GeV/nucleon, though the uncertainties are quite large. They also confirm that the effects of possible variation in the nuclear cross-sections with energy would not alter the value of the path length by more than ten per cent.

Ormes and Balasubrahmanyan (1973) and Webber et al (1973b) have discovered that the ratio of various pairs of primary nuclei groups, e.g. (C + O)/Fe, also decreases with increasing energy. Balasubrahmanyan and Ormes (1973) calculated that this effect cannot be accounted for by an energy dependent path length as derived from secondary/ primary ratios, implying some primary components must have
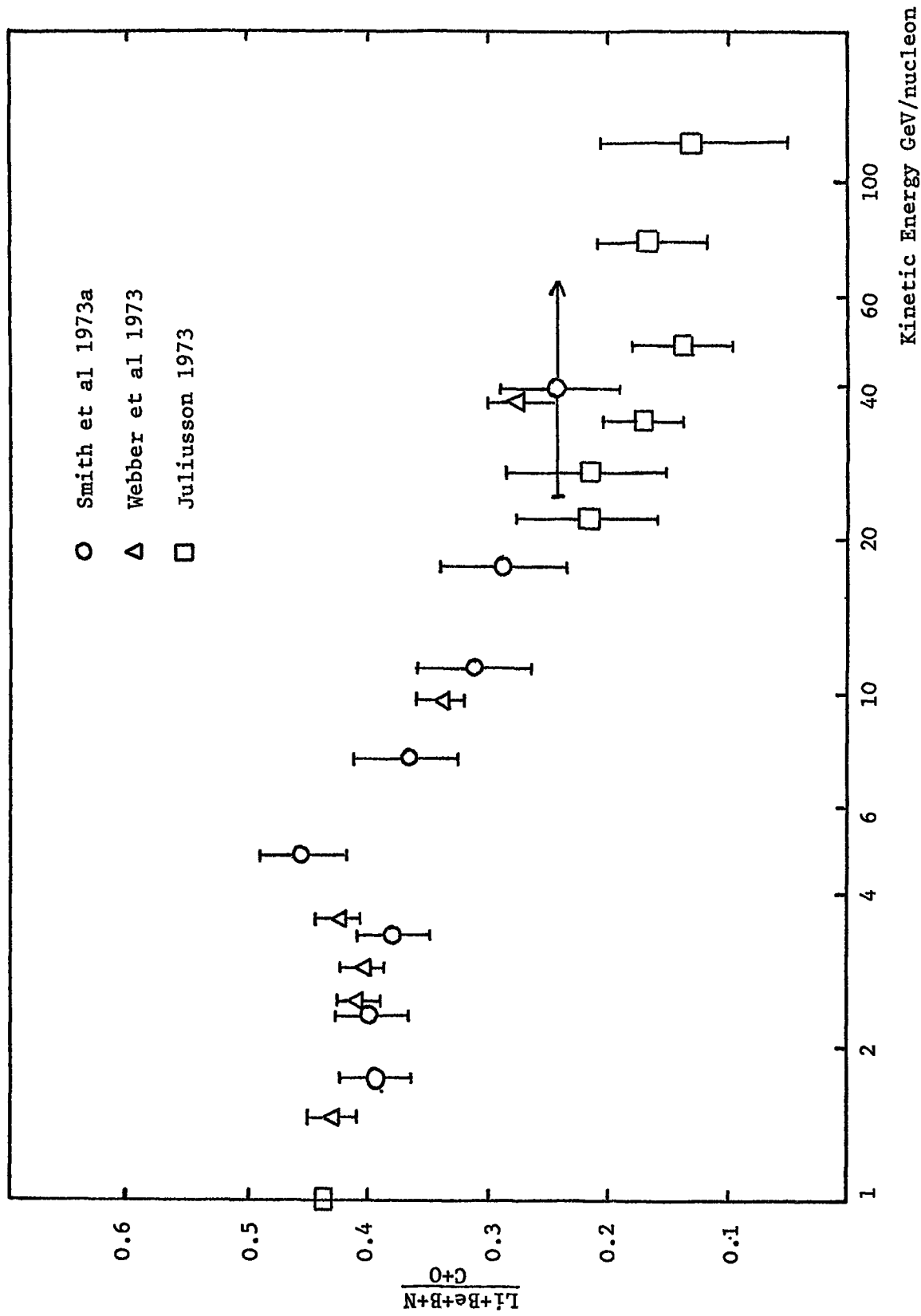
Figure 2.10: The energy dependence of the ratio (Li+Be+B+N)/(C+O) at high energies.

different source spectra. Cesarsky and Audouze (1974)
confirmed that the sources of high energy cosmic rays
must be richer in Fe relative to C + O than the lower
energy cosmic ray sources, while Ramaty et al (1973)
suggest that there may possibly be two source mechanisms,
one which produces the iron and the other responsible for
all the rest of the primary cosmic ray nuclei.

There is very little information about the composition
of cosmic rays at energies greater than 100 GeV/nucleon.
The extensive air shower results at 10^{12}-10^{13} eV are con-
sistent with the balloon measurements at high energies
while the results at 10^{13}-10^{15} eV are inconsistent with
the extrapolation of the Fe spectrum of Ormes et al 1973.
Further measurements, especially with techniques with much
higher charge resolution are needed in this extremely
important range of energies.

2.5 Constancy of the Cosmic Ray Flux

An estimate of the constancy of the cosmic ray flux
over long periods of time may be made by measuring the
abundances of long lived radioactive isotopes e.g. Cl^{36}
Al^{26} Mn^{53} or Be^{10} formed by the interactions of cosmic
rays in meteorites. Such measurements are difficult to
interpret but appear to show that the present day value
of the cosmic ray flux is within a factor of two of the
flux averaged over the last 10^5 to 10^7 years (Geiss 1963,
Lal 1973). The energy region of the cosmic rays producing
most of the transmutations is 10^9 to 10^{10} eV.

References

Anand, K. C. et al., 1968, Canadian J. Phys., 46, S652

Balasubrahmanyan, V. K. and Ormes, J. F., 1973, Astrophys. J.,
186, 109

Barnden, L. R. and McCracken, K. G., 1973, Proc. 13th
Int. Conf. on Cosmic Rays, Denver, 2, 963

Bell, M. C., 1974, Thesis, University of Durham

Burger, J. J. and Swanenburg, B. N., 1971, Proc. 12th Int.
Conf. on Cosmic Rays, Hobart, 5, 1858

Cachon, A., 1962, Proc. 6th Interam. Sem. on Cosmic Rays,
La Paz. Vol. 2 (University of San Andreas), 39

Cesarsky, C. J. and Audouze, J., 1974, Astr. Astrophys.,
30, 119

Daudin, J., Auger, P., Cachen, A., Daudin, A., 1956, Nuovo
Cimento, 3, 1017.

Delvaille, J., Kendziorski, F., Greisen, K., 1962, J.Phys.
Soc., Japan, 17, Suppl. III, 76

Dodds, D., Strong, A.W., Wolfendale, A.W., Wdowczyk, J.,
1974, J.Phys.A (to be published)

Durgaprasad, N. et al, 1970, Phys. Rev. D, 1, 1021

Elbert, J. W. et al, 1973, Proc. 13th Int. Conf. on Cosmic
Rays, Denver, 1, 213

Elliot, H., Thambyahpillai, T. and Peacock, D. S., 1970,
Acta Phys. Acad. Sci Hung., 29, suppl. 1, 491

Garcia-Munoz, M., 1973, Proc. 13th Int. Conf. on Cosmic
Rays, Denver, 5, 3513

Geiss, J., 1963, Proc. 7th Int. Conf. on Cosmic Rays,
Jaipur, 3, 434

Gloeckler, G., Jokipii, J. R., 1967, Astrophys. J., _148_, L41

Gombosi, T. et al., 1974, Preprint

Grigorov, N. L. et al., 1971, Proc. 12th Int. Conf. on Cosmic
Rays, Hobart, _5_, 1746

Hildebrand, B. et al., 1963, Proc. 8th Int. Conf. on Cosmic
Rays, Japan, _3_, 101

Holmes, J., 1974, Thesis, University of Oxford

Juliusson, J. E., Meyer, P. and Muller, D., 1972, Phys. Rev.
Lett., _29_, 445

Juliusson, J. E., 1973, Proc. 13th Int. Conf. on Cosmic
Rays, Denver, _1_, 178

Kaufman, S. B., Steinberg, E. P., Weisfield, M. W. and
Wilkins, B. D., 1973, Phys. Rev. Lett., _30_, 1221

Kempa, J., Wdowczyk, J., Wolfendale, A. W., 1974, J.Phys.A.
_7_, 1213

Kolomeets, E. V., Nenolochnov, A. N. and Zusmanovich, A. G.,
1970, Acta. Phys. Acad. Sci. Hung., _29_, suppl. 1, 513

Lal, D., 1973, Proc. 13th Int. Conf. on Cosmic Rays, Denver,
_5_, 3399

Lapikens, J. et al., 1971, Proc. 12th Int. Conf. on Cosmic
Rays, Hobart, _1_, 316

Lezniak, J. A. and Webber, J. R., 1971, J.Geophys.Res. _76_,
1605

Murakami, K., Wada, M., Miyazaki, Y., Mishina, Y., 1973,
Proc. 13th Int. Conf. on Cosmic Rays, Denver, _2_, 1028

O'Dell, F. W. Shapiro, M. M. and Stiller, B., 1962, J. Phys.
Soc. Japan, _17_, 23

Ormes, J. F. and Webber, W. R., 1965, Proc. 9th Int. Conf.
on Cosmic Rays, London, 1, 407

Ormes, J. F. and Balasubrahmanyan, V. K., 1973, Nature
Phys. Sci. 241, 95

Ormes, J. F. et al., 1973, Proc. 13th Int. Conf. on Cosmic
Rays, Denver, 1, 157

Ramana Murthy, P. V. and Subramanyan, A., 1972, Proc. Ind.
Acad. Sci. 76A, 1

Ramaty, R. and Lingenfelter, R. E., 1969, Astrophys. J.,
155, 587

Ramaty, R., Balasubrahmanyan, V. K. and Ormes, J. F., 1973,
Science, 180, 731

Rasmussen, I. L., 1974, Origin of Cosmic Rays, ed.
J. L. Osborne and A. W. Wolfendale, De Reidel (to be
published)

Ryan, M. J., Ormes, J. F., Balasubrahmanyan, V. K., 1972,
Phys. Rev. Lett. 28, 985

Shapiro, M. M., 1971, Proc. 12th Int. Conf. on Cosmic Rays,
Hobart, Rapp. Paper, 422

Shapiro, M. M. and Silberberg, R., 1968, Can. J. Phys. 46,
S561

Shapiro, M. M. and Silberberg, R., 1970, Ann. Rev. Nuc. Sci.,
20, 283

Shapiro, M. M. & Silberberg, R., 1974, Phil. Trans. of Royal
Soc. of London, Series A, (to be published)

Sherman, N., 1953, Phys. Rev., 89, 25

Smith, L. H., Buffington, A., Smoot, G. F., Alvarez, L. W.
and Wahlig, M. A., 1973, Astrophys. J., 180, 987

Smith, L. H., Buffington, A., Orth, C. D. and Smoot, G. F.,
    1973a, Proc. 13th Int. Conf. on Cosmic Rays, Denver,
    $\underline{1}$, 177

Stecker, F. W. and Solomon, P. M., 1974, 8th ESLAB Symposium
    (part II), Contexts and Status of γ-ray Astronomy,
    Frascati

Stecker, F. W., Puget, J. L., Strong, A.W. Bredekamp, J. H.,
    1974, Astrophys. J., $\underline{188}$, L59.

Strong, A. W., 1974, J.Phys.A. (to be published)

Von Rosenvinge, T. T., Webber, W. R. and Ormes, J. F., 1969,
    Astrophys. Space Sci., $\underline{5}$, 342

Watson, A. A., 1974, Origin of Cosmic Rays, ed. J. L. Osborne
    and A. W. Wolfendale, De Reidel (to be published)

Webber, W. R., Lezniak, J. A. and Kish, J., 1973, Proc. 13th
    Int. Conf. on Cosmic Rays, Denver, $\underline{1}$, 248

Webber, W. R., Lezniak, J. A., Kish, J. and Damle, S. V.,
    1973a, Astrophys. Space Sci., $\underline{24}$, 17

Webber, W. R., Lezniak, J. A., Kish, J. and Damle, S. V.,
    1973b, Nature Phys. Sci. $\underline{241}$, 96

Wolfendale, A. W., 1973. The primary radiation: a brief
    review; Cosmic Rays at Ground Level, ed. A. W. Wolfen-
    dale, Inst. of Physics

Yiou, F. and Raisbeck, G. M., 1972. Phys. Rev. Lett. $\underline{29}$, 372

Chapter 3   The Galaxy and Interstellar Medium

3.1 Introduction

The purpose of this chapter is to describe the properties of the Galaxy and interstellar medium which are relevant to a study of the propagation and possible origin of the cosmic radiation. Section 3.2 describes the overall structure of the Galaxy and is followed in section 3.3 by a brief review of the properties of the interstellar medium. Section 3.4 discusses the experimental observations of magnetic fields in the Galaxy.

3.2 Structure of the Galaxy

3.2.1   Total Mass

The matter in the Galaxy is in the form of stars, dust and gas, distributed mainly in a flat disk. The total mass of the Galaxy is 2×10^{11} $M_\odot$, ($M_\odot$ = 1 solar mass), the greatest fraction of the matter being in $\sim 10^{11}$ stars. The total mass of gas in the form of atomic hydrogen, as estimated from the 21 cm wavelength emission, is $\sim 5 \times 10^9$ $M_\odot$. Molecular hydrogen, helium and heavier elements may bring the mass of gas in the Galaxy up to $\sim 10\%$ of the total mass of the Galaxy. The ratio of gaseous to stellar material varies greatly with distance from the galactic centre, though the distribution of the dust is similar to that of the gas. The smoothed space density of the dust is $\sim 1\%$ of that of the observed gas.

3.2.2   The position of the sun in the Galaxy

The sun lies within 12 pc of the galactic plane. The centre of the Galaxy is in the constellation Sagittarius at

265.6° RA, -28.9° dec. The distance of the sun from the
Galactic centre can be found by estimating the distance
of RR Lyrae variable stars in the central condensation.
The currently accepted value of 10 kpc has an uncertainty
of $\sim$10%. Before 1963 the sun was thought to be at a
distance 8.2 kpc from the Galactic Centre.

A system of Galactic Coordinates (longitude ℓ, latitude
b) centred on the sun is used to give direction in the
Galaxy. The equator of the system is the galactic plane
and $\ell=0^{\circ}$ is towards the Galactic Centre. With respect to
the average motion of nearby stars the sun is moving at
20 km s^{-1} towards $\ell=60^{\circ}$, b=24°.

3.2.3   The distribution of stars

To describe the structure of the Galaxy the coordinates,
R, distance from the Galactic Centre, and Z, the perpendicular
distance from the plane are used. Figure 3.1 shows a cross-
section of the galaxy, the contours giving the distribution
of mass density in stars in units of the smoothed out density
near the sun. The diameter of the disk is about 30 kpc. The
black spots on figure 3.1 indicate the positions of globular
star clusters projected on to the plane through the sun and
the Galactic Centre. These are the oldest stellar systems
and form a roughly spherical halo of radius 15 kpc. The
surface density of all stars projected on to the galactic
plane is strongly peaked towards the Galactic Centre. At
distances of greater than 1 kpc from the centre, the surface
density of stars falls approximately as exp (-R/4 kpc).
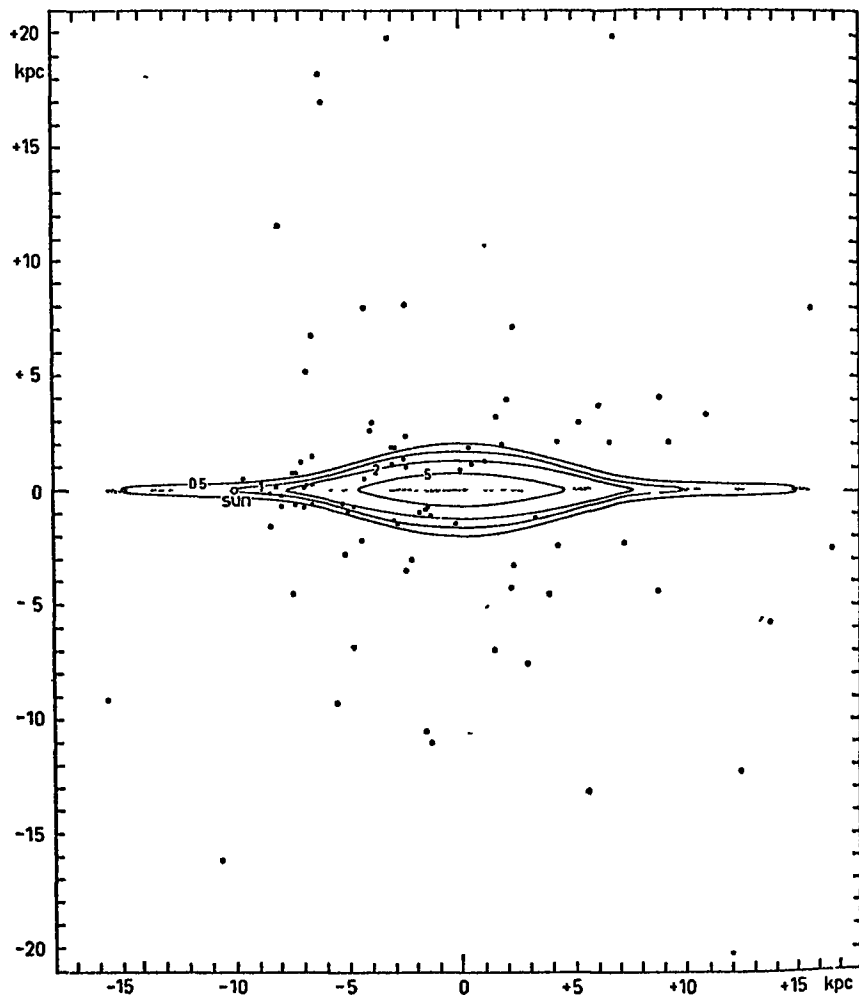
Figure 3.1: Distribution of Globular Clusters projected

on a plane perpendicular to the galactic plane through

the sun and centre, and lines of equal mass density. The

steep increase in density in the inner parts is not indicated.

Shaded parts give a schematic representation of the distri-

bution of interstellar gas and extreme population I.

(J. H. Oort in "Galactic Structure", Chicago, 1965).

The Z-distributions of the various classes of stars and
other constituents of the interstellar medium differ from
one another. The 'thickness' of the disk for a particular
class of object is usually expressed as the equivalent
thickness $(2Z_{eq})$, i.e. the total thickness of the disk the
objects would have if it were a slab of uniform density;
or the distance between half density points $(2Z_{\frac{1}{2}})$. The
relation between these quantities depends on the form of
the Z-distribution. For a gaussian distribution, $Z_{\frac{1}{2}}=0.94\ Z_{eq}$,
while for an exponential distribution $Z_{\frac{1}{2}}=0.69\ Z_{eq}$.

The values of $2Z_{\frac{1}{2}}$ for some representative classes of
stars, in the neighbourhood of the sun, are shown in table 3.1.
The thickness of the disk is seen to increase in the sequence
from young, O stars, through the solar type, G stars, to
white dwarfs.

3.2.4   Spiral Structure

Most external disk-shaped galaxies have a structure of
a spherical or barred nucleus surrounded by spiral arms in
varying degrees of development. At visual wavelengths, the
spiral tracers in these galaxies are O and B type stars,
regions of ionised hydrogen gas and dust lanes. In our own
galaxy visual observations of the structure are limited to
a few kpc due to absorption by dust ($\sim$ 2.2 magnitudes per kpc
in the plane).

The large scale spiral structure is deduced from 21 cm
radio emission from neutral hydrogen. The ground state of
the hydrogen atom is split into two levels with the electron
and proton spins either parallel or anti parallel. A transi-

Table 3.1   Values of $2Z_{\frac{1}{2}}$ for various classes of stars in
the neighbourhood of the sun

Class of Stars	$2Z_{\frac{1}{2}}$ (pc)
O	70
A	160
G, K, M	480
White Dwarfs	700

tion between these two spin states gives radiation of a
frequency 1420.4 M Hz. The natural width of the line is
negligible and it is possible to measure Doppler shifts
down to 0.2 km s^{-1}. The intensity of radiation of a given
frequency, Iν, is usually expressed as a brightness tem-
perature:

$$T_B = \left[\frac{c^2}{2\nu^2 k} \right] I_\nu$$

If, over the 21 cm line profile, the optical thickness
is much less than unity, the brightness temperature is
proportional to the column density of hydrogen atoms. If
the gas motion about the galactic centre is purely rotational
and the rotation curve of the Galaxy is known, the distance
of a portion of gas can be deduced from its radial velocity.
The rotation curve of the Galaxy, for R<R$_\odot$, the solar radius,
can be measured (in a given direction the maximum radial
velocity is that of gas at R = R$_\odot$ sinℓ). At R>R$_\odot$, the rota-
tion curve is deduced from a model of the Galaxy. Figure 3.2
shows a derived rotation curve for the Galaxy. The rotational
velocity in the neighbourhood of the sun is 250$\pm$30 km s^{-1} in
the direction ℓ=90°, inferring a period of rotation for the
sun about the Galactic Centre of 2.5x10^8 yr.

From 21 cm surveys, maps of the spiral structure can be
constructed. Fig. 3.3 is a composite map showing the position
of bright ridges of emission. The sun lies within the so-
called Orion arm. Stellar and radio observations show this
arm to have a pitch angle of 20°. The Orion arm does not
appear to be a major arm but an off-shoot of the Sagittarius
arm. The form of the spiral arms indicates that the Galaxy

θ (km s^{-1})

300

200

100

0   4   8   12   16   20

Galactic Radius (kpc)
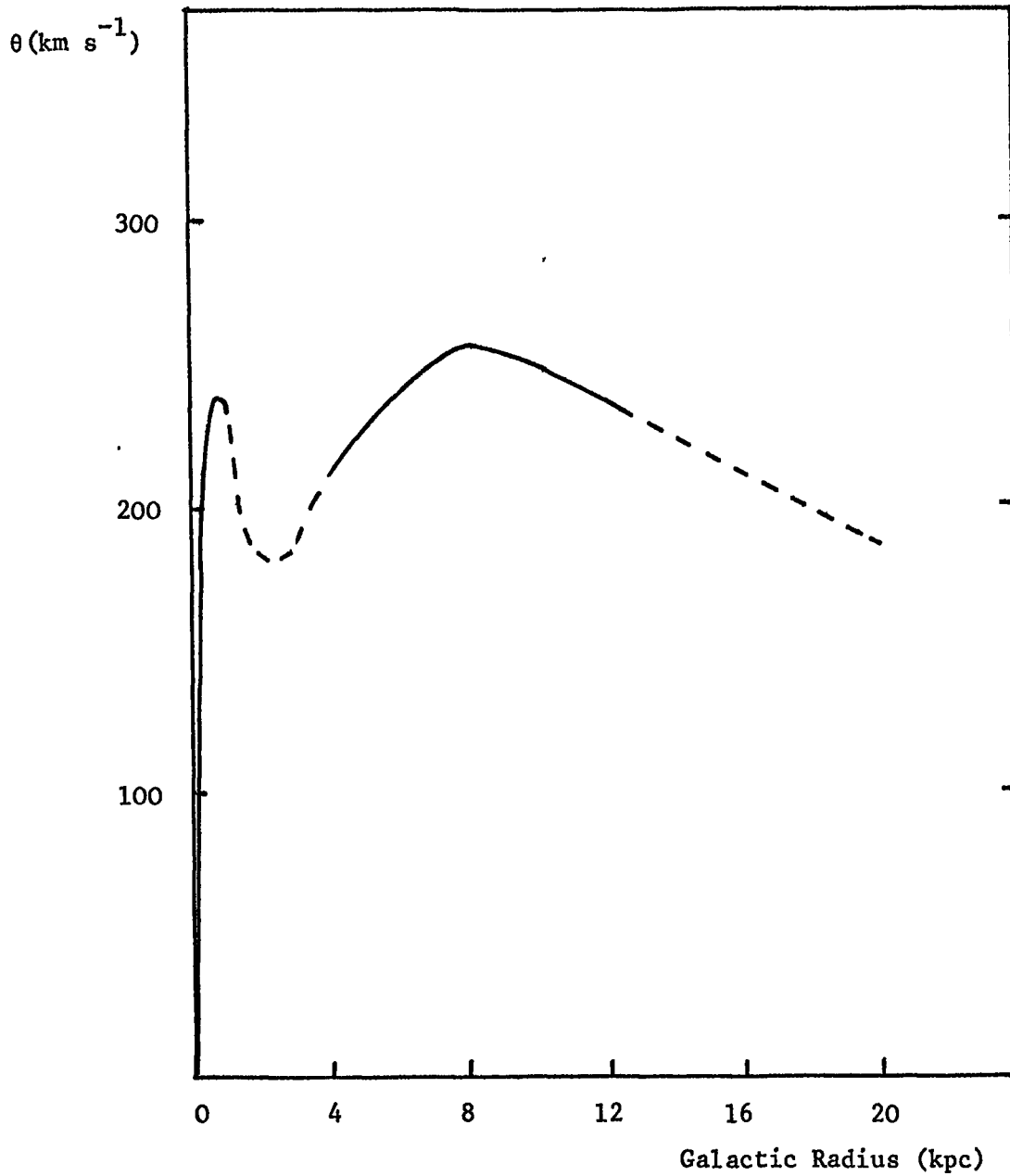
Figure 3.2: Rotation curve of the Galaxy. The portions indicated by continuous lines have been deduced from observations, those indicated by broken lines have been interpolated or extrapolated beyond 12kpc using a model for the Galaxy (Lequeux, 1969).
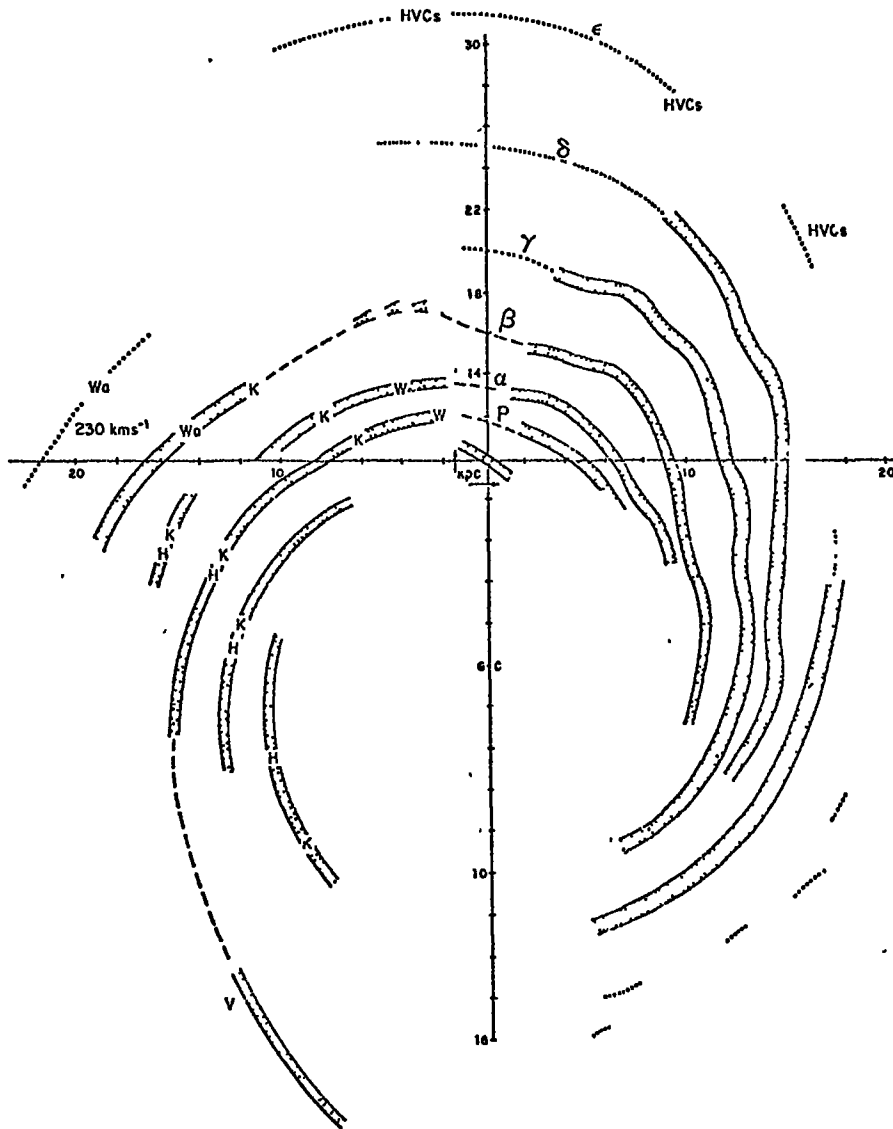
Figure 3.3: A composite map of the spiral structure of our
Galaxy based on a collation of the new data and other sources
of information K=Kerr (1970); H=Henderson (1967); Wa=Wannier et al
(1972); W=Weaver (1970); V=Verschuur (1973)

(G. L. Verschuur, 1973)

is of a type intermediate between Sb and Sc.

The central region of the Galaxy has a complex structure. An interpretation of the situation in the central regions by Sanders and Wrixon (1973) is shown in figure 3.4. The inner, partial or complete, rings of neutral hydrogen are rotating and simultaneously expanding with the velocities shown. The present kinetic energy of expansion of the 3 kpc arm is 10^{53} erg.

To produce such an expansion by a single explosion would require the injection of 10^8 $M_\odot$ 10^7 years ago with a total energy of 3×10^{58} erg. The nuclear disk of neutral hydrogen is also expanding. At the Galactic Centre there is a radio source of synchrotron emission, Sag A, which has a diameter of 6 pc. Observations in the infra-red at $2.2 \mu m$ indicate that the density of normal stars rises to 10^6 pc^{-3} within 1 pc of the Galactic Centre. It has been suggested that there is a massive black hole at the centre of the Galaxy though the observed motion of the gas sets an upper limit to its mass of 2×10^8 $M_\odot$.

Early radio surveys at high galactic latitudes were interpreted as evidence for a halo, of dimensions comparable to the volume occupied by the globular clusters, which contained magnetic field and relativistic electrons. Further surveys with improved resolution showed that a large proportion of the emission came from features in the galactic disk. There is still some evidence, however, for a 'radio disk' of approximate radius 10 kpc with a thickness of up to 5 kpc (Bulanov and Dogel 1974).
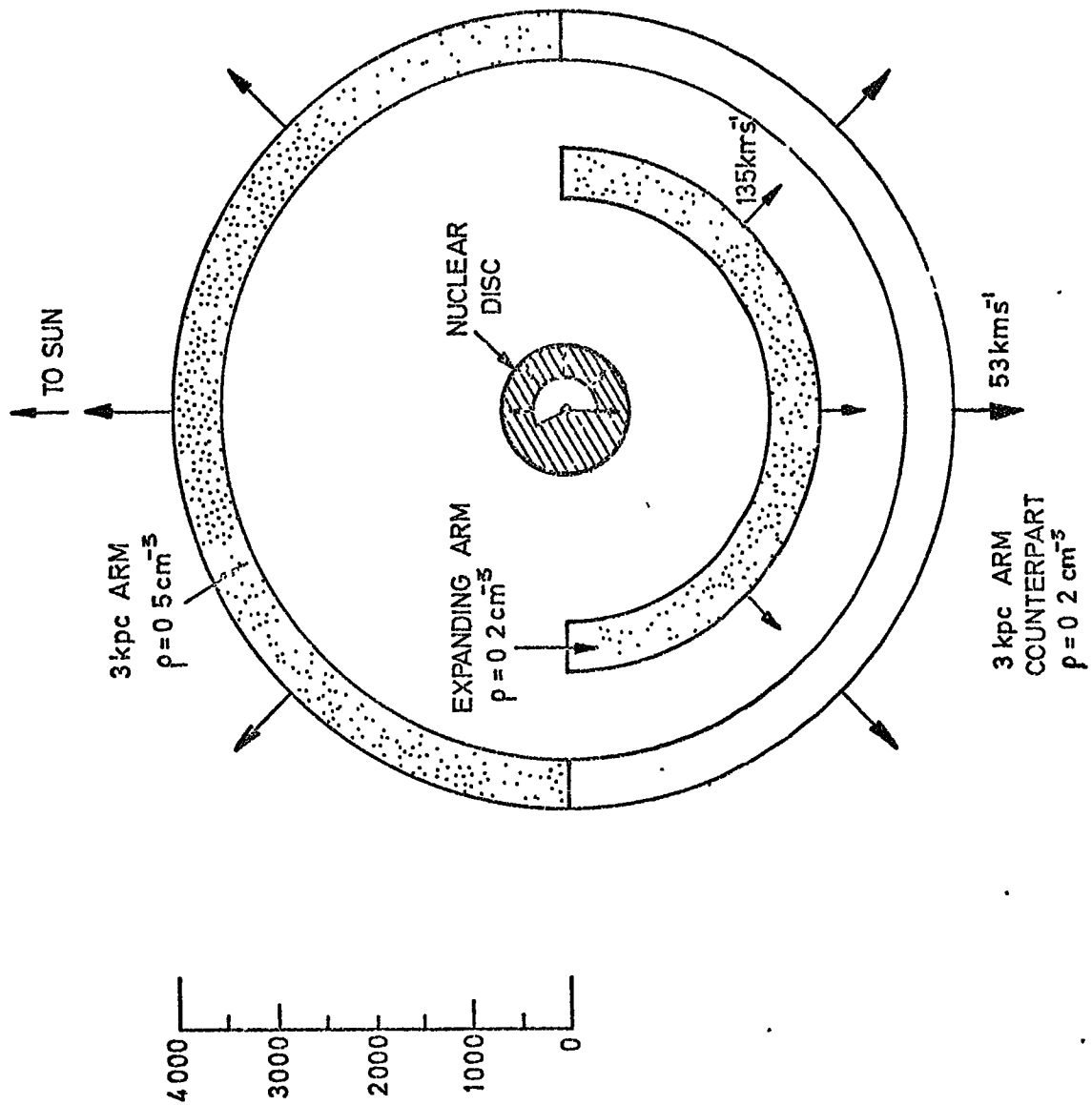
Figure 3.4: Schematic diagram by Sanders & Wrixon (1973) of the central region of the Galaxy.

The persistence of spiral structure in galaxies in spite of the differential rotation can be accounted for by the density wave theory. The spiral tracers are produced due to the compression of the gas as it traverses the density wave. In the Galaxy the rotational velocity of the wave pattern, independent of R, would be 13.5 km s^{-1} kpc^{-1} (Lin 1970). At the position of the sun the waves move with about half the speed of the gas and stars. It would take 3 to $10x10^7$ yr for the sun to traverse a density wave. The density wave theory requires an amplitude of variation of total mass surface density of 10% and an arm to interarm gas density ratio of 5.

3.3 Properties of the Interstellar Medium

3.3.1 Constituents of the Interstellar Medium

The interstellar medium consists of gas, dust and cosmic rays, the latter being considered, as far as the dynamics are concerned, as a hot tenuous gas.

The chemical composition, by weight, of the gas is, hydrogen 70%, helium 28%, heavier elements 2%. The commonly quoted figure for the gas density in the plane is 1 atom cm^{-3}. The gas is either neutral-atomic, ionised, or molecular. These states and their density variations are discussed below. The 'neutral gas' has a low level of ionisation ($\sim 10^{-3}$) which is due to cosmic rays and photo-ionisation of Ca and Na atoms. This level of ionisation is sufficient to 'freeze' the magnetic field, which is discussed in section 3.4, to the gas. The dust grains will also be charged and tied to the field. The dust grains have radii of the order of μm's and probably have

no direct effect on the cosmic radiation. The interstellar
flux of non-relativistic cosmic rays, which could be
important in heating and ionising the gas, cannot be
measured directly due to the shielding effect of the
solar wind.

3.2.2   The Neutral Gas

The neutral gas, which is predominantly hydrogen is
usually termed HI. Clark (1965) interpreted his observa-
tions of the 21 cm line in emission and absorption in terms
of relatively dense, cold clouds immersed in a hotter and
more tenuous intercloud medium. The clouds give sharp
$(2-3 \text{ km s}^{-1})$ emission profiles and sharper absorption
profiles when observed in front of distant radio sources.
From the brightness temperature and the optical depth,
temperature and column densities can be derived for the
clouds: typical values are 60-80K and 3×10^{20} atom cm^{-2}
respectively, although there is a very large scatter
around these values, e.g. temperatures between 10K and
more than 100K have been measured.

Interpretation of the 21 cm data interms of 'standard
clouds', (diameter 10 pc, density 8 cm^{-3}, (Spitzer 1968)),
is by no means unique. Ideally six space and velocity co-
ordinates of the gas are required to define a cloud while
in practice only the direction (ℓ and b) and the radial
velocity (V_r) are known. For a given direction the line
$T_B(V_r)$ is analysed into gaussian components and searches
are made for corresponding components in an adjacent
direction. Whether the 'clouds' are spheres, shells or

sheets is not known. A survey of the cloud size spectrum has been made by Heiles (1967). Heiles found many 'cloudlets' with radius between 1 and 4 pc and typical densities of 2 cm^{-3} in addition to 'standard' clouds.

In nearly all directions at medium and high latitudes, the intercloud medium gives broad ($\gtrsim$ 18 km s^{-1}) and weak (1-20 K) 21 cm emission profiles. Recent unpublished observations by Lazareff and Lequeux show that this medium is sometimes seen in weak absorption, and sometimes not, with spin temperatures ranging from a few hundred degrees to more than 2000 K. Pottasch (1972) has suggested that there may be intermediates between the very hot, low density intercloud medium and the cold clouds.

There have been few attempts to determine the temperature of the intercloud medium. From the width of the diffuse H_α and H_β lines observed in various directions, Reynolds et al (1973) find $T \lesssim 6000$ K. Hachenberg and Mebold (1972) and Baker (1973) find $T \approx 5000$ K using a statistical study of intercloud profiles in extended fields, though their uncertainties are large.

Falgarone and Lequeux (1973) give the following values for the gas in the region of the sun.

Density in the plane:

a)   for the intercloud medium, 0.16 cm^{-3}

b)   for a smoothed average of the cloud material, 0.29 cm^{-3}

Thickness ($2Z_{\frac{1}{2}}$) of the disk:

a)   cloud and intercloud, 360 pc

b)   cloud, 310 pc

c)   intercloud, 550 pc

The value of 0.45 cm^{-3} for the total density of neutral hydrogen is supported by satellite observations of the Lyman α profiles of stars. From measurement of absorption in the arm and interarm regions along the line of sight to strong radio sources the arm-interarm density ratio is estimated to be ~ 8.

For $4.5 < R < 10$ kpc the thickness of neutral gas is approximately constant at ~ 250 pc reducing to 100 pc closer to the centre. The thickness at R>10 kpc increases rapidly except for an anomalous region near $\ell = 140^\circ$ (Jackson and Kellman 1973). At high latitudes high velocity clouds are observed, most of which are approaching the plane. These have been interpreted as material that is either condensing from the intergalactic medium or that is falling back after having been ejected. Figure 3.5 shows the radial surface density distribution of HI which peaks at 13 kpc, contrasting strongly with the stellar distribution. The radial distribution of volume density of HI in the galactic plane peaks at $R \sim 8$ kpc, the decrease at R>8 kpc being compensated by the increasing thickness of the HI disk.

3.3.3 The Ionised Gas

Spheres of ionised hydrogen, termed HII regions, surround young, hot O and B type stars. The gas is ionised completely out to a sharply defined boundary. The radius of the sphere varies as $n_H^{-\frac{2}{3}}$. Table 3.2 shows the radii of HII regions surrounding different types of stars when $n_H = 1$ cm^{-3}. The HII regions are seen optically or as thermal radio sources, the temperature of the gas being 10^4K. It is possible that
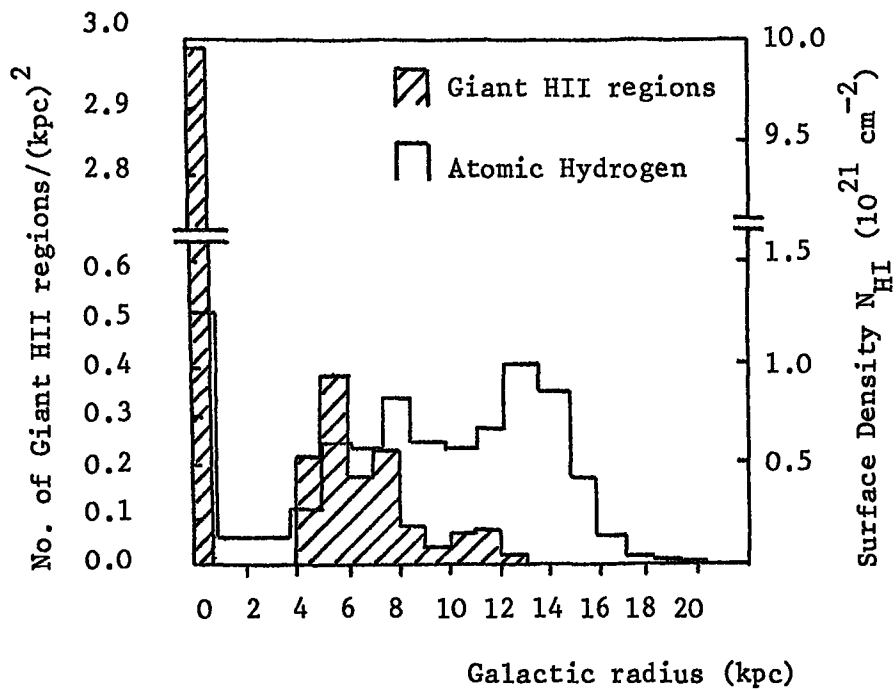
Figure 3.5: Distribution of neutral hydrogen and of giant HII regions as a function of distance from the galactic centre. Both diagrams give surface densities obtained by integration of the coordinate z, perpendicular to the Galactic Plane (Mezger, 1972).

Table 3.2 The radius of HII regions in relation to the
exciting star (Allen, 1973)

Star type	Radius (pc)
O5	100
O8	65
BO	35
B2	15
B5	3
AO	1

HII regions act as sources of most of the kinetic energy in the neutral gas.

'Giant' HII regions (those having a luminosity>4x that of the Orion Nebula) indicate sites of star formation and are useful as spiral tracers. The radial distribution of giant HII regions in the Galaxy is also plotted on figure 3.5.

The mean density of thermal electrons within a few kpc of the sun can be obtained from dispersion measures of pulsars whose distances are known, after discounting the effect of any HII region along the lineof sight. Estimates in the range $n_e = 0.025$ to 0.05 cm^{-3} have been obtained. The recombination rate of electrons and ions is roughly proportional to the square of the density, thus at equilibrium $n_e^2 \alpha n_{HI}$. The thickness of the electron disk should then be greater than that of the neutral gas by a factor of 2 or $\sqrt{2}$ respectively for an exponential or gaussian z-distribution of gas. This is consistent with estimated values of 800 to 1000 pc, derived from rotation measures of extragalactic radio sources (Falgarone and Lequeux, 1973).

3.3.4   Molecular Hydrogen

Molecular hydrogen (H_2) has no radio emission and it is therefore difficult to deduce how much is present in the Galaxy. Although H_2 cannot be directly photo-dissociated by radiation of longer wavelength than the Lyman limit there are indirect processes that limit n_{H2}/n_H in a standard cloud to 10^{-5}. In dense dust clouds, the interior is shielded

and the hydrogen could be mainly in the molecular form. Recent observations of emission from CO molecules imply a peak in the distribution of H_2 at $R \approx 5$ kpc, which may be very significant for the interpretation of γ-ray observations (Stecker and Solomon, 1974).

3.4 Measurements of Magnetic Fields in the Galaxy

3.4.1 Introduction

Magnetic fields have an important influence on the interstellar gas whilst at the same time the gas partly determines the structure of the magnetic field. The energy density of the cosmic radiation is comparable to that of the random motions of the gas and also to the energy density in magnetic fields. As cosmic ray nuclei are charged the strength and configuration of the magnetic field is very important in any discussion of the propagation of cosmic rays in the Galaxy. It is immediately evident that both a large scale field, associated with the spiral arm and interarm features, and small scale fields, associated with gas clouds, cloudlets and supernovae remnants, exist and can be measured in the Galaxy. As yet we have very little observational knowledge about any very small scale features in the magnetic fields of the galaxy, excepting the scale of the solar system cavity.

Information about the strengths and/or the orientations of large scale magnetic fields in the Galaxy has been obtained from measurements of interstellar polarization, galactic loops and spurs, Faraday rotation in both extra-galactic objects and pulsars, and the Zeeman Effect. Each

of these methods of measuring the magnetic field is dis-
cussed in the following paragraphs of this section. The
small scale features of the magnetic fields are discussed
in Chapter 6.

3.4.2   Interstellar Polarization of Starlight

Evidence for the existence of a magnetic field in
the Galaxy was first found in the polarization of starlight.
Chandrasekhar (1946) had predicted that, if Thomson scatter-
ing by free electrons plays an important role in the trans-
fer of radiation in the atmospheres of early type stars,
then the continuous radiation emerging from these stars
should be plane polarized. Hiltner (1949) whilst attempting
to verify Chandrasekhar's prediction, found that radiation
from other types of stars is also polarized and concluded
that the polarization was not associated with each individual
star but was an effect of the radiation passing through
interstellar space. The polarization is independent of
wave length.

The interstellar polarization is caused by dust grains
of asymmetric structure which are lined up by an interstellar
magnetic field. Davis and Greenstein (1951) assumed elong-
ated dust grains containing mostly compounds of hydrogen
with 12% by weight of iron and found that a magnetic field
strength of 10 μgauss was sufficient to align grains of size
10^{-5} to 3×10^{-5} cm to produce the observed ratio of polariza-
tion to colour excess, the short axis of rotation aligning
along the magnetic field lines. The theory predicts that
for uniform, weak magnetic fields with interstellar matter

of constant temperature and composition, the polarization is proportional to the square of the magnetic field strength. Henry (1958) developed similar models with the result that grains would be practically completely aligned for field strengths: >50 μgauss for graphite flakes, >30 μgauss for paramagnetic grains, 1.2 μgauss for ferrites and 0.013 μgauss for iron grains.

Davis and Greenstein (1951) concluded that the direction of the observed polarization vectors indicate a magnetic field parallel to the plane of the Galaxy over regions of several hundred parsecs, being almost uniform along the spiral arm and perhaps making random whirls. This field orientation is consistent with polarization studies of 92 stars by Hoag (1953) and more recently by Seymour (1969) and Verschuur (1970) who analysed 550 stars.

However, studies of the optical polarization data of the local arm by Ireland (1961) and Mathewson (1968), figure 3.6, indicate the presence of a helical field winding itself around the spiral arm. Mathewson's interpretation of a helical field assumes that the spurs of non thermal radio radiation, corresponding to the highly polarized regions at high galactic latitude are part of the helical field structure. There is evidence(Berkuijsen (1973)) that the spurs are old supernovae remnants. Spoelstra (1973) has attempted to derive the direction of the large scale magnetic field from its interaction with the spurs assuming that they are supernovae remnants. Spoelstra's results are shown in figure 3.7.
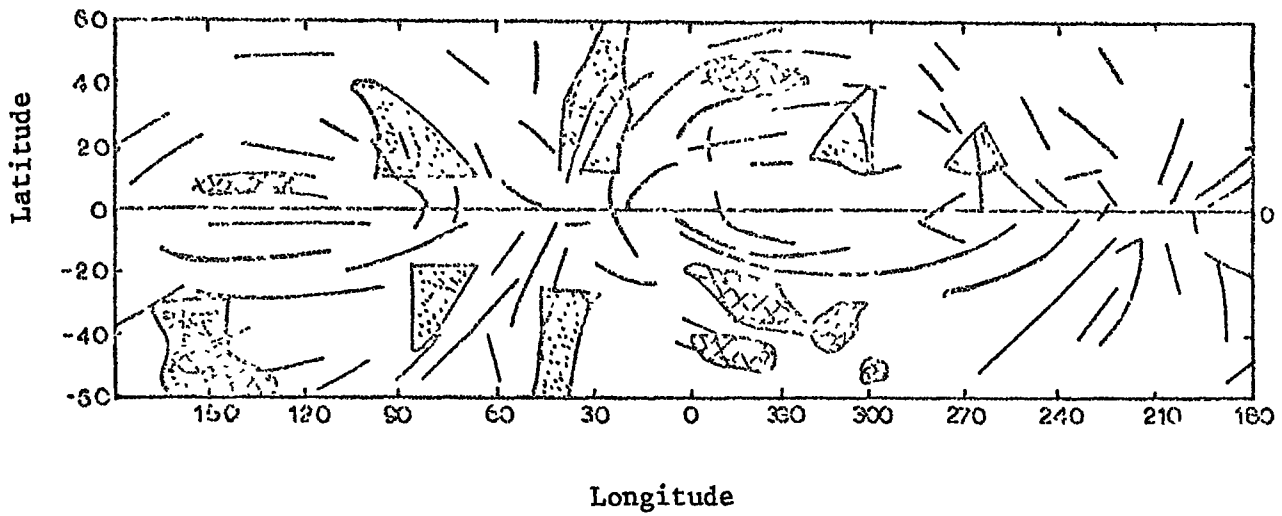
Figure 3.6: "Flow patterns" of E-vectors of optical

polarization measurements.

Radio spurs are shaded.

Hatched areas are strongly polarized at 408 MHz.

(Mathewson, 1968).
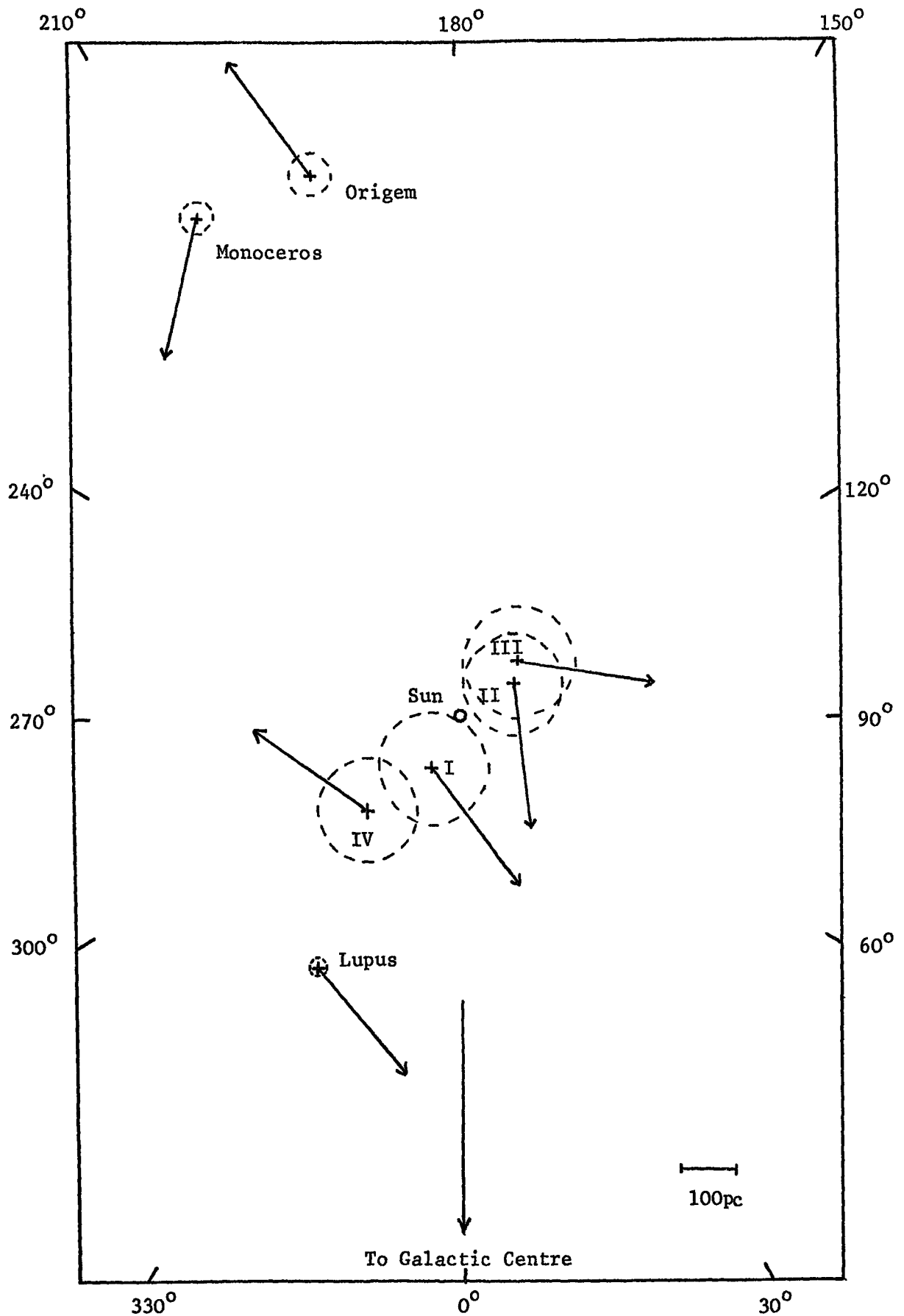
Figure 3.7: Spatial orientation of 7 Galactic Loops projected on the Galactic plane. The arrows indicate the direction of the Galactic magnetic field for each loop.

(Spoelstra, 1973)

To estimate the magnitude of the magnetic field strength from optical polarization studies is very difficult. Spoelstra (1973) gives a field strength of ~ 5 μgauss from the loops and spurs.

3.4.3 Faraday Rotation: Extragalactic sources

When a plane polarized radio wave of wavelength λ traverses an ionized medium in which there is a magnetic field, the plane of polarization undergoes a rotation through an angle, θ, given by:

$$\theta = 8.1 \times 10^{11} \lambda^2 \int H_\ell \, n_e \, d\ell$$

Where λ is expressed in cm, H_ℓ is the longitudinal component of the magnetic field in gauss, n_e is the electron density of the medium in cm^{-3} and $d\ell$ is the element along the line of sight in pc, in which the rotation occurs. The magnetic field is determined by measuring the observed position angle of the plane of polarization of the radiation from a given radio source. This is done for several wave lengths, the resultant plot of θ against λ^2 giving the rotation measure (R.M.), θ/λ^2. Typical values of rotation measure lie between 10 and 100 rad m^{-2}. A positive value of R.M. indicates a line of sight component of the magnetic field directed towards the observer. A knowledge of n_e and ℓ allows the magnitude of the magnetic field intensity to be found. It is necessary to know the region in which the Faraday rotation occurs and the electron density in that region.

One would expect some Faraday Rotation to be produced in the ionosphere. However, since the observed R.M. are about a hundred times greater than the R.M. expected from

the ionosphere alone and the position angles show little
variation at different times of day or night, the effect
due to the ionosphere may be assumed to be insignificant
(Cooper and Price, 1962).

Seielstad et al (1964) find a pronounced variation of
R.M. of extragalactic objects with galactic latitude imply-
ing that the variation is produced mainly in the Galaxy.
However, some sources which are only a few degrees apart
show very different R.M. which may indicate large intrinsic
Faraday rotations in the sources (Gardner et al, 1969).

Figure 3.8 shows a summary of the R.M. of 195 extra-
galactic sources made by Mitton (1972). These data provide
a more uniform coverage of the sky than any previous analyses.
The area of the circle is proportional to the magnitude of
the R.M. Open circles indicate a negative R.M. equivalent
to a field away from the observer. Assuming that most of
the rotation is galactic and that the electron density in
the Galaxy is known, a value for the mean line of sight
magnetic field strength to the edge of the Galaxy can be
found. However, it is probable that the electron density
is not uniform in the Galaxy, resulting in an uneven sampl-
ing of the Galaxy's magnetic field, thus although a value of
$\int N_e H_\ell \, d\ell$ can be found it is not a reliable method for
obtaining magnetic field strengths. (However, if N_e is
taken as 0.05 cm^{-3}, a value of $H_\ell \sim 5$ µgauss is obtained).

Interpretation of the Faraday rotation in extragalactic
objects in terms of magnitude and direction of the magnetic
field is difficult, though the measurements seem to indicate
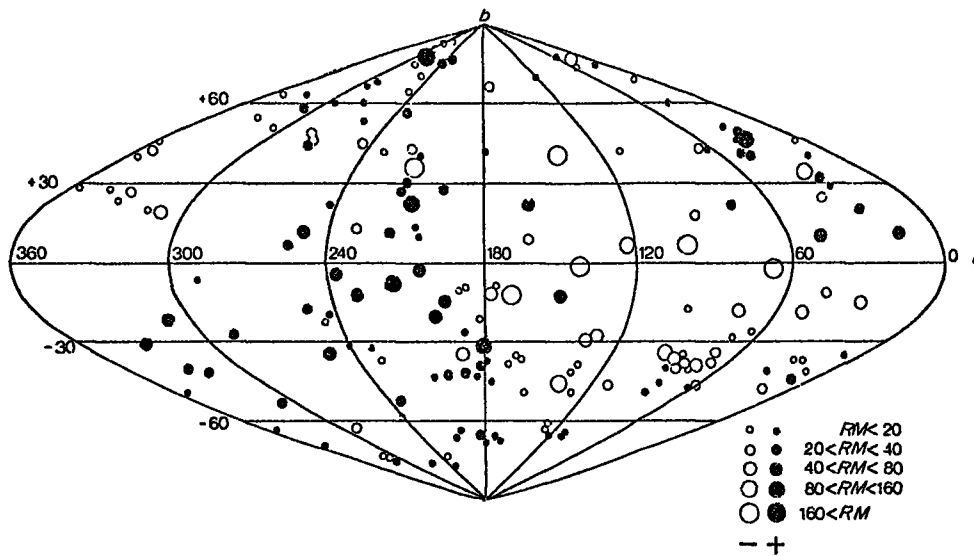
Figure 3.8: The galactic distribution of the rotation measures of 192 extragalactic radio sources.

a longitudinal field directed along the local spiral arm towards $\ell \sim 90°$ with perturbations which may be in the form of a helical component or possibly Spoelstra's supernova remnants.

3.4.4   Faraday Rotation: Pulsars

The problem of estimating the magnetic field strength from R.M. of extragalactic objects due to a lack of knowledge of the electron density is removed when pulsars are used as the source of polarized radio emission. J. G. Davies et al (1968) showed that the arrival time, t, of a radio pulse from a pulsar is a function of frequency due to the passage of the pulse through an ionized medium. For a uniform plasma

$$\frac{dt}{d\nu} = -\frac{8100}{\nu^3} D \qquad \text{sec Hz}^{-1}$$

where D is the dispersion measure in pc cm^{-3} and is equal to the line integral of the electron density to the source;

$$D = \int N_e \, d\ell \qquad pc \; cm^{-3}$$

The mean line of sight component of the magnetic field between the pulsar and the sun, weighted by the thermal electron density is given by

$$\bar{H}_\ell = \frac{\int N_e H_\ell \, d\ell}{\int N_e \, d\ell}$$

Figure 3.9 shows the line of sight magnetic field components in the direction of 38 pulsars as compiled by Manchester (1974). Manchester interprets the results from pulsar observations as being consistent with a simple longitudinal magnetic field, with an average field strength
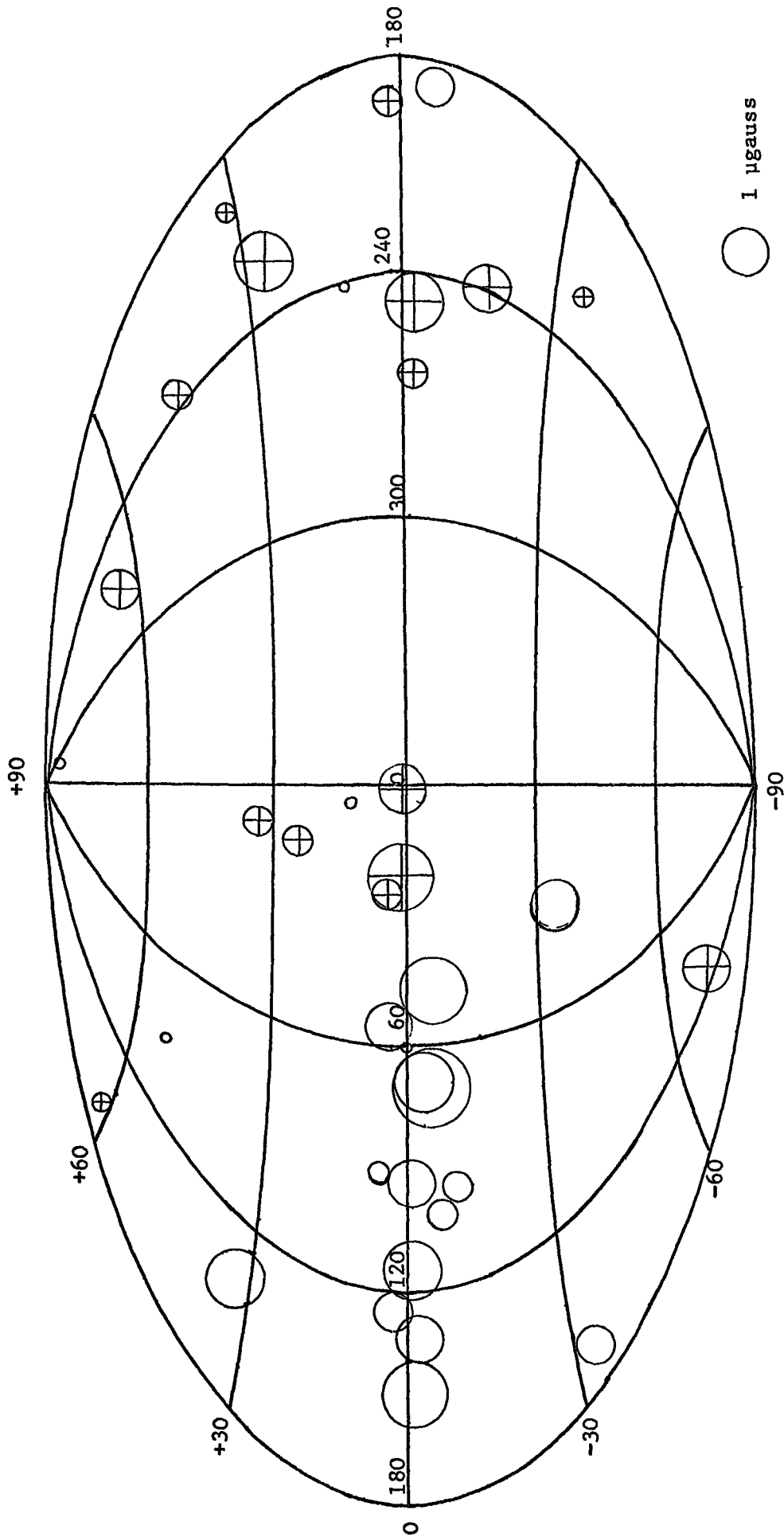
Figure 3.9: Line of sight magnetic field components in the directions of 38 pulsars.

For fields of >0.1 μgauss the area of the circle is proportional to the magnetic field strength. For fields directed towards the observer a plus sign is enclosed.

(Manchester, 1974).

between 2 and 3 µgauss, directed towards $\ell = 90^o$.

3.4.5   The Zeeman Effect

When the Zeeman splitting of the 21 cm hydrogen line was first suggested as a method of determining the magnetic field strength and direction (Bolton and Wild, 1957), it seemed that it would provide a direct measurement of the line of sight magnetic field. The field strengths found are independent of dust, relativistic or thermal electron distributions and represent the field at a particular place. This technique also shows the direction of the line of sight components of the field towards or away from the observer.

Measurements can only be made using the absorption spectra of intense galactic radio sources which result in a restricted sampling of the magnetic field. The complexity of the spectra makes estimation of the field strength difficult. Verschuur (1969) postulated that neutral hydrogen clouds contained "frozen in" magnetic fields and suggested that the magnetic field may be stronger in the clouds as a result of amplification by cloud contraction, proposing that the greater the density of the cloud the stronger the field within it. If a cloud contracts isotropically its density is proportional to $radius^{-3}$ and the field strength is proportional to $radius^{-2}$. The magnetic field strength would therefore be proportional to $density^{2/3}$. Verschuur (1970) attempts to show that the available data give a reasonable fit to this model, figure 3.10, and by extrapolating back to the average interstellar hydrogen density he finds a mean interstellar magnetic field strength of 1 to 3 µgauss.
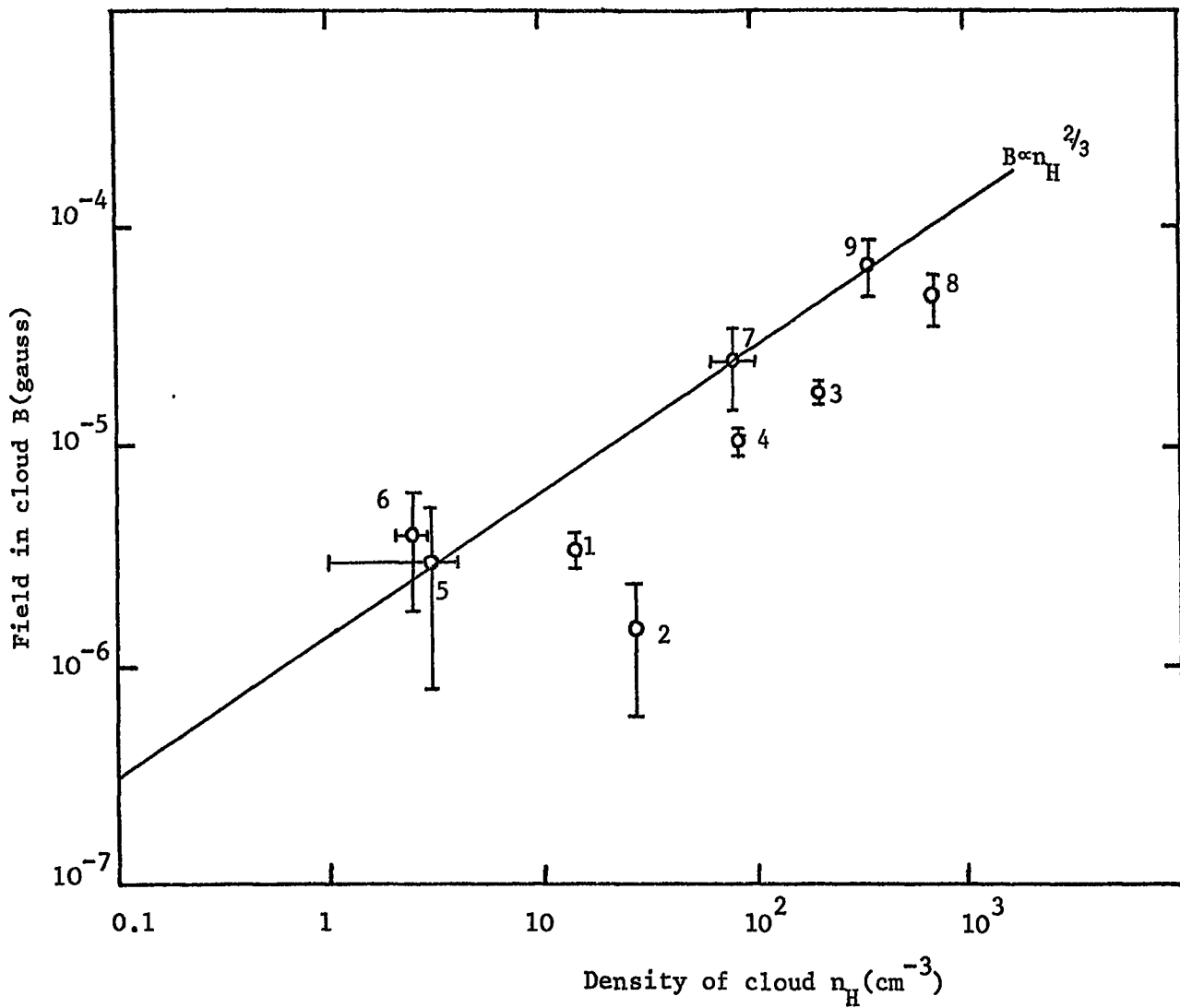
Figure 3.10: Magnetic Fields in neutral hydrogen clouds as a function of their density. (Verschuur 1970).

	Direction	ℓ	b
1.	Tau A	185°	-6°
2.	Tau A		
3.	Cas A	112°	-2°
4.	Cas A		
5.	Cyg A	76°	-16°
6.	Cyg A		
7.	M17	15°	-1°
8.	Orion A	209°	-19°
9.	Orion A		

3.4.6   Conclusions

Table 3.2 gives a summary by Lequeux (1974) of the methods of measurement of the galactic magnetic field and the direction of the field obtained by each method.

The pulsar data is consistent with a large scale longitudinal magnetic field with a strength of a few µgauss. The extragalactic source rotation measures are not inconsistent which such an interpretation, though the interpretation of the optical polarization in terms of a helical field (Mathewson, 1968) is not consistent with a longitudinal field. If the spurs and loops associated with the helical field are confirmed as large supernovae remnants it could be that the helical field has been fitted primarily to an irregularity in the field rather than to the uniform component.

Table 3.3   A summary of the direction of the large scale
magnetic field in the Galaxy for the different
types of measurement, compared to the direction
of the local spiral arm (Lequeux, 1974).

Method	Longitude of field Direction	Distance of measurement from sun
Optical Polarisation	80° (+ local helical field?)	300-4000 pc
Spurs and loops	40°	< 300 pc
Faraday Rotation of Pulsars	$90^o \rightarrow 110^o$	300 pc (mean)
Faraday Rotation of Quasars	110°	$\leqslant$ 2-3 kpc
Local arm direction		
gas	60°-80°	$\sim$ 1 kpc
stars	50°	$\sim$ 1 kpc

References

Allen, C. W., 1973, Astrophysical Quantities, (Athlone Press)

Baker, P. L., 1973, Astron. Astrophys., 23, 81

Berkuijsen, E., 1973, Astron. Astrophys., 24, 143

Bolton, J. G. and Wild, J. P., 1957, Astrophys. J., 125, 296

Bulanov, S. V. and Dogel, V. A., 1974, Astrophys. Space Sci.,
    29, 305

Chandrasekhar, S., 1946, Astrophys. J., 103, 551

Clark, B. C. G., 1965, Astrophys. J., 142, 1398

Cooper, B. F. C. and Price, R. M., 1962, Nature, 195, 1084

Davies, J. G. et al., 1968, Nature, 217 910

Davis, L. and Greenstein, J. L., 1951, Astrophys. J., 114, 206

Falgarone, E. and Lequeux, J., 1973, Astron. Astrophys., 25, 253

Gardner, F. F. et al., 1969, Aust. J. Phys. 22, 107

Hachenberg, O. and Mebold, U., 1972, Communication to the
    1st European Conf. of the I.A.U.

Heiles, C., 1967, Astrophys. J. Suppl. Ser., 15, 97

Henderson, A. P., 1967, Unpublished Ph.D. dissertation,
    University of Maryland

Henry, J., 1958, Astrophys. J., 128, 497

Hiltner, W. A., 1949, Astrophys, J., 109, 471

Hoag, A. A., 1953, Astron. J., 58, 42

Ireland, J. G., 1961, Mon. Not. R. Astr. Soc., 122, 461

Jackson, P. D. and Kellman, S. A., 1973, Astrophys. J., 190, 53

Kerr, F. J., 1970, 'Spiral Structure of our Galaxy', IAU Symp.
    38, Ed. by W. Becker and G. Contopoulos (de Reidel)

Lequeux, J., 1969, 'Structure and Evolution of Galaxies',
    (Gordon and Breach)

Lequeux, J., 1974, 'The Interstellar Medium', Ed. K. Pinkau
    (de Reidel)

Lin, C. C., 1970, 'Spiral Structure of our Galaxy', IAU Symp.
38, Ed. by W. Becker and G. Contopoulos (de Reidel)

Manchester, R. N., 1974, Astrophys. J., 188, 637

Mathewson, D. S., 1968, Astrophys. J., 153, L47

Mezger, P. G., 1972, Course on Interstellar Matter, Saas Fee

Mitton, S., 1972, Mon. Not. R. Astr. Soc., 155, 373

Oort, J. H., 1965, 'Galactic Structure', Ed. by A. Blaaw and
M. Schmidt, (University of Chicago), 455

Pottasch, S. R., 1972, Astron. Astrophys., 20, 245

Reynolds, R., Roesler, F. and Scherb, F., 1973, Astrophys. J.,
179, 651

Sanders, R. H. and Wrixon, G. T., 1973, Astron. Astrophys.,
26, 365

Seielstad, G. A. et al., 1964, Astrophys. J. 140, 53

Seymour, R. A. H., 1969, Mon. Not. R. Astr. Soc. 142, 33

Spoelstra, T. A. Th., 1973, Astron. Astrophys., 24, 149

Spitzer, L., 1968, Diffuse Matter in Space (Interscience)

Stecker, F. W. and Solomon, P. M., 1974, 8th ESLAB Symp.
(part II), Contexts and Status of γ-ray Astronomy,
Frascati

Verschuur, G. L., 1969, Astrophys. J., 155, L155

Verschuur, G. L., 1970, 'Interstellar Gas Dynamics', IAU Symp.
39, (de Reidel), 150

Vershuur, G. L., 1973, Astron. Astrophys. 27, 73

Wannier, P. Wrixon, G. R. and Wilson, R. W., 1972, Astron.
Astrophys., 18, 224

Weaver, H. F., 1970, 'Spiral Structure of our Galaxy', IAU Symp.
38, Ed. by W. Becker and G. Contopoulos (de Reidel)

Chapter 4   Theories concerning the origin and the propaga-

tion of cosmic rays in the Galaxy

4.1 Introduction

Assuming that most of the cosmic ray sources are in the

Galaxy, the following three questions need to be answered.

1)   What is the nature of the cosmic ray sources?

2)   How are the cosmic rays accelerated to relativistic

velocities?

3)   How do they propagate through the Galaxy?

These questions still remain unanswered, although

several viable theories have emerged from the wealth of

observational data that has been collected over the last

few years. In this chapter answers that have been suggested

for these three questions are discussed, though discussion

of the third question continues throughout the remaining

chapters of this thesis.

4.2 The Nature of Cosmic Ray Sources

Bradt and Peters (1950) discovered that the cosmic

rays entering the Earth's atmosphere were made up in part

of nuclei heavier than the proton. From their measured

charge spectrum Bradt and Peters deduced that the ratio

of heavy elements to light elements was greater in the

cosmic radiation than in the solar system abundances and

that the flux of Li, Be and B could be produced by the

spallation of the heavy elements. These discoveries

coincided with the work of Hoyle (1949) on nucleosynthesis

in which he proposed that most of the heavy nuclei in the

Galaxy were formed in the interior of stars and then distri-

buted throughout space when the stars exploded. It was
recognised that the measured abundances of the cosmic rays
would reflect the chemical composition of their sources
and would perhaps give some clues to their acceleration
mechanism.

However, calculation of the primary abundances (i.e.
the abundance just after acceleration) of the cosmic rays
involved a detailed knowledge of the spallation processes
in interstellar space and of the composition of the cosmic
radiation incident on the Earth which was not complete in
the early fifties. When more extensive data on the spalla-
tion cross-sections became available, coinciding with better
charge resolution of the incident cosmic rays, Beck and Yiou
(1968) calculated the primary abundances of some of the
heavy elements, assuming that all the particles traversed
the same amount of interstellar matter.

Since that time many more detailed calculations of the
primary composition have been undertaken, especially by
Shapiro and his co-workers. In their most recent calculation,
Shapiro and Silberberg (1974) have compiled abundance data
from experiments with good charge resolution and have applied
the exponential path length distribution discussed in Chapter 2.
Their results, showing the primary abundances, together with
information about the amount of each element produced by
spallation, are given in figure 2.9.

Assuming that there are no preferential acceleration
effects, the primary abundances calculated by Shapiro and
Silberberg should match the composition of the sources

before acceleration. The overabundance of the heavy elements in the cosmic radiation seems to indicate that their sources must be well evolved objects. For some time it has been thought that supernovae could be the sources of cosmic rays in the Galaxy (Ginzburg and Syrovatskii 1964), as they satisfy the requirement of being well evolved and can also provide enough energy to accelerate the cosmic rays. Recent calculations by Arnett and Schramm (1973) indicate that the large $(C + O/Fe)$ ratio in the cosmic ray sources eliminates supernovae of mass < 8 $M_\odot$ since such supernovae will have burned all their C and O to Fe. Arnett and Schramm suggest that massive supernovae with mass > 8 $M_\odot$ are likely cosmic ray source candidates since they do not burn up all their C and O explosively. The event rate of these supernovae is about the same as for supernovae with 4 $M_\odot < Mass < 8$ $M_\odot$ which is adequate, in terms of energy, to supply the observed cosmic ray flux. These supernovae also leave behind a small dense iron enriched remnant of mass ~ 1.4 $M_\odot$, which could become a pulsar providing an electromagnetic acceleration mechanism and possibly an additional source of iron.

These conclusions may be modified if effects due to preferential acceleration are considered. Recent analysis (Cassé and Goret, 1973, Havnes, 1973) shows that the ratio between the cosmic ray abundance and the universal abundance of each element exhibits a fair degree of correlation with the first ionization potential of the element (figure 4.1). If this correlation is real, it implies that elements with small first ionization potentials, which are more easily

Figure 4.1: Overabundance factor in cosmic ray sources,

as compared to universal matter, plotted as a function
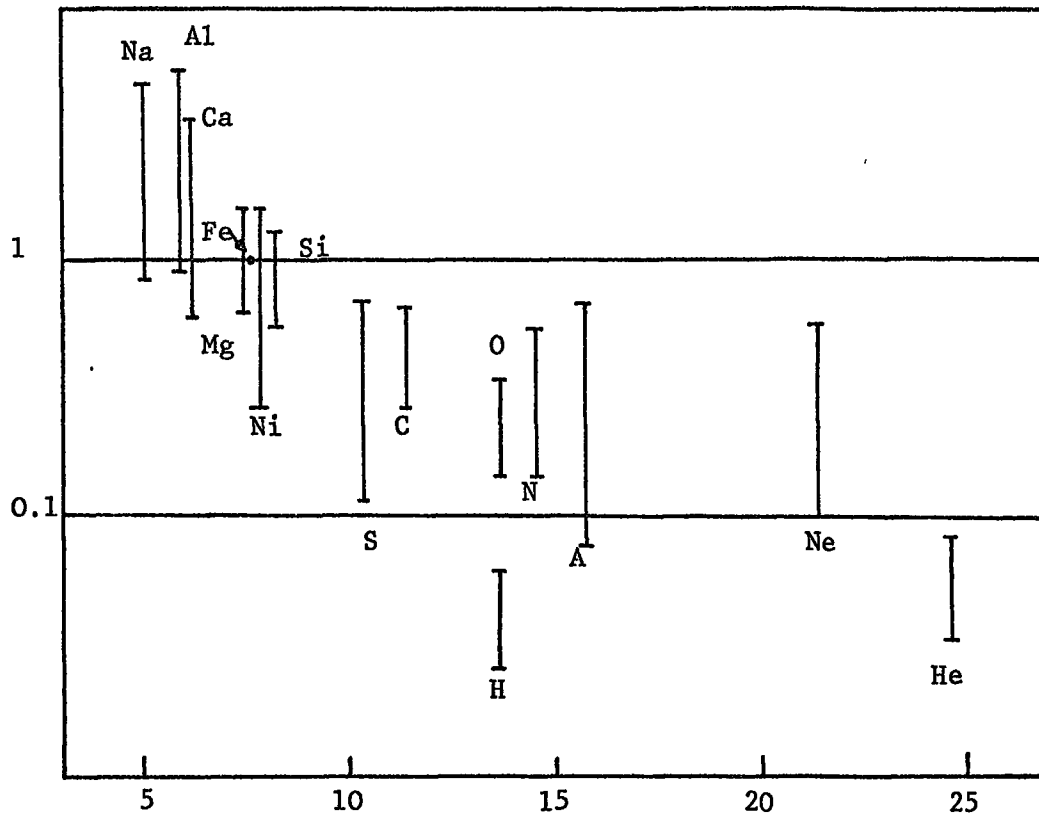
of first ionisation potential of each element (Cassé and

Goret, 1973).

ionized, are accelerated preferentially to those with larger first ionization potentials, suggesting that the acceleration mechanism of cosmic rays is electromagnetic rather than explosive in nature.

The hypothesis of preferential acceleration may be tested by considering the isotopic abundances in the cosmic rays and also by looking at elements with similar first ionization potentials. However, there is very little reliable data regarding cosmic ray isotopes so these tests must be a study for the future.

In the previous chapter the possibility was put forward that the expanding gas in the central region of the Galaxy was due to an explosion in the central region 10^7 yr ago. Any such explosion would probably be a possible source of cosmic rays. Ginzburg and Syrovatskii (1964) argue that the energy required by the explosion, if it were to be the source of cosmic rays, would be more than 3×10^{58} ergs. This is of the same order of magnitude as the energy required to give the gas its kinetic energy of expansion.

However, large explosions at the Galactic Centre may be ruled out as the origin of the cosmic radiation on perhaps three counts.

a) The age of the cosmic rays would be $\sim 10^7$ yr, which is the upper limit to the age of the cosmic rays given by the present measurements of Be^{10} in the cosmic rays.

b) Results for the change in the cosmic rays flux over the last 10^7 to 10^8 yr are not good, but do not indicate any great changes in the flux expected if the origin of the

cosmic rays was in periodic explosions at the Galactic Centre. One might also expect to see a measurable decay in the cosmic ray flux over the last 10^6 years due to leakage from the Galaxy.

c) If a simple diffusion model for the propagation is assumed, the expected anisotropy of the cosmic rays would be $R/c\,\tau$, where R is the distance to the source and τ is the age of the cosmic rays. Assuming a best case of $R=10^4$ pc and $\tau=10^7$ yrs gives anisotropy of 3×10^{-3} which is higher than the observed anisotropy.

Classes of possible cosmic ray sources may be considered in terms of the parameter δt, which is defined as the time between a cosmic ray nucleus being nucleosynthesised and the time that it is accelerated to relativistic velocities. Values of δt lying in three ranges are considered below.

(i) <u>$\delta t = 0$</u>

$\delta t = 0$ means that the acceleration of the cosmic rays would take place in a hydro-dynamic explosion, i.e. the explosion would be the source of both nucleosynthesis and acceleration. In this case the chemical composition of the cosmic ray sources, derived from the observations by subtracting spallation effects, should be identical with the ejecta of the source of explosive nucleosynthesis being considered. If supernovae explosions are considered the distribution of heavy elements expected is likely to be quite "exotic" and is therefore unlikely to present the similarity between the cosmic ray source abundances and the universal abundances that is observed.

Consider a specific example, that of the r-process elements. The ratio of r/s elements in the cosmic ray sources is apparently larger than the ratio in universal abundances, though the uncertainties are large. From these data various workers conclude that the cosmic rays come from supernovae, because the r-process indicates explosive nucleosynthesis. However, consider what happens when the r-process takes place. A large number of neutrons are required since the rate of neutron capture by the heavy elements in the star core must be faster than the decay rates of the newly formed nuclei, which can occur on the scale of seconds. The required density of neutrons would be ~1 to 10^3 g cm^{-3} and in such situations a large fraction of all the Fe would be transformed to heavier elements giving a r/Fe ratio of order one. The observed ratio r/Fe in the cosmic radiation is ~10^{-6} which is inconsistent with the above argument. A similar conclusion may be drawn from the ratio N/C+O which makes it difficult to believe that the cosmic rays are just the ejecta from any kind of explosive situation.

(ii) $\delta t \gg 10^6$ yr

In models with $\delta t \gg 10^6$ yrs the original source of the matter accelerated is completely forgotten in the composition of the cosmic rays. Models in this range of δt include those of Fermi acceleration in the interstellar medium and origin in White Dwarfs. The chemical composition of the cosmic rays expected from a Fermi acceleration model would be very similar to that of the universal matter, the differences

being explained in terms of preferential acceleration.

Measurements of interstellar matter, by satellites such as Copernicus, have revealed that some elements are heavily depleted compared to universal matter. Calcium is particularly underabundant, the ratio of Ca/H in the interstellar medium to Ca/H in universal abundance is $\sim 10^{-3}$. Magnesium shows a similar behaviour having a ratio of ~ 0.1 between the interstellar medium and universal abundances. It is found that all the elements which are depleted in this way are the elements which are good at making stones on the earth, and the depletion in interstellar space is explained in terms of the missing matter making up dust grains etc.

In the cosmic ray source abundances the abundance of Ca is small and no real conclusions can be drawn as to its presence in the cosmic ray sources after subtracting spallation effects. However for Mg the situation is much clearer, the abundance of Mg in the cosmic ray sources showing no depletion relative to the universal abundance.

This point works against the idea that the cosmic rays are just accelerated from ordinary interstellar matter (Reeves 1974).

(iii) $o \leq \delta t \leq 10^6$ yr

The reason for choosing an upper limit of 10^6 yr is because 10^6 yr is essentially the time taken by a supernova to explode; go through the remnant stage and disappear, mixed with interstellar matter. In this type of model acceleration takes place in an expanding supernova remnant.

There is a relationship between the supernova and the cosmic rays though not at the moment of explosion. For example, it is known that the Crab Nebula is accelerating electrons to give the synchrotron emission and also because of their energy losses the electrons could not have been accelerated at the moment of explosion.

As the supernova remnant expands, the ejecta of the explosion mix with the interstellar medium and it is this mixture that is accelerated in the remnant, accounting, at least qualitatively, for the quasi similarity of the cosmic ray and universal abundances. If the ratio of matter mixed to ejecta is large quasi similarity with small differences is achieved. Reeves (1974) has illustrated this point with a cook-book for galactic cosmic rays (figure 4.2). The composition of the ejecta and the number of units of interstellar matter required have been invented to fit the cosmic ray data. The real game, however, is to go backwards from the cosmic ray data and the composition of the interstellar medium to find the composition of the ejecta.

Reeves (1974) concludes that the models with $0 \leq \delta t \leq 10^6$ yr are the most plausible to fit the data on the composition of cosmic rays.

### 4.3 Possible Acceleration Mechanisms for Cosmic Rays in the Galaxy

The amount of energy involved in the acceleration process may be estimated from the energy density and lifetime of the cosmic rays in the Galaxy. The energy density of the cosmic ray flux near the Earth is ~ 1 eV cm^{-3}. Assuming this to be

(a) explode a S.N. in the Galaxy

(b) start a central pulsar

(c) Wait 10^2 to 10^3 yr for remnant to develop: one unit

of stellar exotic ejecta is then mixed with ~10

unit of interstellar gas

50% CNO		73% H		72% H
30% Mg Si	**+**	25% He	**=**	18% He
20% Fe		1% CNO		5% CNO
		0.3% Mg Si		3% Mg Si
		0.1% Fe		2% Fe

One unit of   Ten units of   G.C.R.

ejecta   interstellar   "sources"

matter
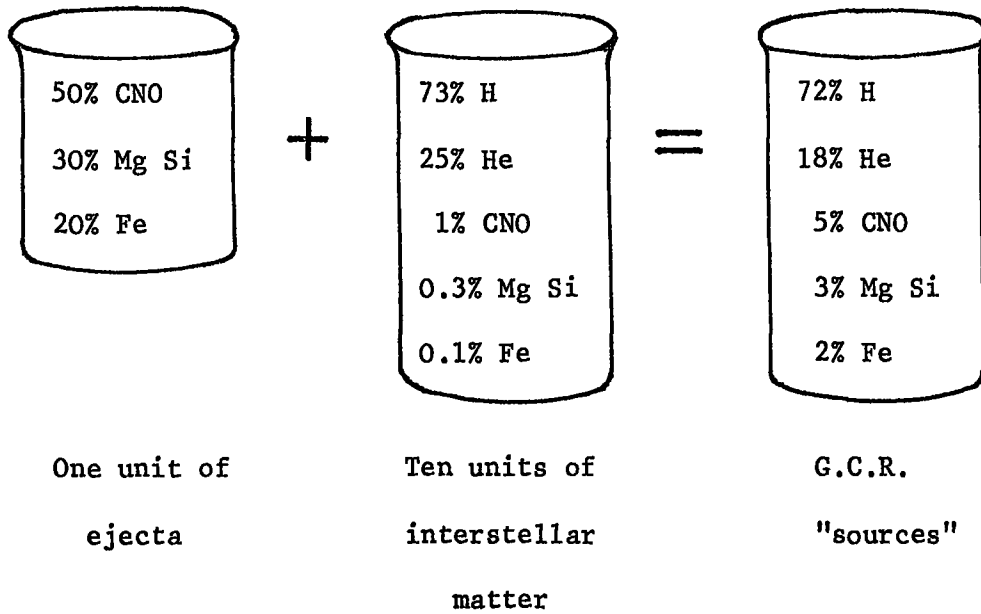
(d) accelerate with pulsar wave.

Figure 4.2: A cook-book for Galactic Cosmic Rays (Reeves, 1974).

the average energy density of cosmic rays throughout the Galaxy and assuming the cosmic rays are confined to a disk of radius 15 kpc and thickness 1 kpc, the total energy in the cosmic rays is $\sim 2 \times 10^{67}$ eV. If an escape time from the confining region of 3×10^6 yr is adopted, the total power required by the sources to maintain the present energy density is $\sim 10^{49}$ erg yr^{-1}. If supernovae explosions are assumed to be the source of cosmic rays and an average rate of 1 supernova per 30 yr is taken, then $\sim 3 \times 10^{50}$ ergs from each explosion must be used in the acceleration process. A type II supernova releases on average $10^{51} - 10^{52}$ ergs.

The means by which a supernova could possibly accelerate particles to relativistic velocities are still not fully understood, although it seems plausible that they could be accelerated electromagnetically in the expanding shell produced by the remnant. Colgate and White (1966) have carried out hydrodynamic analyses of supernovae explosions to investigate the possibility of direct acceleration of cosmic rays by the shock wave produced in the explosion. By assuming a particular stellar model they predicted a cosmic ray energy spectrum in good agreement with observations although the efficiency of the process is very low, $\sim 10^{-3}$, since most of the energy goes into mass motions of the gas at sub relativistic velocities.

Gull (1973) has considered the evolution of a supernova remnant and has shown that there exists a more plausible location for the acceleration process. The remnant slows down due to the 'snow plough' effect as it collects an increasing amount of interstellar matter in front of it.

The denser material of the supernova remnant penetrates the layer of interstellar matter by means of the Rayleigh-Taylor instability. The resulting turbulence amplifies the magnetic field within sections of the shell and there-by accelerates the cosmic rays. The efficiency of this process is $\sim 10^{-2}$ which is high enough to account for the observed cosmic ray flux and also, the interpenetration of the remnant and the interstellar medium allows the required degree of mixing, discussed in the previous section, to take place. Particles can be accelerated up to energies $\sim 10^{18}$ eV by this process (Gurevich and Rumyantsev 1973).

An alternative source of cosmic ray particles, especially of the F_e component, could be pulsars. Goldreich and Julien (1969) pointed out that the electric field induced by the rotating magnetic field is strong enough to pull charged particles from the surface of the neutron star leading to the formation of a dense magnetosphere. Unfortunately, the presence of a magnetosphere complicates calculation of the electromagnetic fields as they cannot be described by the vacuum-dipole solution. However, if it is assumed that the field at large distances from the pulsar, where the density of the magnetosphere is negligible, is that of a rotating dipole, then it is possible to calculate the trajectory of a test particle. Gunn and Ostriker (1969) investigated the interaction between test particles and the low frequency electromagnetic waves that are produced by oblique rotators and concluded that the test particles could be accelerated up to energies of $\sim 10^{21}$ eV when the pulsar is young and rotating very rapidly.

Karakula et al (1974) have calculated the form of the cosmic ray spectrum expected from pulsars using the model of Ostriker and Gunn for pulsar characteristics and experimental data on pulsar frequencies. Karakula et al suggest that pulsars could be the dominant source of cosmic rays in the energy range $10^{14} - 10^{16}$ eV and that the change of slope in the cosmic ray spectrum at 3×10^{15} eV may be explained in terms of the process by which pulsars lose their energy.

It is possible that some cosmic rays are accelerated by the Fermi process (Fermi 1949, 1954). Any constriction in the interstellar magnetic field, where the field increases from B to B_{max} will reflect all incident particles with a pitch angle, θ, such that:

$$\sin^2 \theta > B/B_{max}$$

When a particle travelling with velocity $\underline{v}$ is reflected from such a mirror, moving with velocity $\underline{u}$ ($u \ll v$), the particle experiences a gain in energy given by

$$\Delta E = \frac{-2E(\underline{u} \cdot \underline{v})}{c^2}$$

The probability of an approaching collision is greater than that of an overtaking one, therefore there will be a net gain in energy of particles propagating in a region of randomly moving magnetic irregularities. Fermi showed that such a situation could produce a power-law spectrum with an integral exponent, $-tc^2/\tau V_A^2$, where t is the mean time between collisons, τ is the cosmic ray lifetime in the accelerating region, c is the velocity of light and V_A is the Alfvén velocity.

In the interstellar medium the Alfvén velocity is $\sim 10^6$ cm s^{-1} and the mean cosmic ray lifetime is $\sim 3 \times 10^6$ yr. The observed exponent of -1.7 requires a mean time between collisions of $\sim 6 \times 10^{-3}$ yr which at relativistic velocities corresponds to a collision mean free path of 2×10^{-3} pc, several orders of magnitude less than the observed length scales of irregularities in the galactic magnetic field of about 10 to 30 pc. Furthermore this process is unable to accelerate particles to energies $> 10^{12}$ eV where their gyro-radii are greater than their mean free path for collision. It is therefore unlikely that Fermi acceleration in the interstellar medium is the dominant method of accelerating cosmic rays although it may be dominant in smaller scale regions of turbulence such as supernova envelopes.

4.4 Cosmic Ray Propagation in the Galaxy: Diffusion and Compound Diffusion

The mode of propagation of cosmic rays in the Galaxy must be consistent with a) the low anisotropy observed at all energies, b) the path length in the galaxy of ~ 5 g cm^{-2} at energies of a few GeV/nucleon, which possibly implies a containment time of $\sim 3 \times 10^6$ yr, and c) an energy dependent path length at energies above a few GeV/nucleon. To reconcile these stringent limits with a galactic origin for the bulk of the cosmic radiation, it is apparent that the galactic magnetic field must regulate the propagation of the particles and their escape from the Galaxy. Direct knowledge of the detailed structure of the interstellar magnetic field is poor however and information about the field structure is more likely to come from constraints due

to cosmic ray properties, than a knowlege of the propagation
is to come from the magnetic field structure.

The widely used approach to the cosmic ray propagation
problem, introduced by Fermi (1949), has been to postulate
that particles random walk in some fashion through an
irregular magnetic field so that the cosmic ray density
satisfies a diffusion equation. The effective diffusion
mean free path is, to some extent, a free parameter
although any deduced value must be consistent with our
knowledge of the magnetic field and the interstellar medium.
Even for the interplanetary field, for which there is much
observational data, no complete theory exists at present
for accurately determining diffusion coefficients from the
power spectrum of field fluctuations. A survey of the
various approaches to this problem has been made by Fisk et al
(1974).

Ginzburg and Syrovatskii (1964) and others have argued
that the cosmic ray propagation approximates to three dimen-
sional diffusion. A natural, though not unique, choice for
the diffusion mean free path is 10 to 30 pc, the character-
istic scale of the observed magnetic field inhomogeneities.
The general equation for the concentration of cosmic rays,
$N(\underline{r}, t, E)$, as a function of space, time and energy is

$$\frac{\partial N}{\partial t} - \nabla \cdot (D \nabla N) + \frac{\partial}{\partial E}\left[\frac{\partial E}{\partial t} N\right] + \frac{N}{T} = Q(\underline{r}, t, E)$$

The diffusion coefficient, D, may be a function of direction,
position and energy. For three dimensional isotropic diffus-
ion $D = \lambda c/3$, where the diffusion mean free path λ may vary
with energy. The third term on the left hand side represents

energy loss of the particles during propagation, which is important for electrons but may be neglected for nuclei. In the fourth term T is defined by

$$\frac{1}{T} = \frac{1}{T_c} + \frac{1}{T_e}$$

T_c is the nuclear collision loss time used in the calculation of the production of secondary nuclei by spallation. When the proton component of the cosmic radiation is considered T_c may be neglected if it is assumed that the "grammage", deduced from the heavier nuclear composition, applies to protons as well. T_e is an escape time for the cosmic rays from the Galaxy which has sometimes been used instead of taking a spatial boundary to the diffusion region. This approximation may be valid when the object of the calculation is to obtain a distribution of spallation products but it cannot be used when the object is to obtain a value for the anisotropy of cosmic rays at a given point in the Galaxy. The term $Q(\underline{r},t,E)$ is the source function. It could be a δ-function in space and time, corresponding to production of cosmic rays in discrete events such as supernova explosions.

The solution of the three dimensional diffusion equation for various boundary conditions and source regions was discussed by Ginzburg and Syrovatskii (1964). At that time it was generally accepted that radio observations indicated the existence of a spherical halo to the Galaxy with a radius, R, of ~15 kpc, filled with relativistic electrons and also occupied by the nuclear component of the cosmic

rays. For cosmic ray production in the disk and free escape from the halo boundaries the escape time[*] of the cosmic rays would be

$$\tau \approx \frac{R^2}{2\lambda c}$$

A $\lambda = 10$ pc gives $\tau \approx 3 \times 10^7$ yr. The mean effective gas density in the halo and disk together would be lower than the local interstellar density by the ratio of the volume of the disk to that of the halo, so that this escape time is quite consistent with the observed grammage. The sun is sufficiently close to the plane of symmetry of this system to account for the low anisotropy of the cosmic rays. More detailed observations have led to a reinterpretation of the radio data in terms of a large proportion of the high latitude synchrotron emission coming from relatively nearby, very much expanded supernova remnants. There is also a lack of confirming evidence for radio halos around other spiral galaxies. However, calculations on the electron spectrum and radio background radiation reported by Bulanov and Dogel (1974) indicate a spheroidal halo extending ~ 10 kpc from the disk. A firm choice between disk and halo confinement regions must await the determination of the proportion of Be^{10} (half-life: 1.6×10^6 yr) surviving in the cosmic ray spallation products with a greater precision.

For a disk confinement region extending a distance h on either side of the galactic plane and free escape from the boundaries, the escape time would be

$$\tau \approx \frac{h^2}{\lambda c}$$

[*] The escape time of the cosmic rays from the confining region, here the Galactic halo, is not the measured quantity, i.e. the mean age of the cosmic rays observed at the Earth. However unless there is a large contribution from young, nearby sources, the two times should not differ significantly.

With λ =10 pc as before and h≈100 pc the escape time would be ~3000 yr. To obtain the observed grammage a diffusion mean free path λ<0.1 pc is required. The grammage is related to the age of the particles reaching the earth rather than the mean escape time from the Galaxy, although unless the effects of nearby discrete sources are considered the two times are not very different. Also with λ=10 pc the anisotropy would be too large unless the earth were very symmetrically positioned with respect to the source distribution.

If cosmic rays are produced by random discrete sources in the Galaxy, such as supernovae, the density and anisotropy at a given point will vary with time. Sometimes the anisotropy will be much lower than the average. Ramaty et al (1970) have calculated the probability distribution of anisotropies for given values of λ , assuming three dimensional diffusion with one source per hundred years situated in a disk 200 pc thick. Their results for the cosmic ray anisotropy, lifetime and the ratio of light to medium nuclei as a function of λ are shown in figures 4.3 and 4.4. Ramaty et al suggest that the diffusion mean free path is confined to the range 10^{-2} pc$\lesssim \lambda \lesssim 10^{-1}$ pc, the upper limit being determined by the observed isotropy and the lower limit by the requirement that different nuclei have a distribution of path lengths. They find this range consistent with the observed L/M ratio.

The mean free path λ required for three dimensional diffusion to satisfy the cosmic ray data is very small compared to the size of the observed magnetic field irregularities. Lingenfelter et al (1971) introduced the concept of
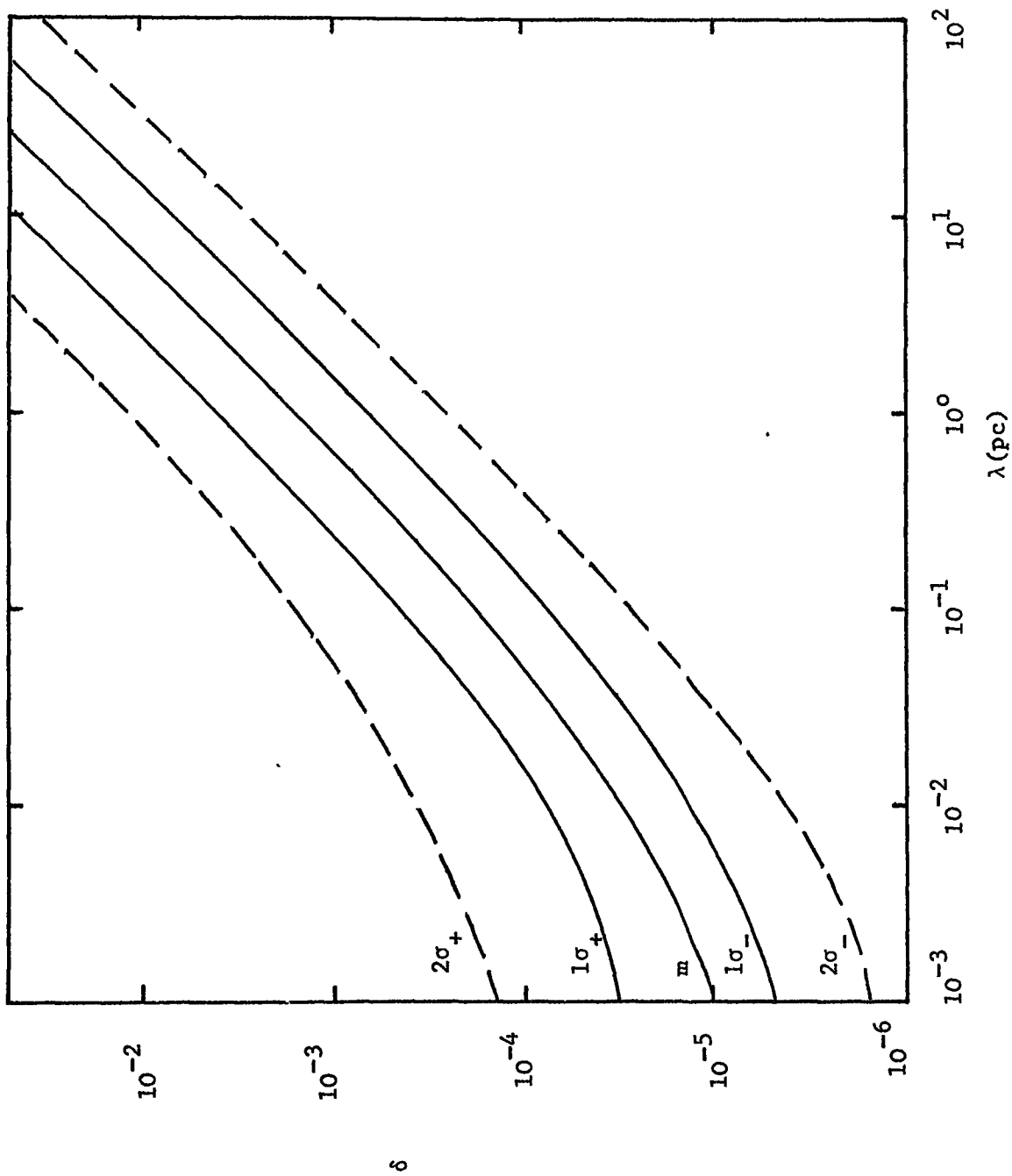
Figure 4.3: Cosmic Ray Anisotropy as a function of the diffusion mean free path λ. The probability that for a given λ the anisotropy is less than the value corresponding to the $2\sigma_+$, $1\sigma_+$, m, $1\sigma_-$, $2\sigma_-$ levels is 0.98, 0.83, 0.5, 0.17, 0.02 respectively (Ramaty et al, 1970).
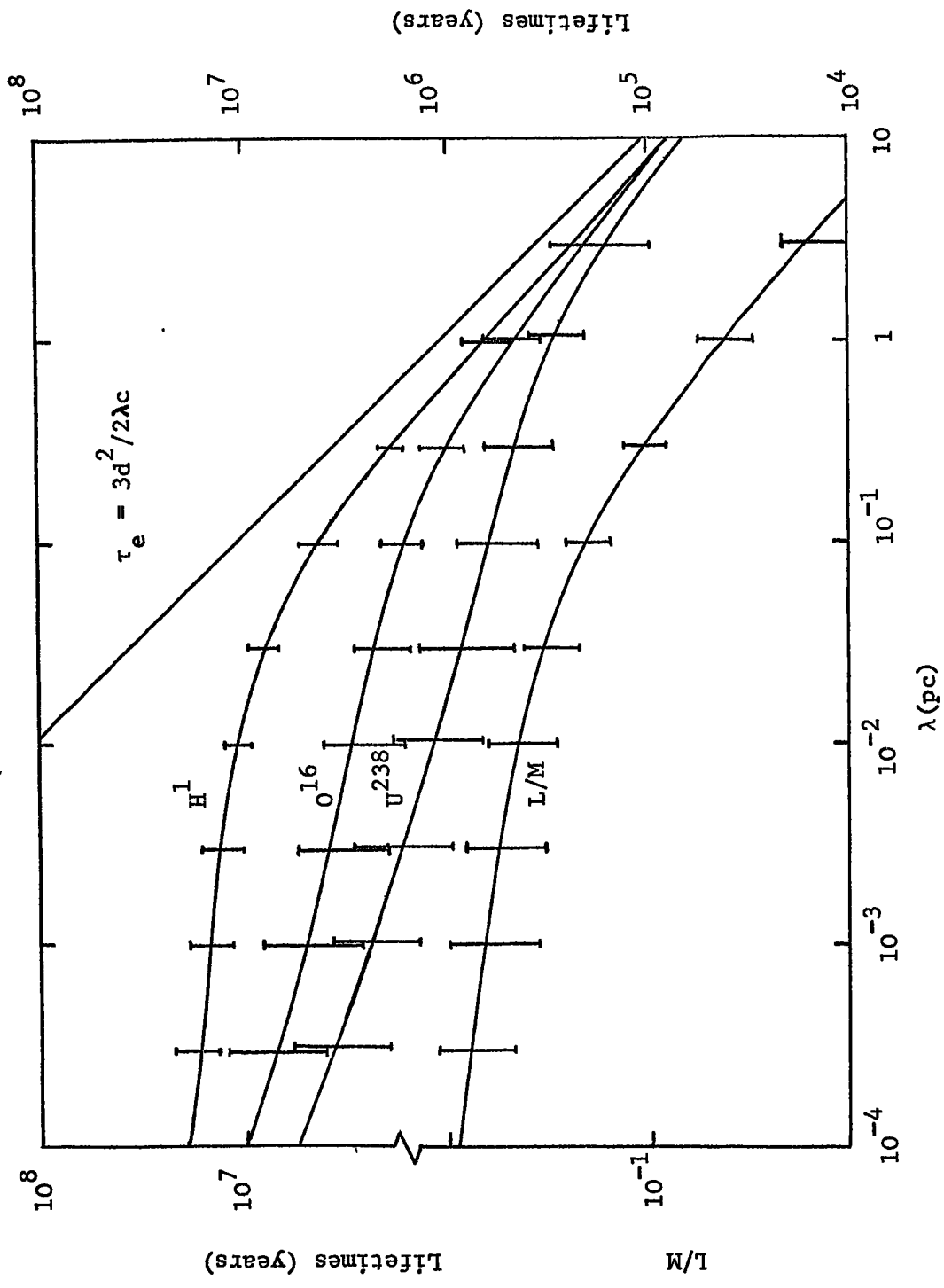
Figure 4.4: Cosmic ray lifetimes and the ratio of light nuclei to medium nuclei as a function of diffusing mean free path. (Ramaty et al, 1970).

compound diffusion in order to satisfy the requirement of small anisotropy using a diffusion mean free path consistent with the observed field irregularities.

Jokipii and Parker (1969) conclude that, although cosmic rays may be tightly bound to the magnetic field lines, which on average run approximately parallel to the galactic plane, each individual field line will be expected to random walk to the surface of the disk due to the turbulent nature of the galactic magnetic field. The particles reach the surface of the disk after travelling ~1 kpc, where the pressure of the cosmic ray gas causes a bubble to inflate, allowing the particles to disengage from the galactic magnetic field.

Lingenfelter et al (1971) propose that the cosmic rays remain on their field line where they propagate by one-dimensional diffusion, with a mean free path λ_p, due to scattering from minor irregularities in the field, while the field lines experience three dimensional random walk with step size λ_m. The probability density of particle displacement, s, along a field line in time, t, is then

$$f_1 (s,t) \, \alpha \, (\lambda_p t)^{-\frac{1}{2}} \exp \left[\frac{3s^2}{4\lambda_p ct} \right]$$

while the probability density for a three dimensional displacement r of a field line of length s is

$$f_2 (r,s) \, \alpha \, (\lambda_m s)^{-\frac{3}{2}} \exp \left[\frac{-3r^2}{4\lambda_m s} \right]$$

The compound probability density for a net displacement r

in time t is thus

$$f(r,t) = \int_{r}^{ct} f_1(s,t)\, f_2(r,s)\, ds$$

The result is that the net displacement of particles is proportional to $t^{\frac{1}{4}}$ rather than $t^{\frac{1}{2}}$ as in simple diffusion and anisotropies $\delta \approx 10^{-4}$ can be obtained with $\lambda_p \approx \lambda_m \approx 30$ pc. The escape time from the confinement volume is about 2×10^7 yr.

Criticisms and modifications to these basic models are presented in the remaining chapters of this thesis.

References

Arnett, W. D. and Schramm, D. N., 1973, Astrophys. J. Lett.,
184, L47

Beck, F. and Yiou, F., 1968, Astrophys. Lett., 1, 75

Bradt, H. L. and Peters, B., 1950, Phys. Rev., 80, 943

Bulanov, S. V. and Dogel, V. A., 1974, Astrophys. and Space
Sci., 29, 304

Cassé, M. and Goret, P., 1973, 13th Int. Conf. on Cosmic
Rays, Denver, 1, 584

Colgate, S. A. and White, R. H., 1966, Astrophys. J., 143, 626

Fermi, E., 1949, Phys. Rev., 75, 1169

Fermi, E., 1954, Astrophys. J., 119, 1.

Fisk, L. A., Goldstein, M. L., Klimas, A. J. and Sandri, G.,
1974, Astrophys. J., 190, 417

Ginzburg, V. L. and Syrovatskii, S. I., 1964, The Origin of
Cosmic Rays (Oxford: Pergamon)

Goldreich, P. and Julien, W. H., 1969, Astrophys. J., 157, 869

Gull, S. F., 1973, Mon. Not. R. Astr. Soc. 161, 47

Gurevich, K. E. and Rumyantsev, A. A., 1973, Astrophys. Space
Sci., 22, 79.

Havnes, O., 1973, Astr. Astrophys. 24, 435

Hoyle, F., 1949, Mon. Not. R. Astr. Soc. 109, 369

Jokipii, J. R. and Parker, E. N., 1969, Astrophys. J., 155, 799

Karakula, S., Osborne, J. L. and Wdowczyk, J., 1974, J.Phys.A,
7, 437

Lingenfelter, R. E., Ramaty, R. and Fisk, L. A., 1971,
Astrophys. Lett., 8, 93

Ramaty, R., Reames, D. V. and Lingenfelter, R. E., 1970,

Phys. Rev. Lett., 24, 913

Reeves, H., 1974, The Origin of Cosmic Rays, Ed. J. L. Osborne

and A. W. Wolfendale (de Reidel)

Shapiro, M. M. and Silberberg, R., 1974, Phil. Trans. of

Royal Soc. of London, Series A (to be published)

Shapiro, M. M., Silberberg, R. and Tsao, C. H., 1970, Acta.

Phys. Acad. Sci. Hung., 29, Suppl. 1, 479

Chapter 5 <u>One-Dimensional Diffusion along Magnetic Field Lines</u>

5.1 <u>Criticism of the Compound Diffusion Model</u>

In the previous chapter the concept of Compound Diffusion was discussed as a possible mode for the propagation of cosmic rays in the Galaxy. Lingenfelter et al (1971) conclude that a mean free path for the one-dimensional diffusion along a field line, λ , as large as 30 pc is sufficient to reduce the overall anisotropy to the observed level. However, Allan (1972) has emphasised the point made by Ginzburg and Syrovatskii (1964) that the anisotropy observed at the earth is on one particular field line. Allan argues that Lingenfelter et al, in their discussion of compound diffusion, ignore the parameter of the field configuration which decides whether or not particles will in fact be trapped on the lines of force. Some degree of order must be present, even in a stochastic field, if the adiabatic invariant is to be preserved. The field must be reasonably uniform in the direction perpendicular to the field lines for a distance of the order of the particles gyroradius. Allan defines a new parameter; the width of a tube of force, i.e. the distance over which the field lines are reasonably parallel to one another. At greater distances the field line directions are uncorrelated. A condition necessary for compound diffusion to apply is that the majority of particles must remain wholly within single tubes of force throughout their motion, therefore the characteristic width of a tube must be many times the gyroradius.

Measurements of the anisotropy are concerned largely

with energies $\gtrsim 10^{11}$ eV. At 10^{11} eV a proton in a field of $3x10^{-6}$ gauss will have a gyroradius of $\sim 10^{-4}$ pc, so that for compound diffusion to be valid each tube of force must have a width of about 10^{-2} pc. Anisotropy is related to a lack of balance in the cosmic ray flux passing through some test area in opposite directions. If a test area, with dimensions small compared with the width of a tube of force, is used, then the measured anisotropy will be that associated with one-dimensional diffusion along the tube. This may be termed the 'micro-anisotropy'. If, however, a test area is used which embraces many tubes of force, the measured anisotropy will be the mean of the separate contributions from each tube of force. The random walk of the field lines ensures that not all of these contributions will be of the same sign, consequently the overall anisotropy over a large area is less than that within one individual tube. It is this overall or 'macro' anisotropy that is the quantity calculated by Lingenfelter et al.

Experiments which look for an anisotropy in the cosmic ray flux are run for a few years in order to obtain adequate statistics. During this time the solar system moves with a velocity ~ 20 km s^{-1} relative to the Galactic frame, but even so travels no more than $\sim 10^{-4}$ pc, much less than the required width of a tube of force for compound diffusion to apply.

The anisotropy measured would, therefore, be the anisotropy within a single tube of force. The predictions of the compound diffusion model do not agree with experiment when this fact is taken into account.

5.2 Calculation of the 'micro-anisotropy': Continuous injection

Jones (1971) has used the model of one-dimensional diffusion along a randomly wandering field line (equivalent to the tube of force defined by Allan (1972)) and has considered the case where cosmic rays are injected continuously and uniformly along the field line. Figure 5.1 shows a schematic representation of a possible configuration of the magnetic field line that passes through the earth. The 'edge' of the galactic disk is taken to mean that distance sufficiently far from the central plane such that the bubble blowing instability takes place allowing a free escape of the cosmic rays from the 'ends' of the field lines. The anisotropy and mean age of the cosmic ray flux seen by the observer at a given point on the field line will be constant in time and dependent solely on the distances to the two ends measured along the line.

Jones notes that we do not know the configuration of the field line that contains the earth and derives a probability distribution for the positions of possible end points. For the assumed uniformly distributed sources the relative frequency distribution of streaming velocities (directly related to anisotropy) is then obtained. The distribution peaks at zero streaming velocity corresponding to the earth being at the mid point of its field line. The experimental upper limit to the anisotropy determines the range of positions about the exact mid-point of the line in which the earth may lie. A very low anisotropy is always possible but from the size of this range relative to the

Cosmic Rays
Escape

"Edge" of Galactic Disc

$+z_1$

"Our" Field Line

z

y

Earth

Ave. Field
<B>

"Edge" of Galactic Disc

$-z_1$

Cosmic Rays
Escape
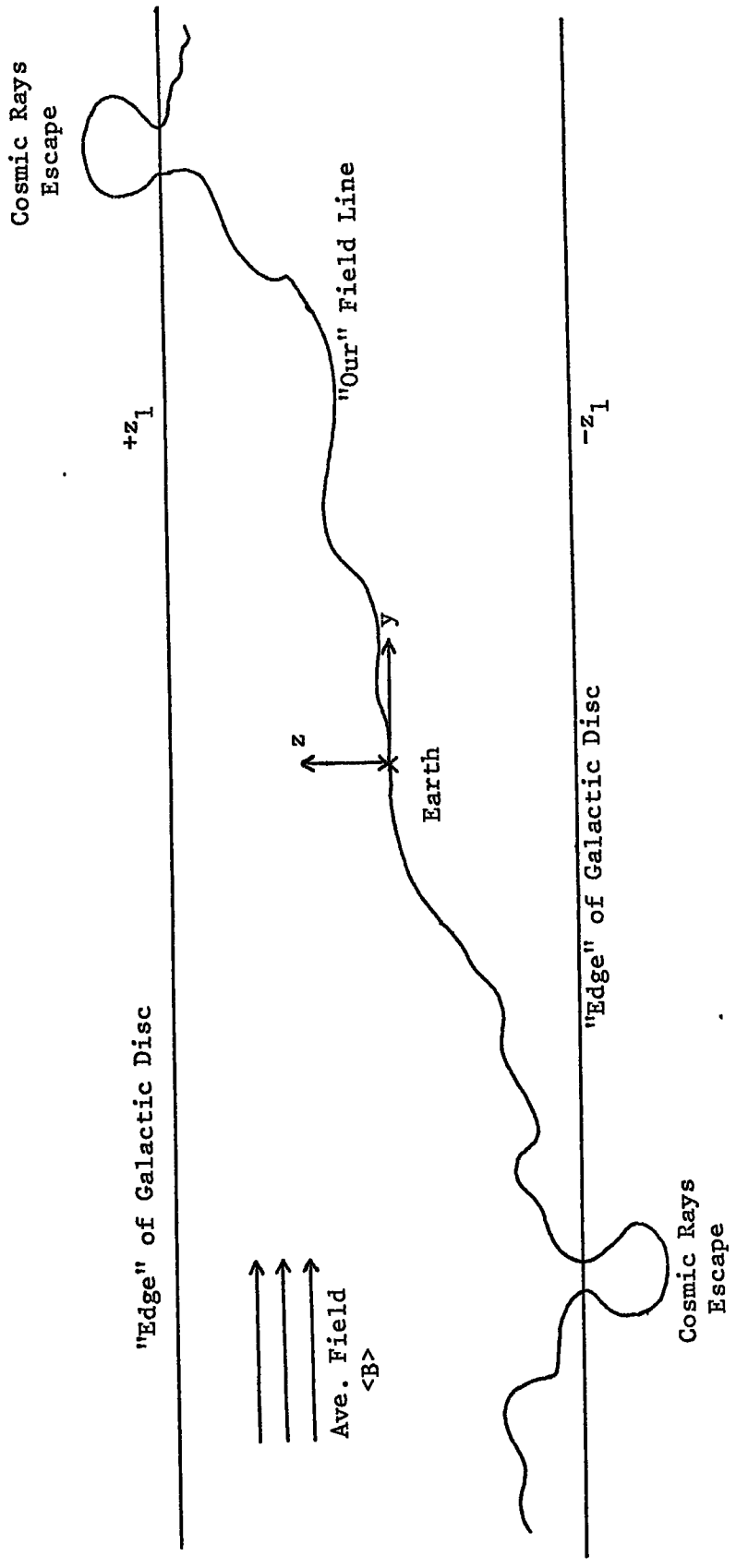
Figure 5.1: Schematic representation of a possible configuration of the magnetic flux tube that passes through the Earth.

length of the field line one may make a judgement of the
probability of the earth actually being in the required
position.

Analysis of Jones's results using a diffusion mean
free path of 10 pc gives the result that the probability
that an anisotropy $\delta \leq 10^{-3}$ is observed is 1.7%.

5.3 Calculation of the 'micro-anisotropy': Discrete sources

5.3.1 The Model

Jones's model may be developed by considering a rather
more physically likely source distribution. Instead of
using a uniform and continuous injection of cosmic rays,
instantaneous point sources randomly distributed in space
with a poissonian distribution in time interval are con-
sidered. No energy dependence is introduced into this
model. Due to the effects of the interplanetary magnetic
field, there can be no measurement of the galactic cosmic
ray anisotropy below 10^{11} eV. For comparison with experi-
mental data on anisotropy this model need only refer to
particles above 10^{11} eV. At lower energies hydromagnetic
waves may be generated by the streaming of cosmic rays
through interstellar gas. These waves scatter the
particles and restrict their streaming velocity to the
Alfvén velocity. Kulsrud and Cesarsky (1971) have con-
sidered the damping of these waves due to collisions bet-
ween the charged and neutral particles of the interstellar
gas. The energy density of cosmic rays with energy $> 10^{11}$ eV
is so low ($\sim 5\%$ of that on all the cosmic rays), that the
growth rate of the waves is much less than their damping

rate in a gas with a density equal to that in the galactic disk. It must be proposed therefore that the irregularities causing the scattering are due to some externally produced general turbulence in the interstellar gas.

The one dimensional diffusion model will break down at sufficiently high energies that the cosmic ray particles are no longer strongly bound to the field lines. Motion of charged particles normal to the magnetic field may be due to gradient or curvature drifts. Consider the gradient drift of a particle moving a distance λ along a field line between successive scatters. The drift velocity due to a gradient in a magnetic field is given by:

$$V_{Drift} = - \frac{V_\perp}{2} \frac{\rho}{B} \nabla B$$

where $V_\perp$ is the component of the particle velocity perpendicular to the field direction, ρ is the larmor radius and ∇B is the magnetic field gradient. Over a distance λ along the field the displacement due to this drift motion will be:

$$\frac{\lambda}{V_{11}} V_{drift}$$

where V_{11} is the velocity component parallel to the field. Assuming a field strength of 3 μgauss and lengths in units of parsecs, the distance drifted will be approximately

$$\left(\frac{E}{10^{11} \text{ eV}} \right) \left(\frac{\nabla B}{B} \right) \left(\frac{\lambda}{6} \right) 10^{-4} \text{ pc} \qquad *$$

The direction of the drift is mutually perpendicular to the field line and the field gradient. The direction of the gradient will vary with position along the field line. If

---

* This formula omits a factor $a^{\frac{1}{2}} \langle V_\perp \rangle / \langle V_{11} \rangle$, where $a\lambda$ is the length over which the field gradient is constant in direction. $\langle V_\perp \rangle / \langle V_{11} \rangle \approx 1.6$ and $a \leqslant 1$. Therefore $a^{\frac{1}{2}} \langle V_\perp \rangle / \langle V_{11} \rangle$ is of order 1.

the direction changes randomly at least every step λ along the field line, the net distance drifted as a particle diffuses a distance L along the field line will be no more than

$$\left[\frac{E}{10^{11} \text{ eV}} \right] \left[\frac{\frac{\nabla B}{B}}{} \right] \left[\frac{L}{6} \right] \ 10^{-4} \text{ pc}$$

For example, a proton of energy 10^{12} eV in diffusing the whole length of a 3 kpc field line would drift by a net distance of 0.5 pc if $(\nabla B/B)$ were as large as 1 pc^{-1}. It is not yet possible to determine the magnitude of magnetic field gradients in the interstellar medium from present observations.

Drift due to field line curvature could be comparable to the gradient drift only if the field lines had frequent bends with a radius of curvature less than 1 pc. Such a large curvature does not agree with the picture of field line wandering discussed by Jokipii and Parker (1969).

The energy at which one-dimensional propagation breaks down depends not only upon the net drift but also upon the rate of separation of field lines in the interstellar field, which is discussed in Chapter 6. By an energy of 10^{14} eV, the larmor radius of a proton in a 3 μgauss field is 0.03 pc and considerable transfer from one field line to another will be occurring over the lifetime of the cosmic rays. Above 10^{14} eV it is probably more reasonable to turn to the propagation model developed by Bell et al (1974) where cosmic rays are scattered by magnetised gas clouds.

The one-dimensional diffusion equation which governs the propagation in the present model is given by eq. (i)-2.

(Appendix)

Cosmic rays are assumed to escape freely when the field line reaches the boundary of the disk. The boundary conditions are therefore: the concentration, N, is zero at x=o and x=h for all time, t, where h is the length of the field line. For a source which is instantaneous in time at t=o and represented by S $\delta(x-x_0)$, where S is the source strength, the solutions to (i)-2 for N(x,t) are given by equations (i)-4 and (i)-5. The flux is

$$J = - D \frac{\partial N}{\partial x}$$

and the one dimensional anisotropy is given by

$$\delta = \frac{J}{NV}$$

The velocity V is the magnitude of the effective mean velocity of the cosmic rays parallel to the field line. The observed distribution of arrival directions of particles at a point on the line will in fact be three dimensional rather than one-dimensional due to the particles being distributed in pitch angle. Assuming that the scattering along the field lines causes complete mixing of pitch angles, V = c/3 and the anisotropy is

$$\delta = \frac{3J}{Nc}$$

For a number of sources occurring at x_i and t_i the individual concentrations N_i and fluxes J_i can be summed and the resultant concentration, anisotropy and mean age, $\bar{\tau}$, can be calculated. $\bar{\tau}$ is given by

$$\bar{\tau} = \frac{\sum_i N_i (t-t_i)}{\sum_i N_i}$$

To do this a set of sources was generated, randomly distributed in space along the field line and following a poissonian distribution of time intervals with an average time τ_s/h between sources.

The length of the field line passing through the earth and the position of the earth relative to its ends are both unknown. A probability distribution of the lengths of field lines was therefore calculated using the stochastic model of the interstellar magnetic field of Jokpii and Parker (1969). The magnetic field lines random walk due to their being carried bodily by the turbulent motion of the gas. The gas motions are considered to be uncorrelated after a distance in the galactic plane of 100 pc.

To calculate the probability distribution the simplification was made that after each 100 pc step in the galactic plane, the field line has been displaced either up or down by a distance of 45 pc. As the earth is close to the mid plane of the galaxy the condition that the field line passed through the mid plane was demanded. Using a Monte Carlo approach, the distribution of lengths to reach the boundaries of the disk, taken to be 130 pc above and below the mid plane, was calculated. This field line length distribution, I, is shown in figure 5.2.

The value of the vertical displacement of the field line after each step is estimated from the distribution of vertical interstellar gas velocities and the rate of change of gravitational acceleration with distance from the galactic plane. The estimated value of 45 pc used to generate the

probability distribution is rather uncertain so a second distribution, II, was generated using a vertical displacement of 35 pc. This is also shown in figure 5.2.

In order to proceed with the calculation, a value has to be adopted for the average time interval between sources. Possible instantaneous point sources of cosmic rays are novae and supernovae which are estimated to occur in the Galaxy at rates of about 260 yr^{-1} (Sharov, 1972) and one per 26 yr (Tamman 1970) respectively. To convert these rates to intervals between sources on a particular field line one must have an estimate of the effective cross-sectional area surrounding a field line from which there is input of cosmic rays from sources i.e. how close to the line, which passes through the earth, a source must lie in order that we should observe cosmic rays from it.

In the first few years after a supernova explosion the magnetic field in the remnant will be sufficiently high for the cosmic rays to be trapped. As the remnant expands, the magnetic field within it decreases and the cosmic rays will eventually escape and become attached to an interstellar field line. The problem of transfer of cosmic rays from the remnant to the galaxy as a whole is a complex one which is not well understood. The effective radius of the source at the stage that cosmic rays are transferred is a necessary parameter of the present computation. The path length of the material (in g cm^{-2}) traversed in the remnant is also of interest. If it is a significant fraction of the total
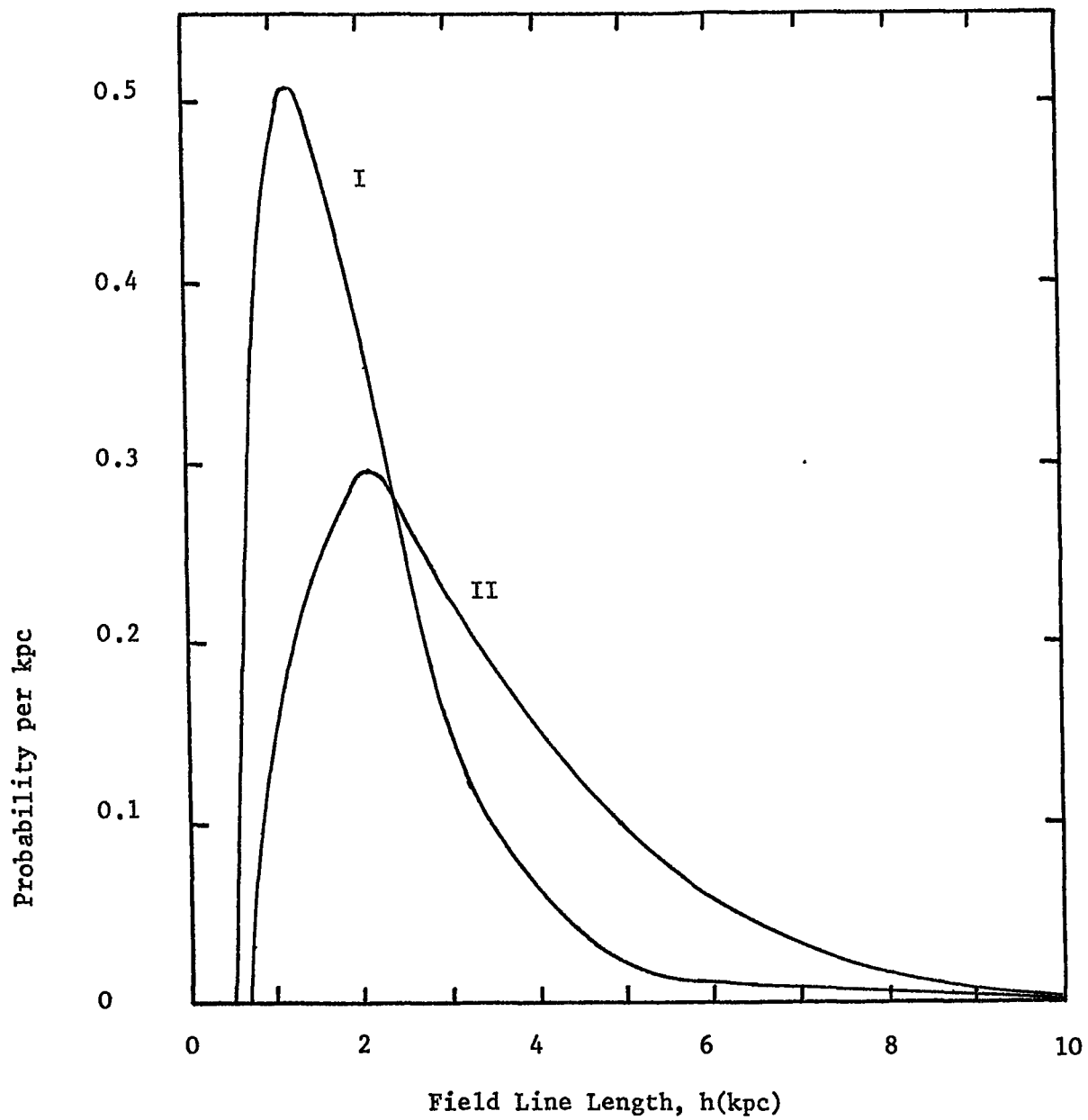
Figure 5.2: Length distribution of magnetic field lines in the galactic disk for two field models.

it may provide an explanation of the observed energy
dependence of path length of the cosmic rays. Ostriker
and Gunn (1971) have developed a model for the expansion
of a supernova remnant with continuous energy input from
a pulsar. For their 'standard' type 2 supernova the magnetic
field falls to a value about twice that of the galactic
field after 3000 yr. The radius of the remnant is then
10 pc. As an upper limit to the effective source radius
one can take the radius of the remnant when it merges into
the interstellar medium. This occurs when the expansion
velocity falls to 10 km s^{-1}, the same velocity as the
turbulent motions of the interstellar gas. The radius is
then about 30 pc. Assuming that supernovae are distributed
uniformly in the galactic disk values of τ_s=(average time
interval between sources on a field line)x(length of the
field line) of 1.4×10^7 and 1.6×10^6 yr kpc are obtained for
effective source radii of 10 pc and 30 pc respectively.
Taking into account the age of the cosmic rays, a few sources
would contribute to the flux at any one time.

The frequency of novae and their energy release are
high enough that they must also be considered as possible
cosmic ray sources although their ability to accelerate
particles to energies >10^{11} eV is in considerable doubt.
In the absence of information on the confinement of particles
in an expanding nova shell, one can only consider an upper
limit to the effective source radius corresponding to the
shell merging with the interstellar medium. For a shell of
10^{-4} $M_\odot$ having an initial velocity of 10^3 km s^{-1} this radius

is 0.4 pc, giving $\tau_s = 1.4 \times 10^6$ yr kpc.

In the present calculation two values of τ_s were used, 4×10^6 yr kpc and 2×10^7 yr kpc in order to show the effect of variation of the interval between sources.

5.3.2   Results of the Calculation

The concentration of the cosmic rays, the anisotropy of the flux and the mean age of the cosmic rays were calculated at given positions, on lines of given length and at successive steps in time small compared to the mean time interval between sources. To find the effect of varying the diffusion coefficient D, three values were used: 0.102 pc^2 yr^{-1}, 0.307 pc^2 yr^{-1} and 1.02 pc^2 yr^{-1}, corresponding to diffusion mean free paths, λ, of 1 pc, 3 pc and 10 pc. The calculations were made using a range of values of λ expected to give a reasonable probability of a low anisotropy without giving too high a mean age for the cosmic rays.

Jokipii has put forward an argument against a mean free path of less than 1 pc. Any waves that scatter cosmic rays of energy $>10^{11}$ eV in the disk region must be generated by turbulent motion of the gas. Energy will thus be transferred from the gas to the cosmic rays, i.e. the cosmic rays will experience a degree of Fermi acceleration and the waves will be damped. The characteristic time for acceleration is proportional to λ and for $\lambda \approx 1$ pc it approaches the age of the cosmic rays. The force of the argument is reduced however, in that the cosmic rays of energy $>10^{11}$ eV contain only a small portion of the total cosmic ray energy

density, therefore the required energy input to the waves from the gas need not be excessive.

Figure 5.3 shows an example of the time variation of the concentration, mean age and anisotropy of the cosmic rays. These particular values were obtained at the mid point of a field line 3 kpc long for the case $\lambda = 3$ pc and $\tau_s = 4 \times 10^6$ yr kpc. Many similar runs were generated and a record was kept of the fraction of the time that the anisotropy was less than 10^{-4}, 4×10^{-4}, and 10^{-3}. This fraction can be equated to the probability of an observer at that position on the line seeing an anisotropy less than the stated value.

In figures 5.4, 5.5, 5.6 and 5.7 this probability is plotted as a function of field line length h and relative position x/h along the line for some values of τ_s and D. The probability of seeing only a very small anisotropy is in general highest for the longest field lines. Comparison of figures 5.4 and 5.6 shows that an increase in D leads to a lower probability of seeing $\delta < 10^{-3}$ at all positions on all field lines. Comparison of figures 5.5 and 5.6 shows that on the shorter lines, an increased frequency of sources leads to a somewhat higher probability of $\delta < 10^{-3}$. Comparison of figures 5.4 and 5.7 shows the magnitude of the decrease in probability when a more stringent limit ($\delta < 10^{-4}$) is taken for the anisotropy.

A check was also made on the constancy of the cosmic ray concentration. A record was kept of the probabilities (i.e. the fraction of time) that the instantaneous concentration is within a factor of two of the concentration
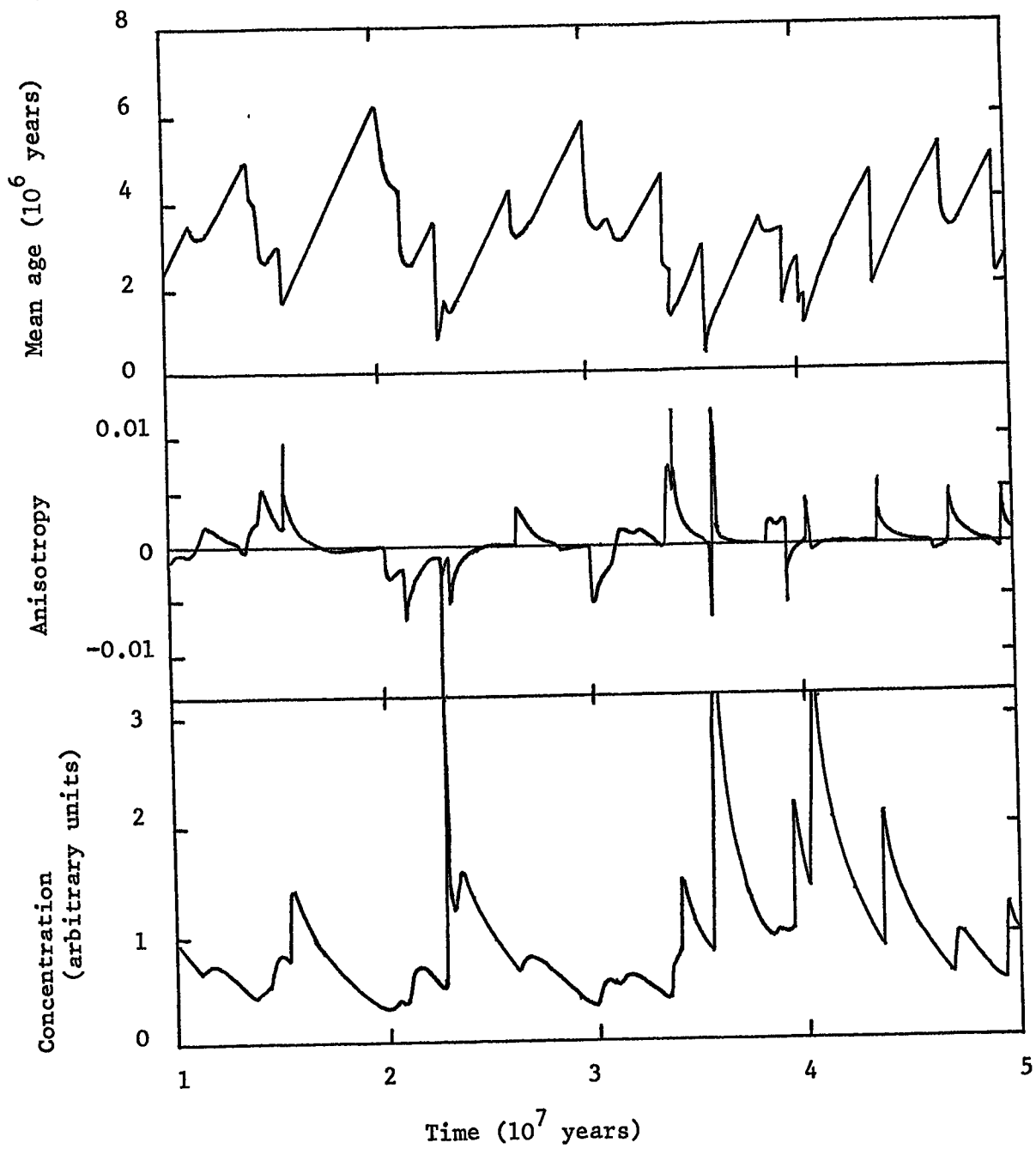
Figure 5.3: Example of the time variation of concentration, mean age and anisotropy of cosmic rays at the mid point of a field line of length 3 kpc.
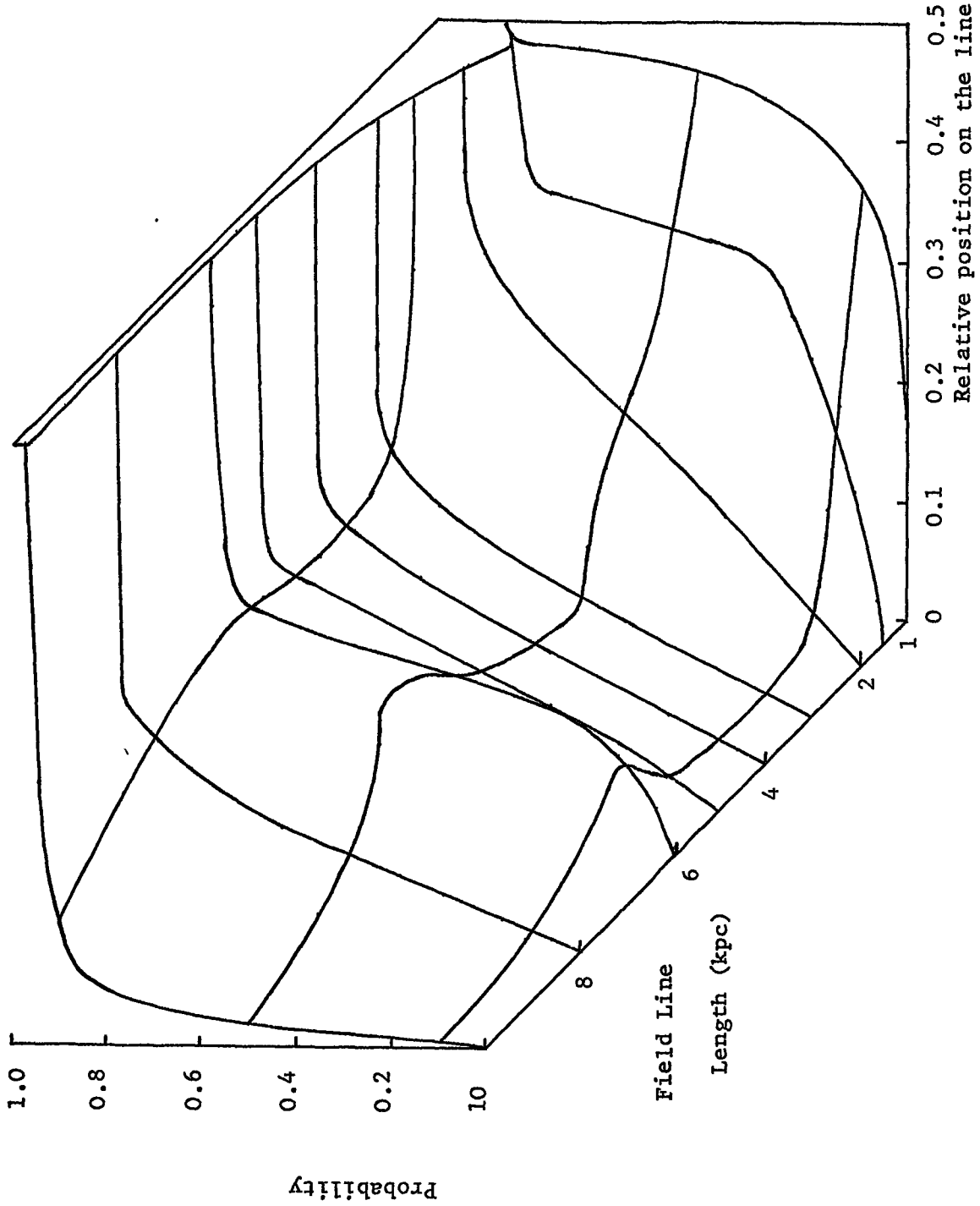
Figure 5.4: Probability that $\delta < 10^{-3}$ as a function of field line length and position on the line for $\lambda = 1 \text{pc}$ and $\tau_s = 4 \times 10^6 \text{ yr kpc}^{-1}$. The contours represent probabilities of 0.9, 0.5 and 0.1.
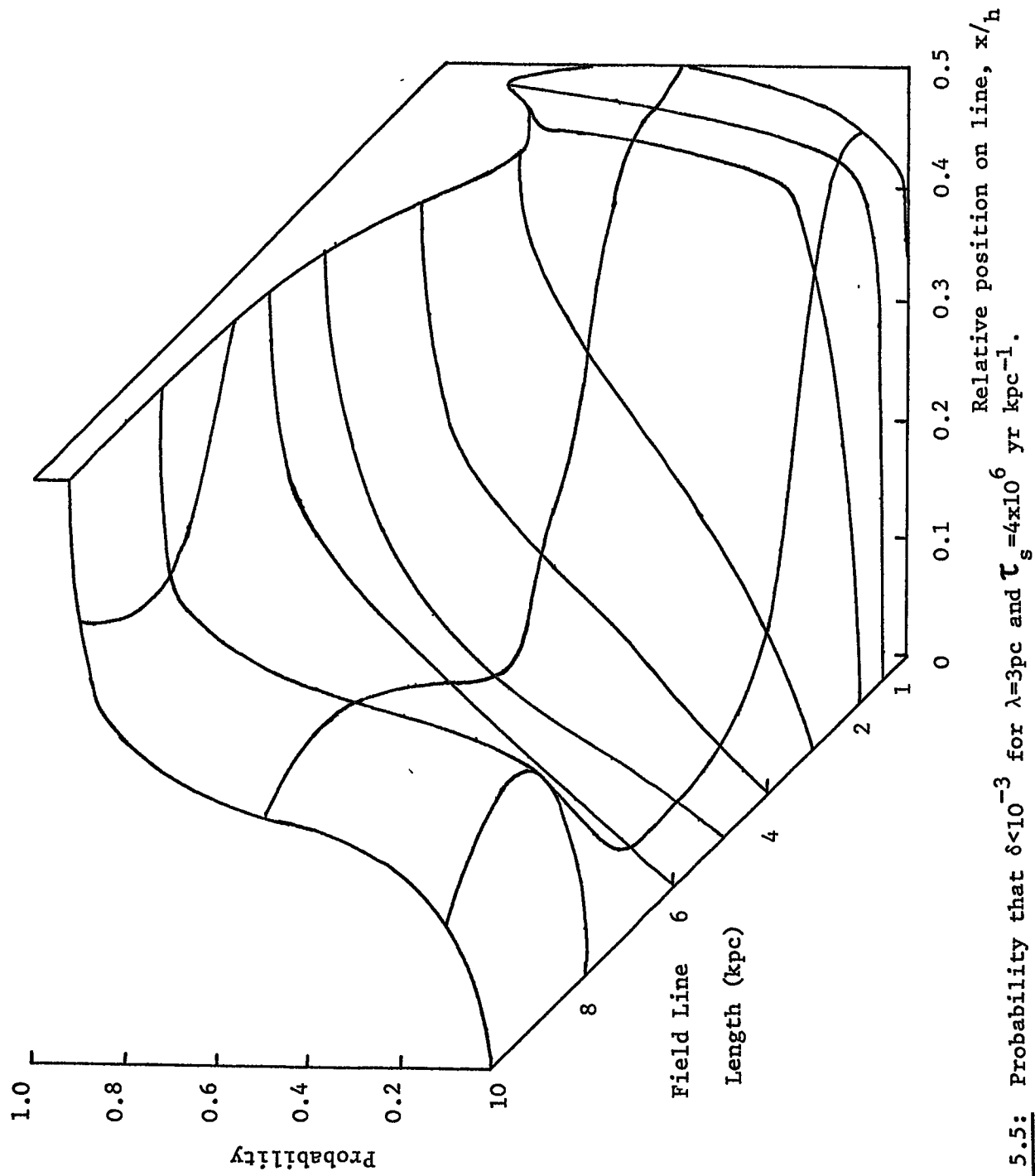
Figure 5.5: Probability that $\delta < 10^{-3}$ for $\lambda = 3\text{pc}$ and $\tau_s = 4 \times 10^6$ yr kpc^{-1}.
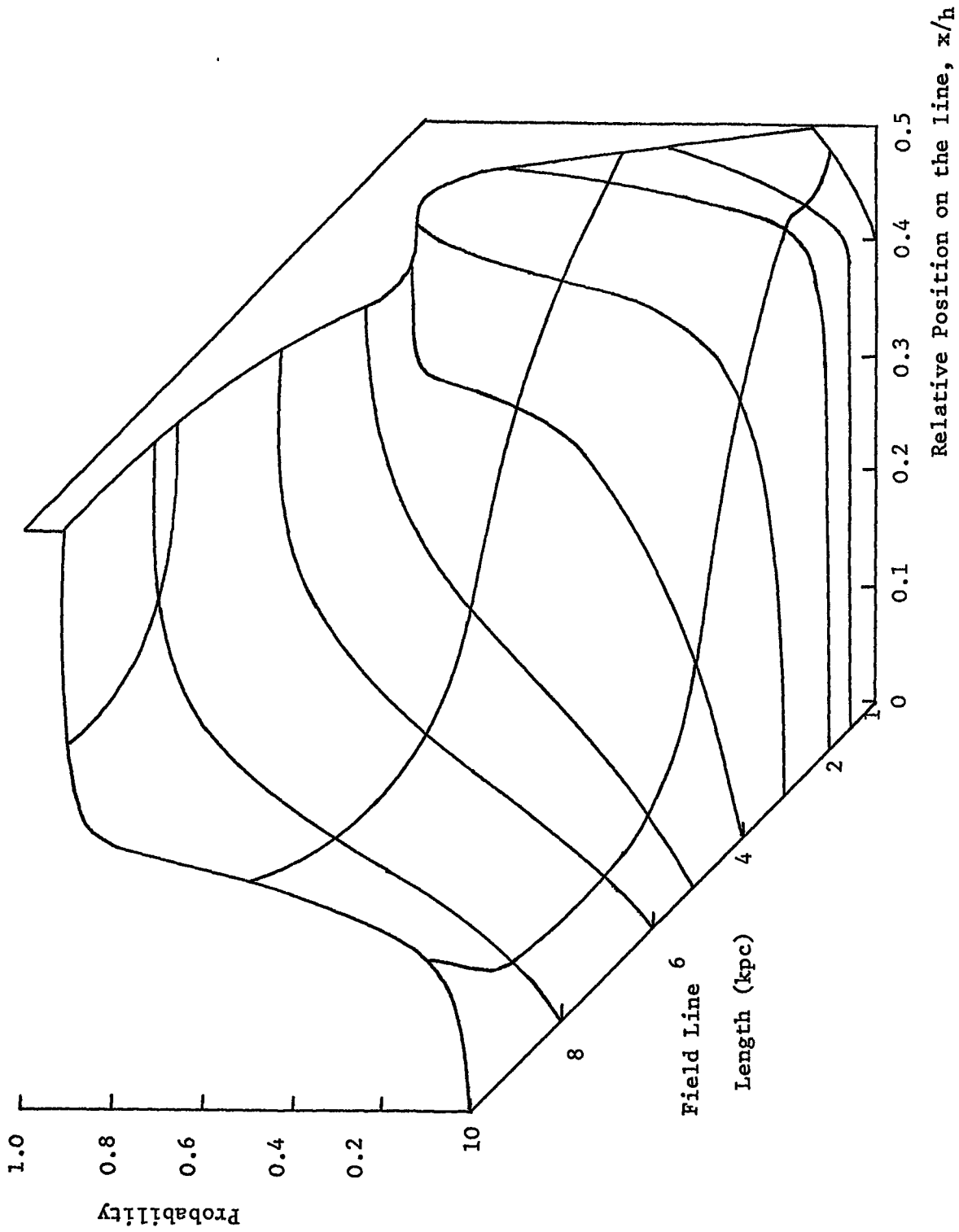
Figure 5.6: Probability that $\delta < 10^{-3}$ for $\lambda = 3$ pc and $\tau_s = 2 \times 10^7$ yr kpc^{-1}.
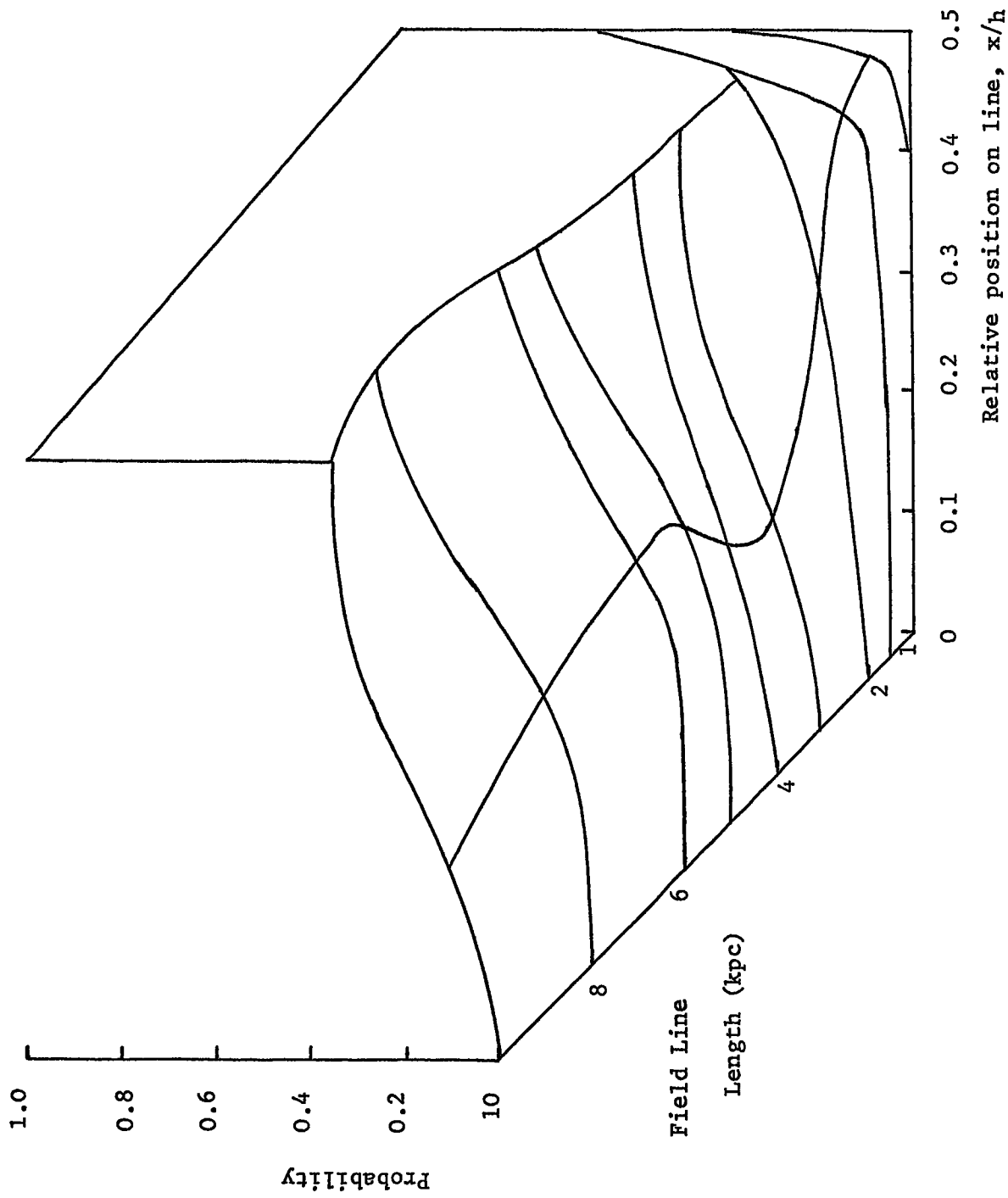
Figure 5.7: Probability that $\delta < 10^{-4}$ for $\lambda = 1\text{pc}$ and $\tau_s = 4 \times 10^6$ yr kpc^{-1}

averaged over the previous 10^5, 10^6 and 10^7 yr. These
probabilities are in general greater than or equal to the
probability that $\delta < 10^{-3}$. There is in addition a strong
correlation between the anisotropy and concentration. The
occurrence of a nearby source will simultaneously increase
the concentration and the anisotropy, thus the relatively
low observed limit to the anisotropy is a more stringent
condition than the rather imprecise limit on the variation
of the concentration (which applies to much lower energy
particles than we are considering here). It is therefore
assumed that the condition for the constancy of concentra-
tion will always be met when the anisotropy is as low as
the observed value.

In order to find the overall probability of observing
anisotropies less than the upper limiting values it is first
assumed that there is an equal probability of the earth
being at any position along the field line and then the
probability of observing a low anisotropy is averaged over
the length of the field line. These probabilities, as a
function of length, were then folded into the field line
length distributions. Table 5.1 gives the probabilities
for the three anisotropy levels for the twelve combinations
of field line length distribution, D and τ_s.

In order to see the effect of having considered discrete
sources instead of a uniform distribution, the corresponding
probabilities were calculated for the latter case too. In
this case the anisotropy is a unique function of the
distance, $x - \frac{1}{2}h$, from the mid point of the field line

Table 5.1 Probabilities of observing given anisotropies for the case of discrete sources for various values of D (pc^2 yr^{-1}) and τ_s (yr kpc)

Field line Distribution	δ	D=0.102		D=0.307		D=1.02	
		$\tau_s=4\times10^6$	$\tau_s=2\times10^7$	$\tau_s=4\times10^6$	$\tau_s=2\times10^7$	$\tau_s=4\times10^6$	$\tau_s=2\times10^7$
I	$<10^{-3}$	0.43	0.34	0.16	0.086	0.046	0.020
I	$<4\times10^{-4}$	0.24	0.14	0.084	0.056	0.018	0.009
I	$<10^{-4}$	0.091	0.060	0.038	0.037	0.004	0.002
II	$<10^{-3}$	0.61	0.54	0.32	0.21	0.11	0.051
II	$<4\times10^{-4}$	0.38	0.29	0.17	0.12	0.044	0.026
II	$<10^{-4}$	0.12	0.11	0.054	0.06	0.011	0.005

Table 5.2 Probabilities of observing given anisotropies for a continuous source distribution for various values of $D(pc^2\ yr^{-1})$

Field line Distribution	δ	D=0.102	D=0.307	D=1.02
I	$<10^{-3}$	0.39	0.16	0.049
I	$<4\times10^{-4}$	0.18	0.065	0.020
I	$<10^{-4}$	0.049	0.016	0.005
II	$<10^{-3}$	0.51	0.24	0.081
II	$<4\times10^{-4}$	0.28	0.10	0.032
II	$<10^{-4}$	0.081	0.027	0.008

$$\delta = \frac{\lambda(2x - h)}{xh - x^2}$$

The probability of observing an anisotropy less than δ can then be equated to the fraction of the total length of the field line within which this condition is satisfied, so the probability is given by

$$P = \left[1 + \left(\frac{2\lambda}{\delta h}\right)^2\right]^{\frac{1}{2}} - \frac{2\lambda}{\delta h}$$

These values are folded into the field line length distribution to give the overall probabilities in table 5.2.

The simplifying assumption that the earth can be at any position on its field line will introduce some error. Since the earth is known from astronomical evidence to be near the central plane of the galactic disk, it is also more likely to be near the centre, rather than the ends, of its field line, and the shorter the field line the more likely it is to be central. As a check, for one set of parameters, the actual probability distribution of the earth's position was folded in. The result was an increase in the overall probability of a low anisotropy by a factor of 1.25. All the probabilities in tables 5.1 and 5.2 should be enhanced by a factor of this order.

The mean age of the cosmic rays at a given position also fluctuates with time as shown in figure 5.3. The average of these ages is independent of the position on the field line but varies with field line length, λ and τ_s. Table 5.3 gives values of the average age for various values of λ and τ_s, the quoted values corresponding to the most probable field line length in each case.

Table 5.3　Average age of cosmic rays (10^6 yr) for various values of τ_s (yr kpc) and λ.

τ_s	$\lambda=1$ pc	$\lambda=3$ pc	$\lambda=10$ pc
4×10^6	7	4.5	2
2×10^7	11	7	6

The variation of the cosmic ray concentration with time shown in figure 5.3 gives an indication of the expected degree of variation of concentration from one point to another in the Galactic disk. At present there are no observations of the proton component to support or refute this. If we are by chance at a period when the anisotropy is low, the local concentration will also be at a relatively low value, about half of the average value throughout the disk, although it should be pointed out that the mean age of the cosmic rays would be higher than the average.

Comparison of the amount of synchrotron radiation from the disk with the measured electron energy spectrum suggests that the local electron component of the cosmic rays is indeed somewhat lower than the average.

5.3.3   Conclusions

Comparison of the probabilities in tables 5.1 and 5.2 shows that for the same field line length distributions and values of D, the probabilities are within a factor of two. The assumption of random discrete sources, when the interval between sources is of the order of 10^7 yr kpc does not give a very different result from that for the simpler assumption of a uniform source distribution. This is surprising since the interpretation of the probability is different in the two cases. In the former case, it is the chance that we are at a point in the earth's cosmic ray history when the fluctuating cosmic ray anisotropy is at a low value: in the latter case, it is the chance that we happen to be situated near enough to the centre of our field

line. For short lines, where the overall probability is low the uniform source distribution gives a probability of 1 over a narrow region of the field line about its mid point, while the random sources give a much lower probability per unit length spread over a larger fraction of the field line.

The field line length distribution II gives a higher set of probabilities than I since it favours longer field lines. Similarly, a smaller value of λ gives lower anisotropies and higher probabilities. A constraint on lowering λ is imposed by the limit to the age of the cosmic rays. The figures in table 5.3 show that even for $\lambda = 3$ pc, which gives a reasonably high probability of a low anisotropy, the age is rather greater than that deduced from the observations of Be^{10} although it should be emphasised that the Be^{10} age refers to a lower energy region. Increasing λ to 10 pc brings the mean age closer to the observations but reduces the probability of a low anisotropy considerably. It is interesting to note that the smaller value of τ_s gives both higher probability of the anisotropy criterion being satisfied and a lower age.

Although the observed properties of the cosmic ray flux may well be the result of our being at a particular time in the earth's cosmic ray history, the probabilities for the model given in table 5.1 are rather small if the anisotropy at 10^{11} eV is less than 10^{-4} and $\lambda > 3$ pc.

Anisotropies will be reduced if there is a finite probability of the cosmic rays being reflected from the

edge of the disk. This possibility will be explored in a later chapter. The possibility of a large rate of separation of neighbouring field lines, which would invalidate the idea of one-dimensional diffusion along field lines, is discussed in the next chapter.

References

Allan, H. R., 1972 Astrophys. Lett., 12, 237

Bell, M. C., Kota, J. and Wolfendale, A. W., 1974 J.Phys.A, 7, 420

Ginzburg, V. L. and Syrovatskii, S. I., 1964 The Origin of Cosmic Rays (Oxford: Pergamon)

Jokipii, J. R., 1971 Proc. 12th Int. Conf. on Cosmic Rays, Hobart, 1, 401

Jokipii, J. R. and Parker, E. N., 1969 Astrophys. J., 155 799

Jones, F. C., 1971 Proc. 12th Int. Conf. on Cosmic Rays, Hobart, 1, 396

Kulsrud, R. M. and Cesarsky, C. J., 1971 Astrophys. Lett. 8, 189

Lingenfelter, R. E., Ramaty, R. and Fisk, L. A., 1971 Astrophys. Lett. 8, 93

Ostriker, J. P. and Gunn, J. E., 1971 Astrophys. J., 164 L95

Sharov, A. S., 1972 Sov. Astron. Astrophys. J., 16, 41

Tamman, E. A., 1970 Astron. Astrophys. 8, 458

Chapter 6   The effects of interstellar turbulence on the
            structure of the Galactic Magnetic Field

6.1   Introduction

An important concept in the study of the propagation of
cosmic rays in a random or turbulent magnetic field is that
of field line random walk. By this is meant the stochastic
meandering of a magnetic line of force brought about by
turbulent motions of the interstellar medium. In many
cases of interest the random walk of magnetic lines of
force is found to dominate the transport of charged particles
normal to the large scale magnetic field direction. In the
solar wind one finds that the ratio of the diffusion coef-
ficient perpendicular to the field and that parallel to the
field may increase with decreasing energy down to $\sim$20 MeV
for protons (Jokipii 1972). At these low energies the
particle cyclotron radius is less than $\sim 2 \times 10^{10}$ cm which is
an order of magnitude smaller than the $\sim 2 \times 10^{11}$ cm coherence
length of the magnetic fluctuations.

The meandering of the lines of force contributes to the
perpendicular diffusion coefficient in that a particle moving
along a line of force in general also moves normal to the
average magnetic field direction. If, when a particle is
scattered in pitch angle, it finds itself on a new, indepen-
dent line of force, since a particle will move sideways
across field lines by a distance approximately equal to its
Larmor radius by the time it has reversed direction, then
the field line random walk contributes fully to the motion
perpendicular to the average field direction. This will be

true, for example, if the particle cyclotron radius in the average field is of the same order as the coherence scale normal to the average field, $L_{c\perp}$, or larger. However, if the average cyclotron radius, r_c, is much smaller than $L_{c\perp}$, the contribution of the random walk to the perpendicular diffusion depends critically on the rate at which nearby field lines separate, which is in turn sensitive to the spectrum of magnetic field irregularities. If, for example, field lines initially $\sim r_c$ apart separate to $\sim L_c$ apart in one pitch-angle scattering mean free path or less, clearly the random walk of the field lines will contribute fully to the motion perpendicular to the average field and the model of one-dimensional diffusion along coherent magnetic flux tubes discussed in the previous chapter will not be valid.

The remaining sections of this chapter discuss the observations of irregularities in the magnetic field of the galaxy, a possible spectrum for the turbulence in the interstellar medium and attempts to evaluate the rate of separation of neighbouring field lines due to turbulence.

6.2 Observations of irregularities in the galactic magnetic field and turbulence in the interstellar medium

As well as providing information about the large scale magnetic field in the Galaxy, measurements of the polarisation of starlight are able to provide information about the irregularities in the magnetic field. Jokipii et al (1969) have analysed the data of Behr (1959) examining the variance of the polarisation along and perpendicular to the direction of the average field. Jokipii et al show that the correlation

length for the irregular field is of the order of 150 pc,
i.e. the characteristic length over which fluctuations
in the interstellar field are correlated.

Osborne et al (1973) have carried out an independent analysis
using the data of Mathewson and Ford (1970). Osborne et al
consider two magnetic field models, i) the reversing field
model of Thielheim and Langhoff (1968) and ii) a simple
longitudinal field with a z-dependence of $-3.8 \exp\{-(z/0.24\text{kpc})^2\}$.
Osborne et al compare the observed polarisation of starlight
as a function of distance with that calculated from the
coherent field models with irregularities due to gas clouds
and dust. Their best fit to the observed data gives an
expression for the ratio of the magnitude of the random
field to the magnitude of the coherent field in terms of the
separation of the irregularities. The spread in the polaris-
ation data about the best fit can in principle be used to
determine the separation of the irregularities. Osborne et al
determine a value not inconsistent with the Jokipii et al
result of 150 pc.

Jokipii and Lerche (1969) have analysed the Faraday
rotation data for extragalactic radio sources using a similar
approach to that of Jokipii et al (1969) with respect to the
optical polarisation data. Using the data of Berge and
Seielstad (1967) Jokipii and Lerche conclude that the cor-
relation length for the irregular field is $\gtrsim 200$ pc. This
result is at variance with the result from the optical
polarisation data, but is not surprising as Jokipii and
Lerche make no attempt to allow for large intrinsic rotation

measures in the extragalactic sources.

Osborne et al (1973) have analysed the pulsar rotation measure data of Manchester (1972). They compare the measured line of sight component for each pulsar with the field calculated from the coherent field models (i) and (ii). This analysis gives a value of $a\sqrt{L_s} \simeq 15 \ pc^{\frac{1}{2}}$, where a is the relative magnitude of the random field and L_s is the distance between irregularities.

Assuming that the spectrum of electrons at the earth is the same throughout the galaxy, the magnitude of the magnetic field strength may be deduced from the data on synchrotron radiation. A value of ~ 6 µgauss is found. This value is the sum of the regular and irregular fields and indicates that the magnetic energy density in each is of the same order.

Observations of the type mentioned above only allow one to draw very general conclusions regarding fairly large scale turbulence features which are not very important for a consideration of the separation of neighbouring field lines.

It has been observed that scattering of radio emission by small scale irregularities in the interstellar medium can cause the apparent size of a radio source, θ, to increase with wavelength, the exact dependence on wavelength, as well as the angular brightness distribution of the source, depending on the spectrum of irregularities or turbulence. Pulsars are ideal sources for such measurements as they are known to have an intrinsic size much smaller than the scattering irregularity size. Mutel et al (1974) have measured the size of the Crab Pulsar at 26.3 M Hz and have compared

their measurement with measurements and predictions of the
apparent size at different wavelengths. They conclude that
the apparent size of the Crab Pulsar is proportional to
$\lambda^{2.05\pm0.25}$ where λ is the wave length of the observation.
Unfortunately, the measurements to date on the pulsar
broadening are not yet able to account for the effect of
the surrounding nebula with sufficient accuracy to be able
to distinguish between a size spectrum of irregularities
which is a Gaussian or a power law (Mutel et al 1974). In
order to consider the separation of magnetic field lines
one must therefore be thrown back to theoretical arguments
in order to derive a spectrum of irregularities.

6.3 A possible spectrum of turbulence in the interstellar
medium

If the motions in a turbulent fluid are considered,
one may make a harmonic analysis of the instantaneous velocity
field $v(\underline{r},t)$ in the form

$$v(\underline{r},t) = \sum_{\underline{k}} \underline{v}_k(t)\, e^{i\underline{k}\cdot\underline{r}}$$

and ask for the average energy stored in the various wave-
lengths. This may be considered in the following manner.

Considering the state of motion at a given instant,
the fluctuating velocity field may be analysed as the
result of a superposition of periodic variations with all
possible wavelengths. The component with a wavelength λ
may be pictured as corresponding to| eddies of size λ and
since many wavelengths are needed to represent a general
velocity field, a "hierarchy of eddies" may be considered.

This hierarchy will be limited on the side of long wave lengths by the fact that no eddy of size larger than the dimension of the medium in which the turbulence is analysed can occur. It is often more convenient to consider the wavenumber $k = 2\pi/\lambda$ instead of the wavelength λ.

The question may now be asked: what is the energy per unit volume stored in eddies with wavenumbers between k and k+dk? If $\rho F(k)dk$ denotes this energy, $F(k)$ is said to define the spectrum of turbulence where ρ is the density of the medium.

Turbulence may only be maintained by an external agency, like continuous stirring and in the stationary case energy must be dissipated in the form of thermal energy at the same rate at which energy is being supplied.

The equilibrium spectrum for hydrodynamic turbulence was first expressed by Kolmogorov (1941). He concluded that when the Reynolds number tends to infinity the spectrum will follow more and more closely a $k^{-5/3}$ law. Kraichnan (1965) argues that the equilibrium inertial range of hydromagnetic turbulence (the turbulence found in the interstellar medium) in the weak field regime exhibits exact equipartition between magnetic and kinetic energy and that the spectrum will follow a $k^{-3/2}$ law in place of the Kolmogorov law. A $k^{-3/2}$ spectrum has also been derived by Skilling (1974, private communication) using the following argument.

For some range of wavenumber $\Delta k \sim k$ (one 'octave') it is supposed that the magnetic field disturbance has an amplitude Θ relative to the regular field strength B_o, where Θ is the mean angle through which components of the field, with wavenumber $\sim k$, bend in a distance $\sim 1/k$ along the field.

Skilling takes the smallest length scale at which the magnetic field turns through 1 radian in a distance $\sim 1/k$ to be 30pc, the typical distance between clouds in the interstellar medium. The wave energy in one octave (a range of k, Δk taken to be $\sim k$) is $\theta^2 B_0^2/8\pi$, where B_0 is the magnitude (in gauss) of the regular component of the field. The total energy in the turbulence is given by:

$$\text{Total Energy} = \sum_{\text{all octaves}} \frac{\theta^2 B_0^2}{8\pi}$$

Between wave numbers corresponding to wave lengths of 30 pc and 500 pc the turbulence is considered to be fully saturated and θ is defined to be equal to 1 in this region.

The rate of wave-wave interactions in the turbulence is proportional to the product of the incident wave intensities and equals the Alfvén rate, $k\,V_A$, when $\theta=1$, where V_A is the Alfvén velocity. The rate at which energy is transferred from one octave to the next, R, is therefore equal to the product of the total energy present, the Alfvén rate and the product of the two intensities.

$$R = \text{const} . \frac{B_0^2}{8\pi} . k\,V_A . \theta^2 . \theta^2 \quad \text{ergs cm}^{-3}\,\text{s}^{-1}$$

In the steady state R is equal to a constant, therefore

$$k\theta^4 = \text{constant}$$

i.e. $\quad \theta \propto k^{-\frac{1}{4}}$

Returning to the definition of the spectrum of turbulence it follows that $\theta \propto k^{-\frac{1}{4}}$ gives a power spectrum

$$F(k)dk \propto k^{-\frac{3}{2}}\,dk$$

At high wave number, viscosity damps out the turbulent waves in a characteristic time of $1/k^2 \nu$, where ν is the

kinematic viscosity. At the wave number where the time for viscous damping is equal to the time for energy transfer to the next octave a change in slope in the spectrum is expected. The slope of the spectrum after this cut off wave number, k_{max}, is not known but assuming a power law $k^{-\alpha}$, α must be >2 or the expectation value for the r.m.s. gradient of the magnetic field would tend to infinity (Jokipii, 1973). In the case of a Kolmogorov spectrum $\alpha \to 7$ after the cutoff. (Chandrasekhar, 1949). The calculation described in a later section assumes a complete cutoff in the spectrum.

At the cut off the following relationship holds.

$$\frac{1}{k^2_{max}\,\nu} \approx \frac{\theta^2 B_0^2}{8\pi} \bigg/ k_{max}\,V_A\,\theta^4\,\frac{B_0^2}{8\pi}$$

Using values of $\nu = 3 \times 10^{20}$ cm^2 s^{-1} (Chandrasekhar, 1949) and $V_A = 3 \times 10^6$ cm s^{-1} for the interstellar medium the value of the cutoff wave number k_{max} is ~ 350 pc^{-1}. The spectrum of turbulence in terms of θ is shown in figure 6.1.

6.4 The separation of neighbouring field lines

Jokipii (1973) has calculated the rate of separation of magnetic lines of force in a random magnetic field. He calculates the mean square rate of separation in terms of a magnetic field power spectrum. The probability distribution for the separation of two lines of force is assumed to obey a Fokker-Planck equation and Jokipii evaluates the Fokker-Planck coefficients for certain specific forms of the fluctuating magnetic field using a Monte Carlo approach. He concludes that for a power law spectrum $\propto k^{-\alpha}$ with $\alpha < 2$ the
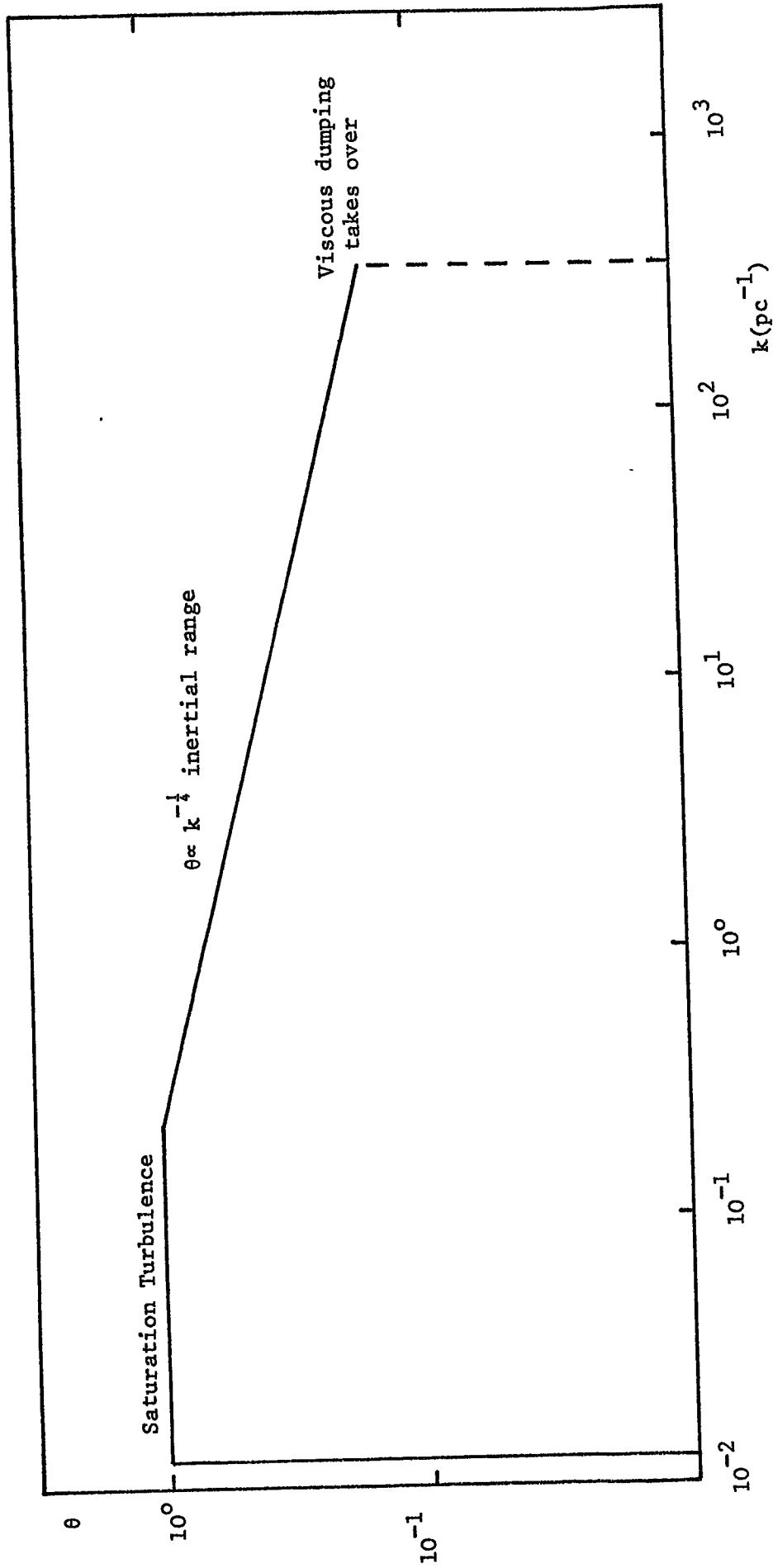
Figure 6.1: The spectrum of turbulence in the magnetic field.

rate of separation of the lines of force can be quite rapid and insensitive to the initial value of the separation.

Using a simplified approach Skilling et al (1974) have calculated the rate of separation of magnetic field lines using a Kolmogorov spectrum of turbulence without a cutoff. In the following a slightly modified version of the Skilling et al treatment is applied to the spectrum of turbulence defined in the previous section.

The separation of two initially parallel field lines due to one octave of waves, centred about a wavelength λ , is considered. The waves are considered to be correlated over a distance of $\sim$ one wavelength both parallel and perpendicular to the direction of the field. There are two cases to consider.

a)   If the initial separation, s_0, is greater than one wavelength, λ , then the angle between the two field lines will be given by θ , where θ is the amplitude of the turbulent field for the octave considered. The change in separation of the lines after a distance of one wavelength along the average field direction will be given by

$$\Delta s = \left\{ s_0^2 + \lambda^2 \tan^2\theta - 2s_0\lambda \tan\theta\cos\beta \right\}^{\frac{1}{2}} - s_0$$

where β is a random phase angle. The probability of the lines moving apart is greater than the probability of them converging. This is shown schematically in figure 6.2.

b)   If $s_0 < \lambda$, the angle between the two field lines will no longer be given by θ but will be some linear fraction of θ depending on s_0. The change in separation of the two field
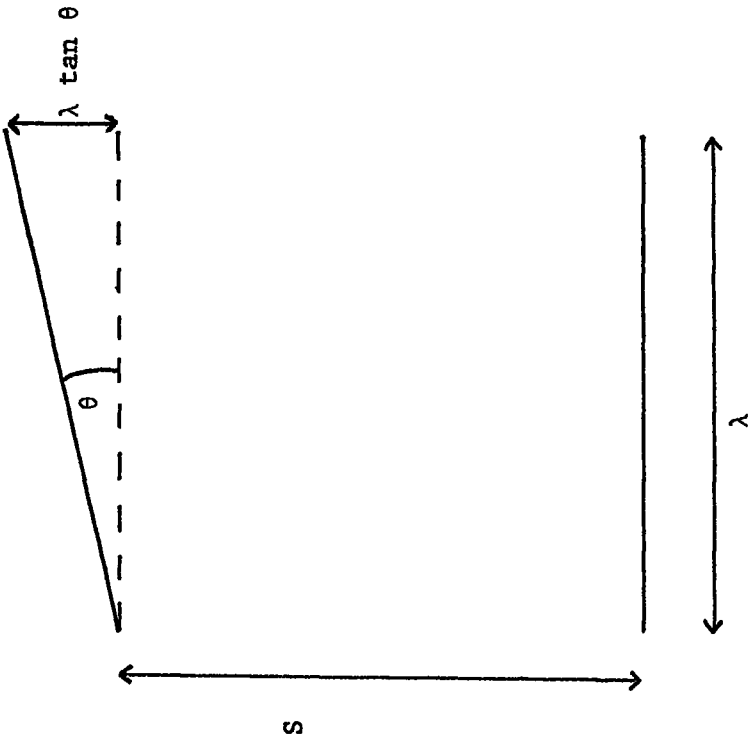
a) View normal to the plane of the field lines
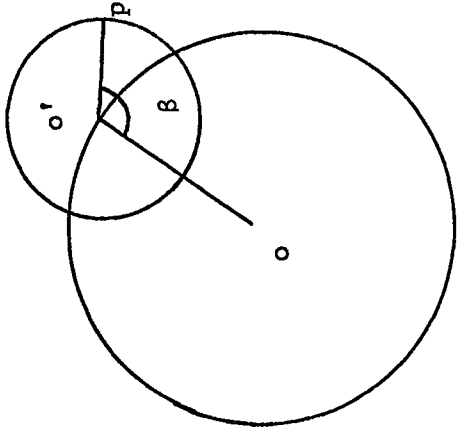
b) End view of separation

$oo' = s_o$

$o'p = \lambda\tan\theta$

Figure 6.2: Separation after 1 wavelength, $s > \lambda$

lines in this regime will now be given by

$$\Delta s = \left\{ s_0^2 + \lambda^2 \tan^2 \left(\frac{s_0 \theta}{\lambda} \right) - 2 s_0 \lambda \tan \left(\frac{s_0 \theta}{\lambda} \right) \cos \beta \right\}^{\frac{1}{2}} - s_0$$

The change in separation of two field lines due to the octave of waves about wave length λ after some distance Δr along the average field is now considered. If $\Delta r < \lambda$, the change in separation after Δr will be

$$\Delta s_\lambda = \frac{\Delta r}{\lambda} \Delta s$$

If $\Delta r > \lambda$, since the waves have a correlation length $\sim \lambda$ the change in separation may be calculated using a random walk calculation with $\Delta r / \lambda$ steps. The value of s_0 is modified by Δs at each distance λ along the field, the value of Δs being calculated for each step by generating a random phase angle .

The change in the separation Δs_λ for an initial separation s_0 after a distance Δr along the field may be calculated for each octave. The total change in the separation after a distance Δr due to the full spectrum of turbulence may then be calculated by adding the Δs_λ independently, each octave of waves being given a weighting appropriate to the spectrum. The initial separation may now be modified by some value Δs_T and the separation after a further distance Δr along the field may be calculated by repeating the process with the new s_0.

Using a value of 0.3 pc for Δr the separation of two field lines after a distance of 30 pc along the average field direction was calculated for several initial separations. The results are shown in table 6.1. The results

Table 6.1   The separation of magnetic field lines as a

function of initial separation

Initial Separation (pc)	Separation after 30 pc (1σ limits) (pc)	Mean Distance along field required for separation to be 100 pc (pc)
10^{-4}	$(2.2 \pm 0.9) \times 10^{-2}$	210
10^{-3}	0.16 ± 0.04	192
10^{-2}	0.52 ± 0.10	185
10^{-1}	1.43 ± 0.15	175
10^{0}	4.87 ± 0.28	150
10	23.17 ± 0.61	100

were found to be insensitive to a change in the value of
Δr used. Also shown in table 6.1 are the distances along
the average field one must go in order to achieve a separa-
tion of 100 pc.

6.5 Conclusions

Using the spectrum of turbulence derived in section 6.3
the rate of separation of field lines is found to be very
rapid for all initial separations corresponding to the
Larmor radii of particles with energies $\sim 10^{11}$ eV, agreeing
with the conclusions of Jokipii (1973) and Skilling et al
(1974).

If the total energy in the turbulence were calculated,
using the spectrum as derived in section 6.3, by summing the
contribution from each octave, the total energy would be
~ 20 times that in the regular component of the magnetic field.
This would directly contradict the observations we have at
the present time, i.e. the synchrotron radiation data, which
indicate a magnetic energy density in the turbulence of the
same order as that in the regular field. The rate at which
energy would have to be supplied to maintain the turbulence
would also be very large.

This contradiction may be overcome by a closer examina-
tion of the derivation of the spectrum which neglects many
factors of order 1. The derivation relies primarily on two
assumptions:-

(i) the amplitude of the field with length scale λ is given
by Θ.

(ii) each of the waves in the turbulence may be considered
to be statistically independent

The first assumption may be good for small θ but for
all $\theta \gtrsim 0.2$ radians, an amplitude of $\sin \theta$ may be a better
approximation. For waves with length scales $\lambda \gtrsim 0.1$ pc, it
is not at all certain that the turbulent waves in the inter-
stellar medium may be considered to be statistically indep-
endent, the energy density may not, therefore, be calculated
by simply summing over each octave independently. One is
not therefore able with any certainty to predict the spectrum
of turbulence for length scales $\lambda \gtrsim 0.1$ pc and the energy con-
dition may be satisfied since it is the turbulence with large
λ which contributes significantly to the energy density.

However, for a consideration of the rate of separation
of neighbouring field lines it is the turbulence with length
scales in the few octaves above the viscosity cutoff, i.e.
small λ, which are important. These length scales are almost
certain to be statistically independent, and apart from
occasional local input from supernovae explosions, will be
fed entirely by wave-wave interactions. They will then
follow a $k^{-3/2}$ law and the conclusions regarding the rapid
rate of separation of the field lines are not radically
altered.

A rapid mixing of field lines does not agree with the
model of coherent magnetic flux tubes discussed in the
previous chapter. The expected mode of propagation for
cosmic ray particles within a field with rapidly separating
field lines would be an isotropic 3-dimensional diffusion.

References

Behr, A., 1959 Nach. Akad. Wiss., Gottingham (Sonderabruck),
126, 201

Berge, G. L. and Seielstad, G. A., 1967 Astrophys. J., 148
367

Chandrasekhar, S., 1949 Astrophys. J., 110, 329

Jokipii, J. R., 1972 Proc. Conf. on Solar-Terrestrial
Relation, Calgary, August 1972

Jokipii, J. R., 1973 Astrophys. J., 183, 1029

Jokipii, J. R. and Lerche, I., 1969 Astrophys. J., 157, 1137

Jokipii, J. R., Lerche, I. and Schommer, R. A., 1969 Astrophys. J.
157, L119

Kolmogorov, A. N., 1941 Compt. Rend. Acad. Sci. URSS, 30,
301 and 32, 16

Kraichnan, R. H., 1965 Phys. Fluids, 8, 1385

Mathewson, D. S. and Ford, V. L., 1970 Mem. R. Astr. Soc.,
74, 139

Mutel, R. L., et al, 1974 Astrophys. J., 193, 279

Osborne, J. L., Roberts, E. and Wolfendale, A. W., 1973
J. Phys. A, 6, 421

Skilling, J., McIvor, I. and Holmes, J. A., 1974 Mon. Not. R.
Astr. Soc., 167, 87p

Thielheim, K. O. and Langhoff, W., 1968 J. Phys. A, 1, 694

Chapter 7   The role of plasma effects on cosmic ray propagation

7.1 Introduction

From the cosmic ray propagation model discussed in Chapter 5, it was found to be very improbable that a model which allowed free escape of cosmic rays from the edge of the galactic disk would give a small cosmic ray anisotropy coupled with a short lifetime in the Galaxy. An effective cosmic ray propagation model must include a process which inhibits the escape of particles across the boundaries of the diffusing region. Interpretation of the cosmic ray chemical abundance data shows that an exponential distribution of cosmic ray path length in the Galaxy must be predicted by any viable propagation model. A 'leaky-box' model gives the required path length distribution and repeated scattering from the leaky box walls may reduce the cosmic ray anisotropy to the observed low value. Skilling (1971) and Holmes(1974) have proposed that the partially transmitting boundaries of a 'leaky box' are formed by Alfvén waves in the ionised component of the interstellar gas.

The generation of plasma waves by cosmic rays in the Galaxy is discussed in section 7.2. The positions of the boundaries, following Holmes (1974), are calculated in section 7.3. The model is developed in the remaining sections of the chapter to include the possibility of diffusion in the galactic disk and discrete cosmic ray sources.

7.2 The generation of plasma waves by cosmic rays in the Galaxy

Since the energy density of the Galactic magnetic field

is very similar to that of the cosmic radiation, ~ 1 eV cm^{-3}, the cosmic radiation is expected to have an influence on the magnetic field. The effects of the cosmic rays on the field are investigated by treating the cosmic rays and the ionised component of the interstellar medium as collisionless plasmas which obey the Vlasov equation:

$$\frac{\partial f}{\partial t} + \frac{\partial}{\partial x} \cdot (f\underline{v}) + \frac{\partial}{\partial p} (f \frac{dp}{dt}) = 0$$

where $f(x,p,t)$ is the distribution function of the particles and dp/dt the force on the particles. Whenever the cosmic ray streaming velocity along the field exceeds a value $\sim V_A$, the Alfvén velocity, magneto-hydrodynamic (MHD) waves are generated (Lerche(1967), Wentzel(1968)). Wentzel (1969) shows that whenever the cosmic rays generate MHD waves, the cosmic rays will be scattered by the waves and thereby have their streaming velocity reduced.

The growth rate of MHD waves, in the cold plasma approximation, has been investigated by Kulsrud and Pearce (1969). They find the growth rate of the waves is given by

$$\Gamma_k = \sum 2\pi^2 q^2 (\frac{V_A}{c})^2 \sum_{n=-\infty}^{\infty} \int dp^3 \; V_\perp^2 \delta (\omega_k - k_{11}v_{11} - n\Omega)$$

$$\left\{ \begin{array}{c} J_n'^2(x) \\ \dfrac{n^2 J_n^2(x)}{x^2} \end{array} \right\} \left[\frac{\partial F}{\partial E} + \frac{k_{11}}{\omega_k p} \frac{\partial F}{\partial \mu} \right]$$

The first sum is over all the various cosmic ray species of charge q. The second sum is over the Bessel functions, J_n, the upper term applying to the magnetosonic mode and the lower one to the Alfvén mode. $F(p)$ is the cosmic ray momentum

distribution, E is the cosmic ray energy, Ω is the gyro frequency, μ is the pitch angle cosine, ω_k is the real part of the MHD wave frequency, V_{11} and $V_\perp$ are the cosmic ray velocities parallel to and perpendicular to the magnetic field and $x = k_\perp V_\perp / \Omega$. This result is valid under the conditions $V_A \ll c$, which is satisfied in the interstellar medium, and $\Gamma_k \ll \omega_k$.

From the δ-function, it is clear that only those cosmic rays which see a Doppler shifted frequency $\omega_k - k_{11} V_{11}$, which is an integral multiple of their cyclotron frequency Ω, can resonate with the wave. Since $\omega_k = k V_A \ll k_{11} V_{11}$, for $n \neq o$ the resonance condition may be replaced by

$$k_{11} = \frac{n\Omega}{V_{11}} \approx n/r_L \quad ,$$

where r_L is the cyclotron radius. For $n=o$, the resonance condition is that the wave has the same phase velocity as the particle, which only occurs for waves propagating nearly perpendicular to the magnetic field or for $V_{11} \approx V_A$. Only the cases $n = \pm 1$, 0 are important (Tademaru 1969).

In the cold plasma approximation the possibility of collisionless (Landau) damping of the waves is ignored. In fact, the magnetosonic mode is heavily damped by this process in interstellar space since the Alfvén velocity is much smaller than the electron thermal velocity. The Landau damping of the Alfvén mode is negligible. Kulsrud and Pearce (1969) find that the dominant linear damping process for the Alfvén waves in the interstellar medium is due to collisions between charged particles moving with the waves and neutral atoms. When the damping rate, Γ_D is much less than

the wave frequency, ω, the ion-neutral collision damping rate is

$$\Gamma_D = \begin{array}{ll} \nu_{in}/2 & \omega \gg \nu_{in} \\ \omega^2/2\nu_{in} & \omega \ll \nu_{in} \; n_i/n_H \end{array}$$

where $\nu_{in} = n_H \langle \sigma V_H \rangle$ is the ion-neutral collision frequency, n_H is the neutral particle number density, n_i is the ion and electron number densities and $\langle \sigma V_H \rangle$ is the average of the ion neutral interaction cross-section and thermal velocity.

If the cosmic ray generated Alfvén waves are to grow, the linear damping rate must be less than the growth rate. For a power law cosmic ray distribution function $F(p) \propto p^{-\gamma}$, Kulsrud and Cesarsky (1971) approximate the growth rate by

$$\Gamma_G = \frac{\pi}{4} \frac{\gamma-1}{\gamma} \; \Omega_H \; \frac{N(>p)}{n_i} \; \left(\frac{V_s}{V_A} - 1\right)$$

where $N(>p)$ is the integral cosmic ray number density and V_s is the cosmic ray streaming velocity. Taking $N(>p) \propto p^{-1.5}$, Kulsrud and Cesarsky find

$$\Gamma_G = \frac{1.69 \times 10^{-10}}{\varepsilon^{1.5}} \left(\frac{V_s}{V_A} - 1\right) s^{-1}$$

where $\varepsilon = cp$ is in units of GeV.

The damping rate Γ_D is also found to be of the order of $10^{-10} \; s^{-1}$ in the plane of the Galaxy, so that cosmic rays of energy greater than a few GeV cannot generate the waves necessary to reduce their streaming velocity to $\sim V_A$. Kulsrud and Cesarsky (1971) conclude that if cosmic rays of energy $\gtrsim 100$ GeV are confined to the Galactic plane by Alfvén waves, the waves must be generated by sources more powerful than the cosmic rays themselves.

Skilling (1971) has argued that the existence of more powerful wave sources to confine the higher energy cosmic rays in the Galaxy is not essential. The density of ionised and neutral particles decreases with height above the Galactic plane, thus Γ_G will increase and Γ_D decrease with height above the plane. As a consequence, Skilling argues that cosmic rays of energy greater than a few GeV need only travel a certain distance out of the plane before they encounter waves which will scatter them. He calculates the distribution function, f(x,p,t) of the cosmic rays in the presence of Alfvén waves by transforming the Vlasov equation to a frame of reference which is moving with the waves and expanding f in inverse powers of the particle-wave scattering frequency. The scattering frequency is determined by equating the growth rate of the waves with their damping rate in the equilibrium condition. The resulting equation for the distribution function is

$$\left(\frac{\partial}{\partial t} + w \cdot \nabla\right) f = \frac{1}{3}(\nabla \cdot w) p \frac{\partial f}{\partial p} - \frac{1}{p^3}\nabla \left[\left(\frac{\Gamma_D B_o}{4\pi^3 m_H \Omega_o V_A}\right) B_o \hat{n}\right] \quad (7.1)$$

where w is the wave velocity, $B_o \hat{n}$ represents the background magnetic field, m_H is the proton mass and p is the cosmic ray momentum. Equation 7.1 is the basic equation for the evolution of the cosmic rays whenever waves are present which resonate and confine the relevant particles. This domain of validity may be called the "wave zone". $\hat{n} \cdot \nabla f$ must be negative in the wave zone since a positive $\hat{n} \cdot \nabla f$ would lead to results such as a negative equilibrium wave energy density, caused by the basic implausibility of

supposing cosmic rays might stream up their own density gradient, instead of down.

The wave zone is contrasted with the "free zone" in which there are no self generated resonant waves and cosmic rays are able to stream freely along magnetic field lines at speeds $\sim$ the velocity of light, assuming no other scattering irregularities are present. A value, $\hat{n}.\nabla f = o$, may be expected in the free-zone as an initial approximation.

7.3 The location of the wave zone/free zone boundary

Equation 7.1 has been used to calculate the location of the wave zone – free zone boundary in the galaxy in the following way (Holmes 1974). Using the relationship between the cosmic ray density, $N(p)$ and the distribution function

$$N(p) = 4\pi p^2 f(p)$$

and assuming only the z-component of the gradients to be important, equation 7.1 reduces to

$$\frac{\partial N(p)}{\partial t} + V_A \frac{\partial N(p)}{\partial z} = \frac{1}{3} \frac{dV_A}{dz} \left[p\frac{\partial N(p)}{\partial p} - 2N(p) \right]$$

$$- \frac{4\pi}{p} \frac{d}{dz} \left[\frac{\Gamma_D B_o^2}{4\pi^3 m_H \Omega_o V_A} \right] \qquad (7.2)$$

$N(p)$ is assumed to follow a power law with exponent -2.5. Equation 7.2 may now be re-written,

$$\frac{1}{N(p)} \frac{\partial N(p)}{\partial t} + \frac{V_A}{N(p)} \frac{\partial N(p)}{\partial z} = -1.5 \frac{dV_A}{dz} - \frac{4\pi}{pN(p)} \frac{d}{dz}$$

$$\left[\frac{\Gamma_D B_o^2}{4\pi^3 m_H \Omega_o V_A} \right] \qquad (7.3)$$

Equation 7.3 is the equation for $N(p)$ in the presence of

waves. In the free zone, the equation for $N(p)$ may be approximated by $\frac{\partial N(p)}{\partial t}=0$, and $\frac{\partial N(p)}{\partial z}=0$ assuming free motion along field lines and a steady state has been attained.

At the boundary $N(p)$ must be continuous. Therefore, since

$$1.5 \frac{dV_A}{dz} + \frac{4\pi}{pN(p)} \frac{d}{dz} \left(\frac{\Gamma_D B_o^2}{4\pi^3 m_H \Omega_o V_A} \right) = 0 \qquad (7.4)$$

at the boundary, the position of the boundary may be estimated. In doing this, the following assumptions and approximations are made.

(i)   The spectrum of cosmic rays is the same everywhere in the free zone, the number density, as a function of energy, given by

$$N(p) = 12_\pi \times 10^{-11} \, p^{-2.5} \quad cm^{-3} \, GeV/c^{-1}$$

(ii) The damping of the Alfvén waves is due to ion-neutral collisions only and is given by

$$\Gamma_D = \tau n_n$$

where $\tau = 3 \times 10^{-9}$ s^{-1} cm^3 and n_n is the neutral particle density at any position in the interstellar medium.

(iii) The density of interstellar matter, neutral and

•   ionised, falls off smoothly as

$$n_n = n_{on} \exp\left(-z^2/z_{on}^2\right); \quad n_i = n_{oi} \exp\left(-z^2/z_{oi}^2\right)$$

where n_{on} is the neutral particle density and n_{oi} the ionised particle density in the galactic plane. It is further taken that

$$z_{on} = z_{oi} = 165 \text{ pc}, \quad n_{on} = 1 \text{ cm}^{-3}, \quad n_{oi} = 0.025 \text{ cm}^{-3}$$

(iv) The magnetic field has a component of strength 3×10^{-6} gauss in the z-direction at all heights, z, above the Galactic plane.

Our present observational knowledge of the interstellar medium is still very poor, especially with regard to such parameters as the rate of change of gas density with height above the Galactic plane, therefore these approximations should be considered as over simplifications of the actual conditions in interstellar space and any conclusions reached using them should be considered with caution. Some of the approximations used above are modified in the calculations presented in chapter 8.

The equation for the height of the boundary, Z_T, above the galactic plane, as a function of cosmic ray kinetic energy, T, now reduces to

$$\frac{Z_T}{Z_{oi}} = \left[\frac{1}{2} \ln \left(\frac{9}{G(T)} \right) \right]^{\frac{1}{2}} \tag{7.5}$$

where $G(T)$ is given by

$$G(T) = \frac{1}{4\pi g} \left\{ \left[(T^2+2Tm)(T+m)^{-1} + (T^2+2Tm)^2 (T+m)^{-3} \right] N(T) \right.$$

$$\left. - (T^2+2Tm)^2 (T+m)^{-2} \frac{dN(T)}{dT} \right\}$$

$$g = \frac{\tau n_{oi} n_{on}}{\pi^2 \Omega_o}$$

and m is the cosmic ray rest mass.

Following Holmes (1974), the probability of a cosmic ray reflecting when interacting with the boundary is taken to be $1 - 2 V_A/c$, where V_A is evaluated at the boundary. (The transmission probability is given by the value of the streaming velocity in the wave zone, of which $2V_A$ is an estimate, divided by the particle velocity in the free zone. The streaming velocity in the wave zone is considered in

more detail in Chapter 8.) At each interaction with the
boundary, the cosmic rays will lose an energy $\sim V_A/c$ x the
energy of the incident particle to the waves due to the
particle-wave interaction. This energy loss is not taken
into account in the calculations presented in this thesis.
An order of magnitude estimate indicates that each cosmic
ray would probably lose only half its energy due to inter-
actions with the boundary during its lifetime in the Galaxy.

Estimates of the boundary heights above the plane and
the probability of reflection are shown as a function of
cosmic ray kinetic energy in Table 7.1

7.4 Three dimensional diffusion within the "free zone"

Given that the cosmic rays are able to generate Alfvén
waves which form effective boundaries at given heights above
the Galactic plane, the problem of the propagation of the
cosmic rays in the free zone may be approximated by a
three dimensional diffusive motion, due possibly
to the interstellar turbulence discussed in the previous
chapter, in a leaky box, with the probability of reflection
from the walls of the box as shown in table 7.1 The solution
to the three-dimensional diffusion equation in a region,
where there are partially reflecting boundaries in the z-
direction and which extends to ∞ in the x and y directions,
containing sources of cosmic rays which are instantaneous
in space and time is given by

$$N(r,t) = \sum_{\text{all sources}} s(r_n, t_n) \left(\frac{3}{4\pi \ell_{11} c(t-t_n)} \right) \exp \left[\frac{-3(x-x_n)^2 - 3(y-y_n)^2}{4\ell_{11} c(t-t_n)} \right]$$

Table 7.1   Boundary height and probability of reflection as
             a function of energy

Energy (GeV)	Boundary Height (pc)	Probability of Reflection
10	275	.9989
10^2	350	.9973
10^3	400	.9936
10^4	450	.9836

$$\sum_{j=1}^{\infty} \frac{\left\{ \sin\frac{\lambda_j z_n}{2a} + \frac{\lambda_j}{2aK}\cos\frac{\lambda_j z_n}{2a} \right\} \left\{ \sin\frac{\lambda_j z}{2a} + \frac{\lambda_j}{2aK}\cos\frac{\lambda_j z}{2a} \right\} \exp\left[\frac{-\lambda_j^2 D_\perp (t-t_n)}{4a^2} \right]}{\int_0^{2a} \left\{ \sin\frac{\lambda_j z}{2a} + \frac{\lambda_j}{2aK}\cos\frac{\lambda_j z}{2a} \right\}^2 dz}$$

(7.6)

where: (i)   z has been defined so that the Galactic plane

is at z=a and the reflecting boundaries are at

z=o and z=2a

(ii)   the reflection probability is r

(iii) $K = \frac{V_\perp}{D_\perp}\left\{ \frac{1-r}{1+r} \right\}$

(iv)   the λ_j are given by the roots of

$\tan \lambda = \frac{2K\lambda(2a)}{\lambda^2 - (2Ka)^2}$

(v) ℓ_{11} is the diffusion mean free path parallel to

the Galactic plane

(vi) $D_\perp$ is the diffusion coefficient perpendicular to

the Galactic plane

(vii) $V_\perp$ is the particle velocity perpendicular to the

Galactic plane and is taken to be c/3.

(viii) $S(r_n, t_n)$ is the strength of the source.

In this chapter the diffusion coefficient is assumed to

be isotropic and diffusion coefficients equivalent to diffu-

sion mean free paths of 30 pc and 10 pc are used in the cal-

culations. (The diffusion coefficients which result from a

consideration of the spectrum of turbulence discussed in

chapter 6, and which will have an energy dependence, are

introduced as a modification to the propagation model in chapter 8).

Using equation 7.6 one is able to calculate the relative contribution to the cosmic ray flux of any source R pc from the sun and age τ. Figure 7.1 shows contour maps of the levels of contribution of individual sources to the cosmic ray flux (assuming each source has the same strength) as a function of distance and age. For example a source at a distance of 100 pc will contribute 100 times more particles at 100 GeV if it is $\sim 4 \times 10^5$ years old than if it is 6×10^6 years old. Similarly for sources $\sim 10^5$ years old, a source ~ 600 pc from the sun will contribute 100 times more particles than a source which is 1.5 kpc from the sun.

7.5 Trial calculation

A trial calculation for a given distribution of sources in space and time may be made to test the validity of the approximations made regarding the constancy in space and time of the cosmic ray flux in the free zone whilst considering 3-dimensional diffusion in the free zone. If one assumes that supernova explosions are the source of cosmic rays one can derive a source distribution from the positions of observable supernova remnants. The total contribution to the cosmic rays from these "observed" sources may be calculated. However, when this contribution is compared to that expected from the total number of supernovae giving appreciable contributions, it is found to be very small indeed. This is due to the fact that sources up to an age of $\sim 5 \times 10^6$ years contribute significantly, whereas observable
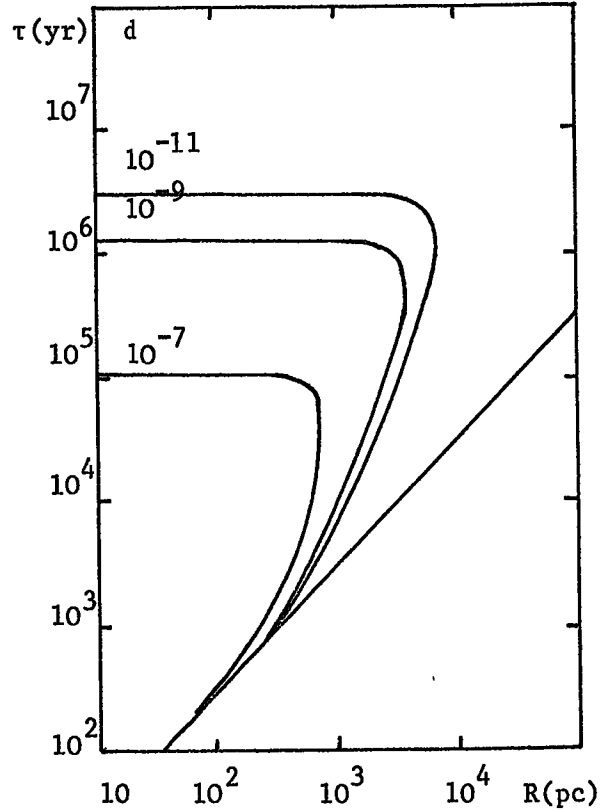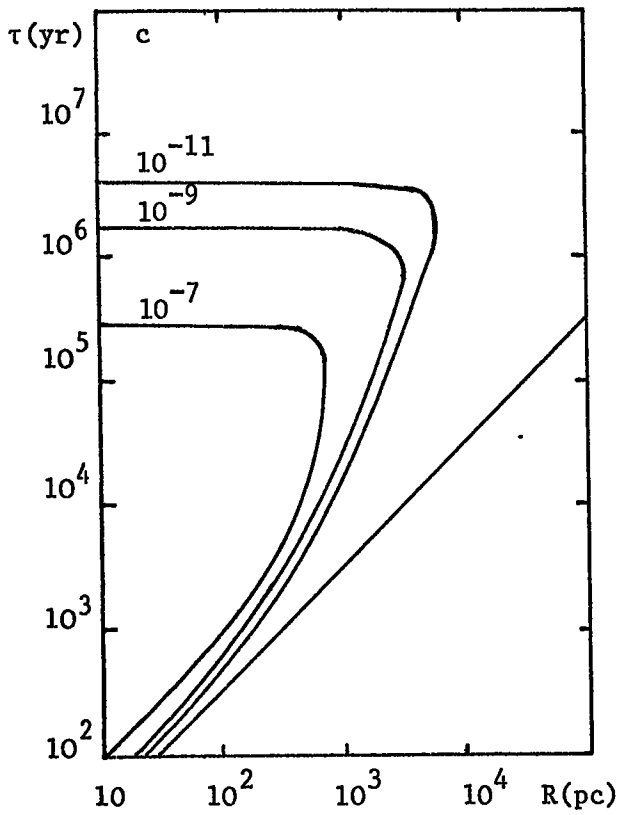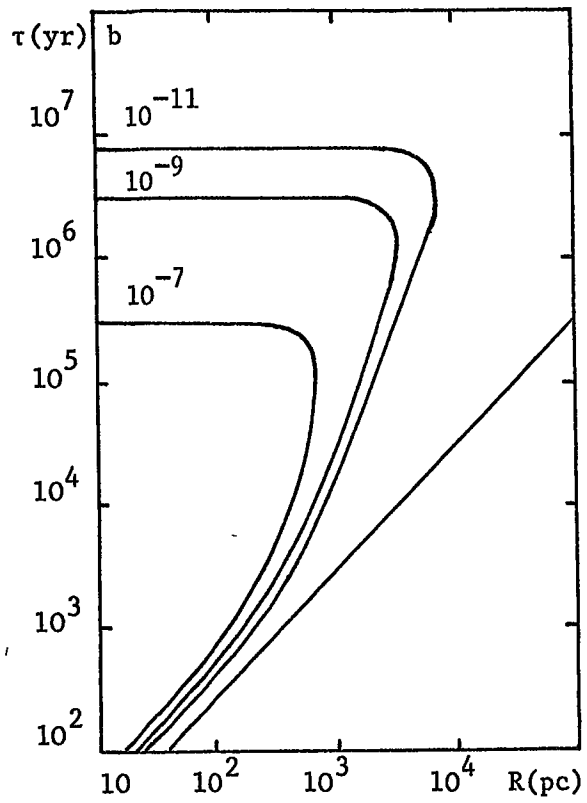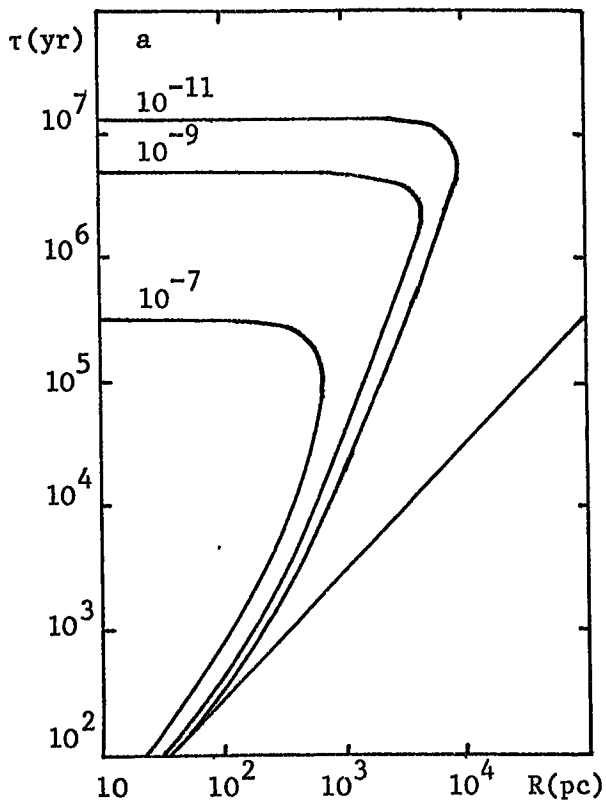
Figure 7.1: Contours showing the contribution (in arbitrary units) of sources of age τ and distance R from the sun.

a) Energy $\simeq 10^2$ GeV, λ=10pc   b) Energy $\simeq 10^3$ GeV, λ=10pc

c) Energy $\simeq 10^4$ GeV, λ=10pc   d) Energy $\simeq 10^4$ GeV, λ=30pc

supernovae remnants fade away after a few x 10^5 years.
Therefore, in order to calculate the expected dependence
of the concentration, anisotropy and matter traversed of
the cosmic rays as a function of energy it is necessary to
use a randomly generated source distribution. In this
trial calculation a source distribution was used which
consisted of initially 50,000 sources* within a 5 kpc
radius of an observer's position and within 100 pc of the
Galactic plane. A supernova rate of one supernova per
50 years in the Galaxy was assumed.

Using the same source distribution for all energies
the concentration, age and anisotropy in the Galactic
plane at the centre of the source distribution, the con-
centration at the boundary and at 10 pc from the boundary
were calculated as a function of time using time steps of
5.4×10^3 years. The required number of new sources was
generated at each step, the existing sources having their
age modified at each step in time.

At each energy the concentration at the boundary was
found to be less than at the galactic plane and there was
a finite negative value of $\partial n / \partial z$ which was not very time
dependent at the boundary. The effect of these two results
is that the energy, T, for which the boundary is at a given
height Z_T has been overestimated. This can be seen by con-
sidering equation 7.4. The boundary was initially calculated
for a momentum p using the term

$$p \; N(p) \; 1.5 \; \frac{dV_A}{dz}$$

* on average uniformly distributed

Now at the same boundary height the corresponding cosmic

ray momentum is p' and this term is replaced by

$$p' \; N(p') \; 1.5 \; \frac{dV_A}{dz} + \; p' \; V_A \; \frac{\partial N(p')}{\partial z}$$

which can be rewritten

$$p' \; N(p') \left[1.5 \; \frac{dV_A}{dz} + \frac{V_A}{N(p')} \; \frac{\partial N(p')}{\partial z} \right]$$

Generalising to the case of a cosmic ray spectrum $\alpha p^{-\gamma}$ the

required correction factor $\delta = p'/p$ is therefore given by

$$\delta = \left[1 + \frac{\frac{V_A}{N(p')} \; \frac{\partial N(p')}{\partial z}}{\frac{(\gamma+2)}{3} \; \frac{dV_A}{dz}} \right]^{\gamma-1}$$

The factor $\frac{1}{N(p')} \; \frac{\partial N(p')}{\partial z}$ is evaluated at the boundary from

the results of the calculation. V_A and $\frac{dV_A}{dz}$ are evaluated

at the boundary. The correction factors to the energy

were found to be small, i.e. $\leqslant$ factor of 2. Compared to the

accuracy with which other important parameters in the cal-

culation (e.g. the transmission probability, the gas density

fall-off and hence the boundary positions) are known, the

correction factors are small and are therefore neglected.

However, the correction factor was found to increase with

decreasing diffusion mean free path. Whenever $1/N(p)$

$\partial N(p)/\partial z$ evaluated at the estimated boundary position becomes

$\sim \frac{\gamma+2}{3V_A} \; \frac{dV_A}{dz}$, no boundary is formed by cosmic rays at that energy

and the diffusion problem becomes one of free escape at some

height above the galactic plane. The cause of the $\partial N/\partial z$ term

is the diffusion approximation. $\partial N/\partial z$ is found to increase with

decreasing diffusion mean free path and no boundary will form whenever the diffusion mean free path $\leqslant 1$ pc. This may be considered in another way. The transmission probability is approximated by the streaming velocity in the wave zone divided by the streaming velocity in the free zone. If the diffusion coefficient in the free zone is small the streaming velocity in the free zone is $<<c$ and hence the transmission probability tends to 1, which is the condition that no reflecting boundary will form.

The mean values, together with the maximum and minimum values, of the concentration in the Galactic plane, the anisotropy and the mean age of the cosmic rays, over a period of time of 10^5 years covered by the calculation are plotted as a function of energy in figure 7.2. The manner in which the concentration falls off is seen as the way in which the propagation modifies the source spectrum; the source spectrum used in the calculation was energy independent. The mean age and amount of material traversed are on the low side of the observed cosmic ray values, but are seen to decrease with energy in a manner not inconsistent with the most recent observations. The amount of material traversed is simply estimated by calculating the amount of matter the cosmic ray would see if it travelled between the boundaries at the velocity of light and multiplying this by the number of times it would be able to cross the free zone at the speed of light in the mean age. The calculated values of the anisotropy fluctuate over 2 orders of magnitude and also fluctuate widely in direction in the Galactic plane. The anisotropy in the z-direction is reduced to a very low level
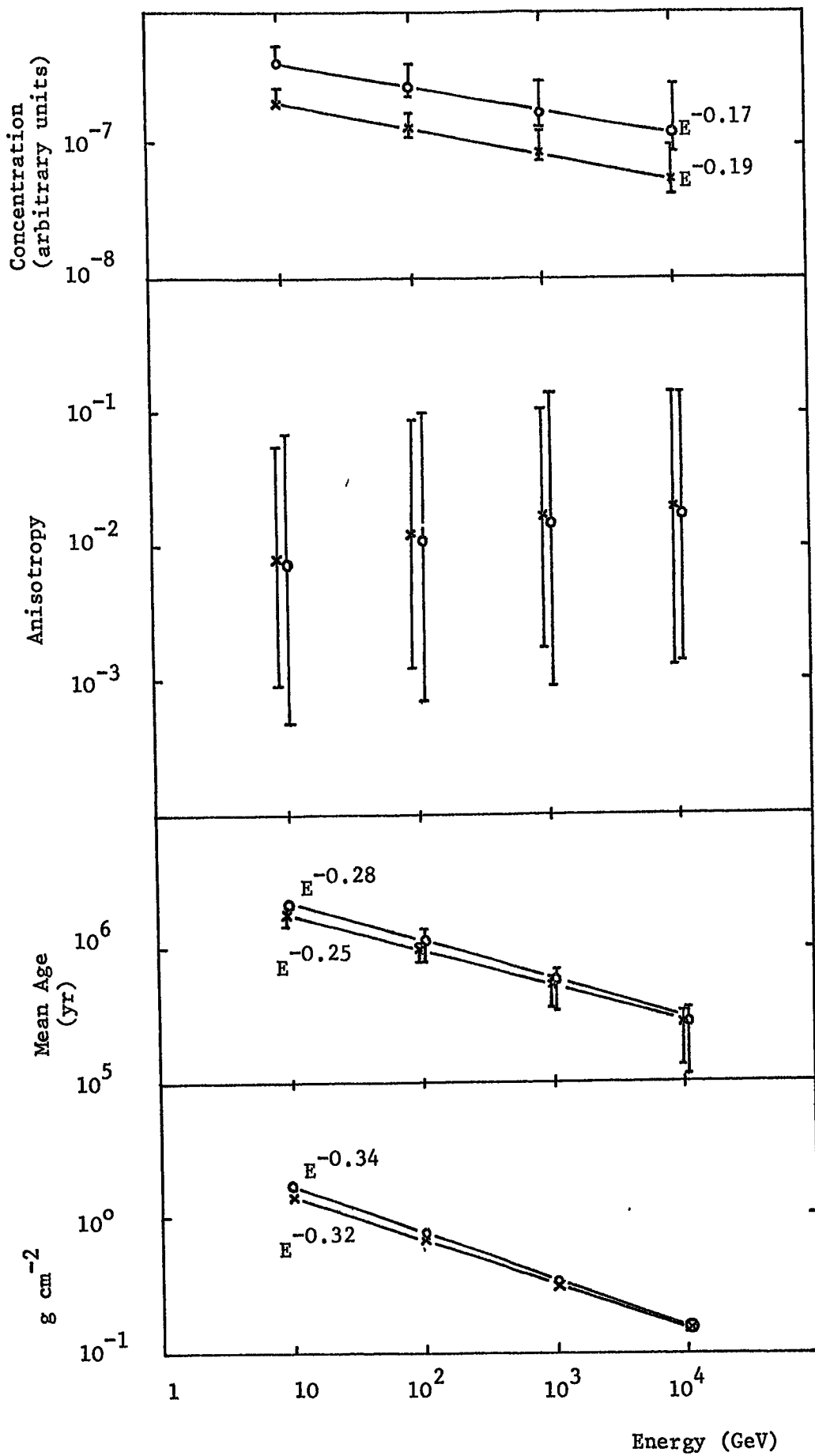
**Figure 7.2:** Results of a time dependent calculation. The upper and lower limits refer to maximum and minimum values.

x λ=30 pc

0 λ=10 pc

by the boundaries. The minimum values calculated are within a factor of $\sqrt{2}$ of the experimental upper limits, however the fraction of the time that the anisotropy is in this range is only small, ~ 0.1–0.2.

From the results of the calculation the value of $\frac{1}{n} \frac{\partial n}{\partial t}$ evaluated at the boundary was compared with the magnitude of $1.5 \, dV_A/dz$ to test the validity of neglecting $\frac{1}{n} \frac{\partial n}{\partial t}$. The ratio

$$\frac{\text{mean value} \left| \frac{1}{n} \frac{\partial n}{\partial t} \right|}{1.5 \, \frac{dV_A}{dz}}$$

is shown in table 7.2 for each energy. It is found that the term $\frac{1}{n} \frac{\partial n}{\partial t}$ in equation 7.3 is not completely negligible, especially at the lower energies. The effect of this term, is that as the concentration at the boundary fluctuates due to the fluctuating source distribution, the boundary position for each energy fluctuates about the mean position shown in table 7.1. A boundary which fluctuates in position with time complicates the solution to the diffusion equation considerably. In the calculations presented in chapter 8, the $\partial n/\partial t$ effect is again neglected, the fluctuations in boundary position assumed to be small and slow for the greater part of the time.

In conclusion, it is plausible that cosmic ray generated Alfvén waves can confine cosmic rays to the Galaxy by forming partially reflecting boundaries above and below the plane of the galaxy provided the scattering in the disk is not too great. No consideration has yet been made for the effect of possible non-linear damping effects on the waves and the

Table 7.2 Comparison of calculated $\frac{1}{n}\frac{\partial n}{\partial t}$ at the boundary with $1.5 \frac{dV_A}{dz}$

Energy (Approx) (GeV)	Diffusion m.f.p. (pc)	mean $\dfrac{\frac{1}{n}\frac{\partial n}{\partial t}}{1.5 \frac{dV_A}{dz}}$	Fraction of time $\left\|\frac{1}{n}\frac{\partial n}{\partial t}\right\| < \frac{1}{3} \; 1.5 \frac{dV_A}{dz}$
10	30	1.591	0.08
10^2	30	0.404	0.39
10^3	30	0.197	0.84
10^4	30	0.087	1.00
10	10	.785	0.28
10^2	10	.265	0.71
10^3	10	.146	0.82
10^4	10	.085	0.93

assumptions regarding the cosmic ray and interstellar medium
parameters require some modification.

References

Holmes, J. A., 1974   Mon. Not. R. Astron. Soc., 166, 155

Kulsrud, R. M. and Cesarsky, G. J., 1971   Astrophys. Lett., 8, 189

Kulsrud, R. M. and Pearce, W. P., 1969   Astrophys. J., 156, 445

Lerche, I., 1967   Astrophys. J., 147, 689

Skilling, J., 1971   Astrophys. J., 170, 265

Tademaru, E., 1969   Astrophys. J., 158, 959

Wentzel, D. G., 1968   Astrophys. J., 152, 689

Wentzel, D. G., 1969   Astrophys. J., 156, 303

Chapter 8 Energy dependent propagation models for cosmic

rays in the Galaxy

8.1 Introduction

The galactic confinement model for cosmic rays, postulating confinement by cosmic ray generated Alfvén waves, introduced in the previous chapter may be extended. In this chapter the effect on the propagation model of using some improved parameters for the cosmic rays and interstellar medium is assessed. In section 8.2 the effect on the position of the reflecting boundaries of variation in the gas density in the Galaxy is considered. In section 8.3 non-linear damping of the Alfvén waves is considered and in section 8.4 the diffusion coefficients expected in the Galactic disk due to a possible spectrum of interstellar turbulence are discussed. Idealised models of cosmic ray propagation are then constructed in the light of the modified parameters and calculations are carried out which enable the model predictions to be compared with the observed properties of the cosmic radiation.

8.2 The variation in boundary position due to variation in

the interstellar gas density

The variation in the estimated boundary position as a function of Galactic radius may be investigated by considering the variation of the interstellar gas density in the Galactic plane, $n_{oII}(R)$ and the variation in the scale height of the gas.

The variation in neutral gas density in the Galactic plane is taken to follow the distribution shown in figure 8.1. The half-thickness of the neutral gas is taken to be constant at 135 pc for Galactic radii <10 kpc and to rise linearly with Galactic radius at radii >10 kpc, reaching a value of 600 pc at 15 kpc Galactic radius. The boundary position above the Galactic plane is calculated as a function of Galactic radius and cosmic ray energy using the same parameters for the cosmic ray flux and interstellar magnetic field as in chapter 7. The result of this calculation is shown in figure 8.2. An increase in the concentration of H_2 at Galactic radii ~5 kpc will not affect the position of the boundary since the scale height of the H_2 is only half that of the neutral Hydrogen and the H_2 is confined mainly to dense clouds.

The boundary position oscillates slowly for radii ≤10 kpc, but rises rapidly at radii >10 kpc. As is the case for the boundary which fluctuates in position with time, the boundary which is not a simple geometrical shape is difficult to deal with simply in a diffusion equation. Consequently, in the propagation models which are presented in the latter part of this chapter, the boundary for a given cosmic ray energy is taken to be at a height above the Galactic plane which is constant with Galactic radius in order that an analytical solution to the diffusion equation may be used. This simplification may not greatly affect the prediction of such observable cosmic ray parameters as the anisotropy and mean age since the increase in confining volume may be compensated
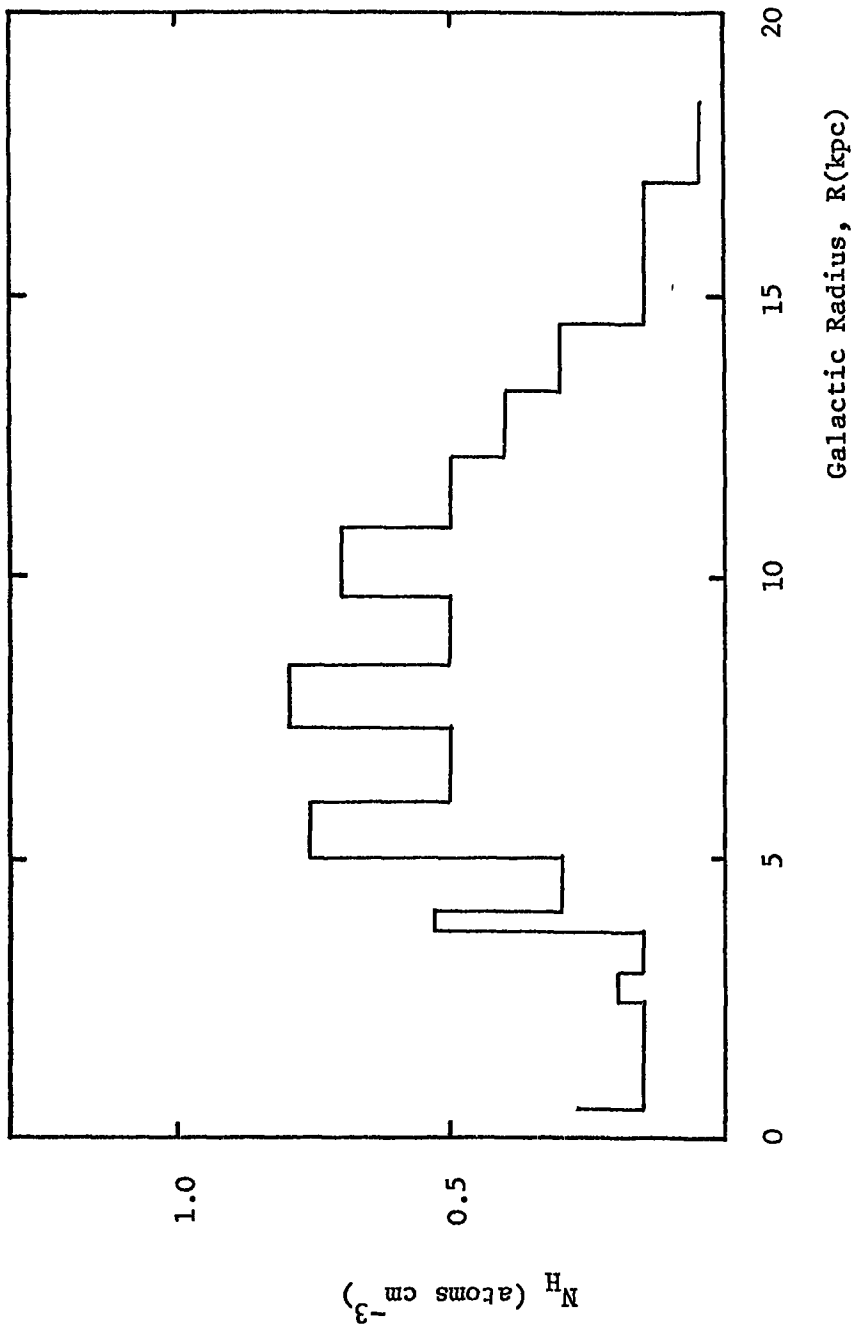
**Figure 8.1:** Distribution of the density of neutral hydrogen in the Galactic Plane.

For R<8 kpc, the summary of recent observations by Puget and Stecker (1974)

has been used, for R>8 kpc the distribution is given by Westerhout (1970).
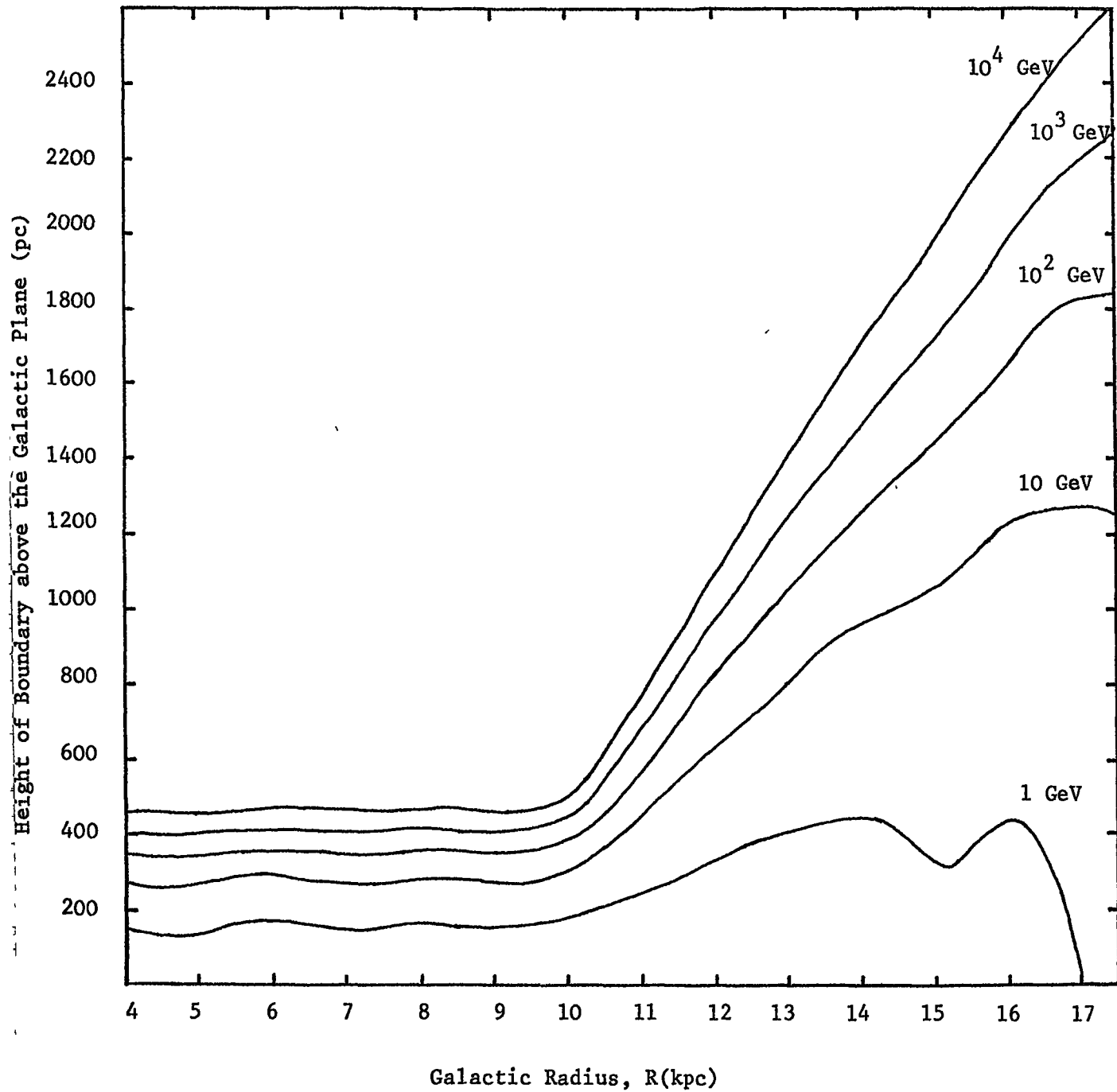
Figure 8.2: Calculated boundary height above the Galactic Plane as a function of Galactic Radius and cosmic ray energy.

for in the Galactic situation by a smaller mean gas density
and an increased cosmic ray diffusion coefficient, if the
turbulence is not so effective, at Galactic radii ≥ 10 kpc.
It would however have a great effect on any calculation to
predict the synchrotron radiation from cosmic ray electrons
in the interstellar magnetic field at high galactic latitudes
in the anti-centre direction. In any such calculation the
full geometry of the confining region would need to be
included.

8.3 The damping of Alfvén waves

Wentzel (1974) has investigated the damping of cosmic
ray generated Alfvén waves in the interstellar medium and
the resulting streaming velocity of the cosmic rays in the
presence of the waves. If the Alfvén waves were not damped,
the cosmic rays would stream at a velocity $\frac{1}{3}$ $(\gamma + 2)$ V_A where
γ is defined by the cosmic ray differential spectrum, $N(p) \propto p^{-\gamma}$
and V_A is the Alfvén velocity. In the presence of damping
in the galactic disk due to friction between the ionised and
neutral hydrogen, the streaming velocity becomes

$$< V > = \frac{1}{3} (\gamma + 2) V_A + \frac{0.19}{\gamma - 1} \left[\frac{T}{10^3 K} \right]^{0.4} \cdot \frac{n_i^{\frac{1}{2}} n_H}{N(>p)}$$

where T is the temperature of the interstellar medium, n_i
is the ionised gas density and n_H is the neutral gas density.

When the neutral gas density becomes very small, non
linear wave-wave interactions are found to dominate the dis-
sipation of Alfvén waves. Whereas for the damping by neutral
hydrogen, the wave spectrum decay rate $-\partial m_k / \partial t \propto m_k n_H$, for
the wave-wave interactions $-\partial m_k / \partial t \propto m_k^2$ where m_k is the

energy density of the waves with wave number k. Wave-wave interactions exist no matter how low the flux of particles may be. This form of wave dissipation may be understood in the following way. The gas pressure is much less than the magnetic pressure, hence the velocity of sound is slow compared to the Alfvén velocity. To first order in wave amplitude, $\underline{B}_1$, the Alfvén waves are compression free. In next order, the grad B_1^2 due to one wave yields some acceleration of gas along $\underline{B}$. This is a forced oscillation travelling at V_A. However, when two oppositely directed Alfvén waves are superposed, the forced oscillation is nearly a standing wave and may disperse as a sound wave. Expressed in terms of phonons, this interaction is the decay of a forward Alfvén wave, i.e. travelling in the direction of the cosmic rays, into a forward sound wave plus a backward travelling Alfvén wave with a slightly longer wavelength. The backward Alfvén wave can similarly decay into a backward sound wave and a forward Alfvén wave with an even longer wavelength. Thus a cascade arises in which Alfvén waves are degraded to ever lengthening wavelength and the resulting sound waves are dissipated in the interstellar medium.

The resulting wave decay rate from this process has been formally derived by Chin and Wentzel (1972). Wentzel (1974) finds that, for a magnetic field of 3×10^{-6} gauss and a cosmic ray density similar to that near the sun, an extra term

$$56 \times 10^5 \ (100 \ \text{pc}/L)^{\frac{1}{2}} \ (p/mc)^{\frac{\gamma+1}{2}} \ \text{cm s}^{-1}$$

is added to the streaming velocity of the cosmic rays in the
wave zone, where m is the cosmic ray mass in GeV, p is the
cosmic ray momentum in GeV and L is the scale height of
particles in the wave zone. The value of L is not known
and in the calculations which follow a wide range of values
for L have been used. Wentzel suggests a value between
100 pc and 1 kpc as the most probable though ultimately L
should be computed from the dynamics of gas and cosmic rays.

An estimate of the streaming velocity of the cosmic
rays in the wave zone is therefore given by

$$<V> = \frac{1}{3}(\gamma+2) V_A + \frac{0.19}{\gamma-1} \left[\frac{T}{10^3 K}\right]^{0.4} \frac{n_i^{\frac{1}{2}} n_H}{N(>p)} +$$

$$56 \times 10^5 \left[\frac{100 \text{ pc}}{L}\right]^{\frac{1}{2}} \left[\frac{p}{mc}\right]^{-\frac{\gamma+1}{2}} \text{cm s}^{-1} \qquad (8.1)$$

A better estimate of the transmission probability at
the wave zone-free zone boundary than the $2V_A/c$ used in
Chapter 7 is therefore given by $<V>/c$[*], where $<V>$ is
evaluated using parameters of the interstellar medium and
cosmic rays at the boundary. The position of the boundary
is not changed by the addition of wave-wave effects, only
its effectiveness in reflecting cosmic rays is altered.

Skilling (1975) has re-examined the motion of cosmic
rays through a moving magnetised medium supporting a
spectrum of hydromagnetic waves and finds that Fermi
acceleration can greatly modify adiabatic energy losses
which have conventionally been thought to accompany con-
vective motion of cosmic rays. This reinforces the argument
for not considering energy loss by the cosmic rays on their

[*] see footnote on page 135

interaction with the boundary.

8.4 The diffusion mean free path in the presence of turbulence

In a turbulent medium, cosmic rays will scatter on turbulence with a wavenumber k of the order of (cosmic ray larmor radius)$^{-1}$ in a resonant manner. If the larmor radius is r_L and θ is the amplitude of the turbulence with wavenumber $k(\sim 1/r_L)$, the mean free path along a magnetic field line will be $\sim r_L/\theta^2$ (Skilling, private communication). Thus for the spectrum of turbulence shown in figure 6.1, the diffusion mean free path along the magnetic field for a cosmic ray with energy $\sim 3\times 10^7$ GeV would be ~ 30 pc. Field lines which are close together at some point in space are expected to separate sufficiently rapidly that the diffusion can be considered to be isotropic due to a particle moving a distance $\sim r_L$ perpendicular to its field line after each scatter. At an energy of 3×10^7 GeV the motion of a cosmic ray particle in the disk of the Galaxy may therefore be approximated by an isotropic 3-dimensional diffusion with a scattering mean free path of 30 pc. For cosmic rays with energies of $\sim 10^3$ GeV the diffusion mean free path would be 0.2 pc. For cosmic rays with energy $< 3\times 10^7$ GeV but greater than an energy corresponding to a larmor radius $r_c \sim 1/k_c$, where k_c is the wavenumber at which the spectrum of turbulence cuts off, the diffusion mean free path will be $\propto (\text{Energy})^{\frac{1}{2}}$.

Particles with a larmor radius $< r_c$ will not be able to interact with the turbulence as frequently as those with larmor radius $> r_c$ since the turbulence will be very weak. The diffusion coefficient along the field lines will

increase with decreasing energy hence particles will not
be scattered from one field line to another as often as at
higher energy. Also in this regime the rate of separation
of neighbouring field lines will not be quite as fast as
for the larger separations. As a consequence the three
dimensional diffusion coefficient will increase with de-
creasing energy. The exact dependence of the increase as
a function of energy will depend critically on the spectrum
of turbulence at wave-numbers greater than the cut off
wave number and the exact rate of separation of field lines.
In the model calculations the energy dependence of the
diffusion coefficient is assumed to be $\propto(\text{energy})^{-2}$ for
particles with larmor radii $< r_c$.

The position of the cut off in the spectrum of tur-
bulence is dependent on the kinematic viscosity of the
interstellar medium, which is in turn dependent on the
interstellar gas density and temperature. The interstellar
gas density and temperature vary widely throughout the
Galaxy and the appropriate value of the kinematic viscosity
is not known to better than a factor ~ 10. In view of these
uncertainties in the position of the cut off in the spectrum
of turbulence, two values of the cut off wavenumber have
been assumed for the model calculations which follow. It
may, in fact, prove easier to establish a limit to the cut
off wave number from the constraints imposed on the model
by the cosmic ray data, than to deduce the kinematic vis-
cosity from the parameters of the interstellar medium as
they are known at the present. In the model calculations

the spectrum of turbulence is assumed to cut off at wave-numbers corresponding to the inverse larmor radii of particles with an energy of 10^3 GeV (Models labelled I) and 300 GeV(II). The cosmic ray diffusion mean free paths as a function of energy resulting from these assumptions are shown in table 8.1. At low energies, $\sim$ few GeV, the rate of separation of magnetic field lines and large scale magnetic field features may provide an upper limit to the diffusion mean free path of $\sim$50 pc.

In the following model calculations, an arbitrary limit on the vertical extent of the turbulence above the plane of the Galaxy of $\pm$ 450 pc is imposed on models I & II. Further models are introduced which allow the turbulence to be effective only within $\pm$ 250 pc of the Galactic plane (Model III) and $\pm$ 150 pc of the Galactic plane (Model IV). Limits of this order on the effectiveness and extent of the turbulence may arise if (i) most of the sources of turbulence are close to the Galactic plane and (ii) conditions in the interstellar medium at large distances from the Galactic plane are such that the cut off in the turbulence spectrum occurs at much smaller wavenumbers than in the Galactic plane. These limits are of greatest importance when the concept of a partially reflecting boundary breaks down at energies $\sim$ few hundred GeV.

8.5 Idealised Models of cosmic ray propagation in the Galaxy

In this section idealised models of the propagation of cosmic rays in the Galaxy are presented. Calculations based on these models show the expected variation in the observable properties of the cosmic rays due to a variation in the

Table 8.1   Diffusion mean free paths (pc) as a function
of cosmic ray energy derived from the spectrum
of turbulence

Energy (GeV)	Model I	Model II
1	50	50
3	50	50
10	50	50
30	50	12
100	20	1.33
300	2.22	0.12
10^3	0.20	0.20
3×10^3	0.35	0.35
10^4	0.63	0.63

propagation parameters which are not uniquely determined by the known parameters of the interstellar medium. Limits may then be set to some of these parameters by comparing the model predictions with the observed cosmic ray properties.

Each model is classified by a capital letter, A to F, representing variation in the boundary conditions of the confining region of the cosmic rays or in the cosmic ray source distribution, and by a Roman numeral, I to IV, representing variation in the diffusion parameters due to the interstellar turbulence spectrum. The features of each model are indicated in table 8.2. For each model the cosmic ray concentration (in arbitrary units) at the position of the earth in the Galaxy, the anisotropy, mean age, and mean amount of matter traversed by the cosmic rays are calculated as a function of cosmic ray energy. The "concentration at the earth" is the factor by which the source spectrum of cosmic rays, i.e. the number of particles emitted as a function of energy by the source, is multiplied to give the spectrum at the earth.

8.5.1 Models A and B

In models A and B the confining region of the cosmic rays is a disk extending to infinite radius with partially reflecting boundaries above and below the plane of the disk. The reflecting boundaries are considered to be due to cosmic ray generated Alfvén waves and the boundary position as a function of cosmic ray energy is calculated using the method described in Chapter 7, with the following parameters for the interstellar medium.

Table 8.2   Classification of idealised models for cosmic ray propagation

Model	Geometry of confining region	Value of L assumed	Source Distribution
A	Reflecting Boundaries at $\pm Z_T$ Extending to ∞ radius in plane of Galaxy	10^4 pc	uniform within 12 kpc of Galactic Centre
B	As A	100 pc	As A
C	Reflecting Boundaries at $\pm Z_T$ and at Galactic radii of 15 kpc	2500 pc	As A
D	As C	500 pc	As A
E	As C	500 pc	Exponential
F	Spiral arm structure	500 pc	Exponential

Model I : Cut off in spectrum of turbulence at wave number corresponding to inverse Larmor radius of 10^3 GeV cosmic ray

Model II : Cut off in spectrum of turbulence at wave number corresponding to inverse Larmor radius of 300 GeV cosmic ray

Model III : Turbulence only effective in regions within ±250 pc of Galactic Plane

Model IV : Turbulence only effective in regions within ±150 pc of Galactic Plane

The scale height of the neutral gas, $Z_{on} = 150$ pc

The scale height of the ionised gas, $Z_{oi} = \sqrt{2}\ Z_{on}$

The neutral gas density in the Galactic plane, $n_{on} = 1$ cm^{-3}

everywhere

The ionised gas density in the Galactic plane, $n_{oi} = 0.025$ cm^{-3}

The temperature of the interstellar medium, $T = 10^{3}$K

The magnetic field component in the Z direction, at all positions above and below the Galactic plane is 3×10^{-6} gauss

The cosmic ray number density is taken to be $N(p) = 12\pi \times 10^{-11}$ $p^{-2.5}$ cm^{-3} GeV/c^{-1}

The streaming velocity of the cosmic rays at the boundary is assumed to be given by equation 8.1 and values for L, the scale height for particles in the wave zone of 10^{4} pc for model A and 100 pc for model B are assumed. These represent two extreme values for L.

Models I and II for the cosmic ray diffusion coefficients are introduced, and noting that a cosmic ray generated Alfvén wave boundary is not formed whenever the cosmic ray diffusion mean free path is less than ~ 1 pc, the boundary positions above the plane of the Galaxy and the cosmic ray transmission coefficients across the boundary are shown in table 8.3. In the situation where no boundary is formed, i.e. the transmission coefficient $=1$, the solution to the diffusion equation is found by setting the cosmic ray concentration to be zero at $Z = \pm 450$ pc where $Z = 0$ pc defines the Galactic plane. Elsewhere, the solution to the diffusion equation given in section 7.4 is applied.

Table 8.3 Boundary position above the Galactic Plane and cosmic ray transmission coefficient as a function of energy

Model	AI		AII		BI		BII	
Energy (GeV)	Boundary Position (pc)	Transmission Coefficient	Boundary Position (pc)	Transmission Coefficient	Boundary Position (pc)	Transmission Coefficient	Boundary Position (pc)	Transmission Coefficient
1	230	5.335×10^{-4}	230	5.335×10^{-4}	230	7.134×10^{-4}	230	7.134×10^{-4}
3	286	7.057×10^{-4}	286	7.057×10^{-4}	286	1.107×10^{-3}	286	1.107×10^{-3}
10	334	9.972×10^{-4}	334	9.972×10^{-4}	334	1.988×10^{-3}	334	1.988×10^{-3}
30	371	1.417×10^{-3}	371	1.417×10^{-3}	371	3.676×10^{-3}	371	3.676×10^{-3}
100	406	2.195×10^{-3}	406	2.195×10^{-3}	406	7.769×10^{-3}	406	7.769×10^{-3}
300	436	3.485×10^{-3}	450	1.0	436	1.62×10^{-2}	450	1.0
10^3	450	1.0	450	1.0	450	1.0	450	1.0
3×10^3	450	1.0	450	1.0	450	1.0	450	1.0
10^4	450	1.0	450	1.0	450	1.0	450	1.0

The sources of the cosmic rays are assumed to be instantaneous in space and time, confined to a region within 12 kpc of the centre of the Galactic disk being evenly distributed in this region and assumed to occur at a rate of 1 per 50 years in the Galaxy. The sources are randomly generated, though the same source distribution is used for each calculation.

The cosmic ray concentration, mean age and anisotropy at the earth are calculated as a function of energy at several times over a period of 10^6 years in order to investigate the time variation of the observable cosmic ray properties. For Model A the concentration of cosmic rays with energy ~ 1 GeV is investigated as a function of Galactic radius.

The results of the calculation are shown in figures 8.3 and 8.4 where values for cosmic ray concentration, anisotropy and mean age at an arbitrary time t=o and the minimum and maximum fluctuations of these quantities over a period of 10^6 years are plotted. Also plotted is the mean amount of material that the cosmic rays have traversed calculated following the method described in Chapter 7.

The time fluctuations in the concentration are very small especially at low energy and certainly do not contradict the data on the constancy of the cosmic ray flux over such periods of time from meteorite studies (Lal 1973). In later models time fluctuation studies are not carried out.

An alarming feature of these models is the bump which appears in the concentration versus energy plot as the mode
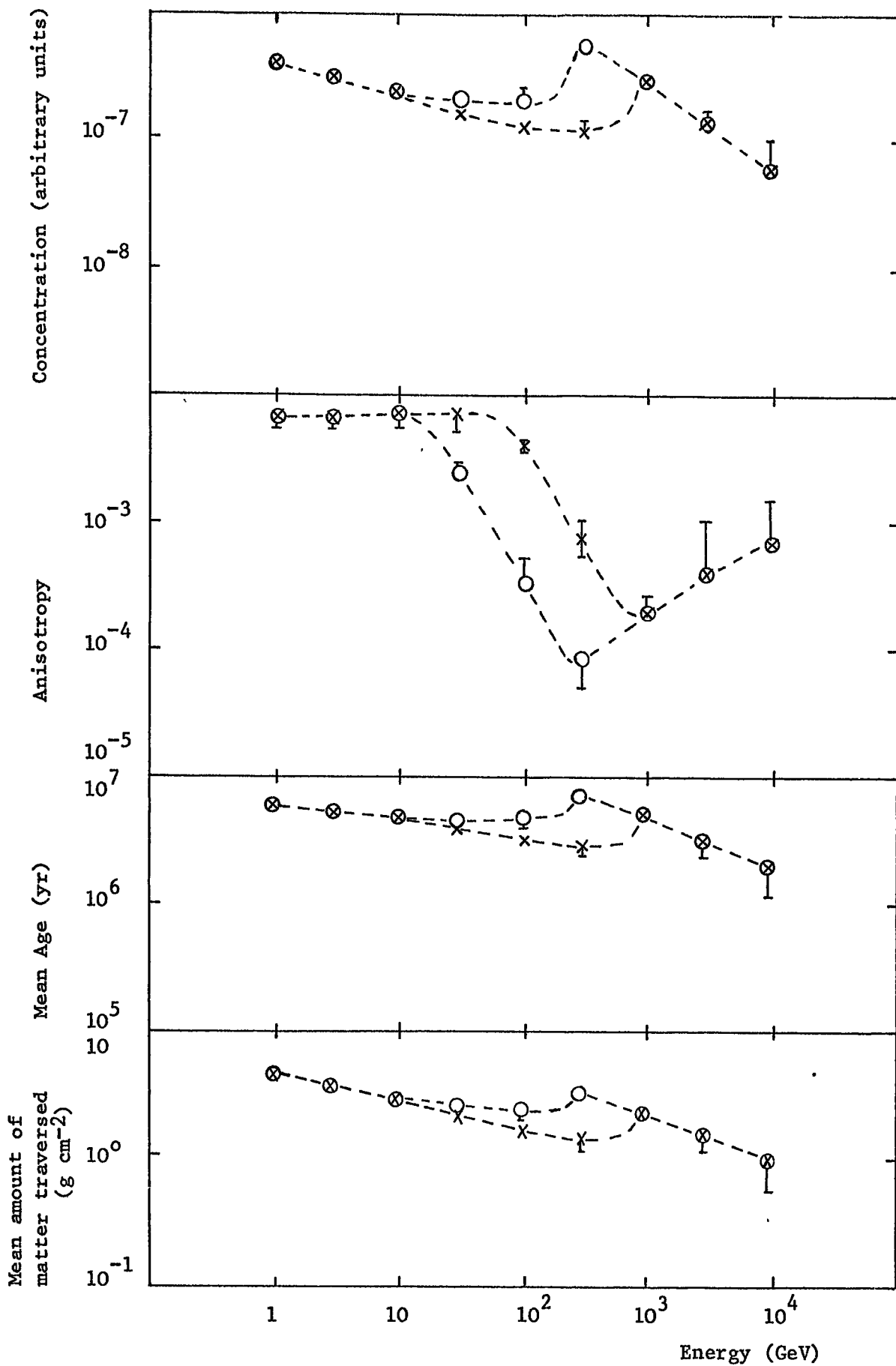
Figure 8.3: Calculated concentration, anisotropy, mean age and matter

traversed as a function of energy for Model A.

x   Model I)
0   Model II) calculated at t=0

The error bars indicate the maximum and minimum values calculated
over a period of 10^6 years. The dotted lines are drawn to guide
the eye.
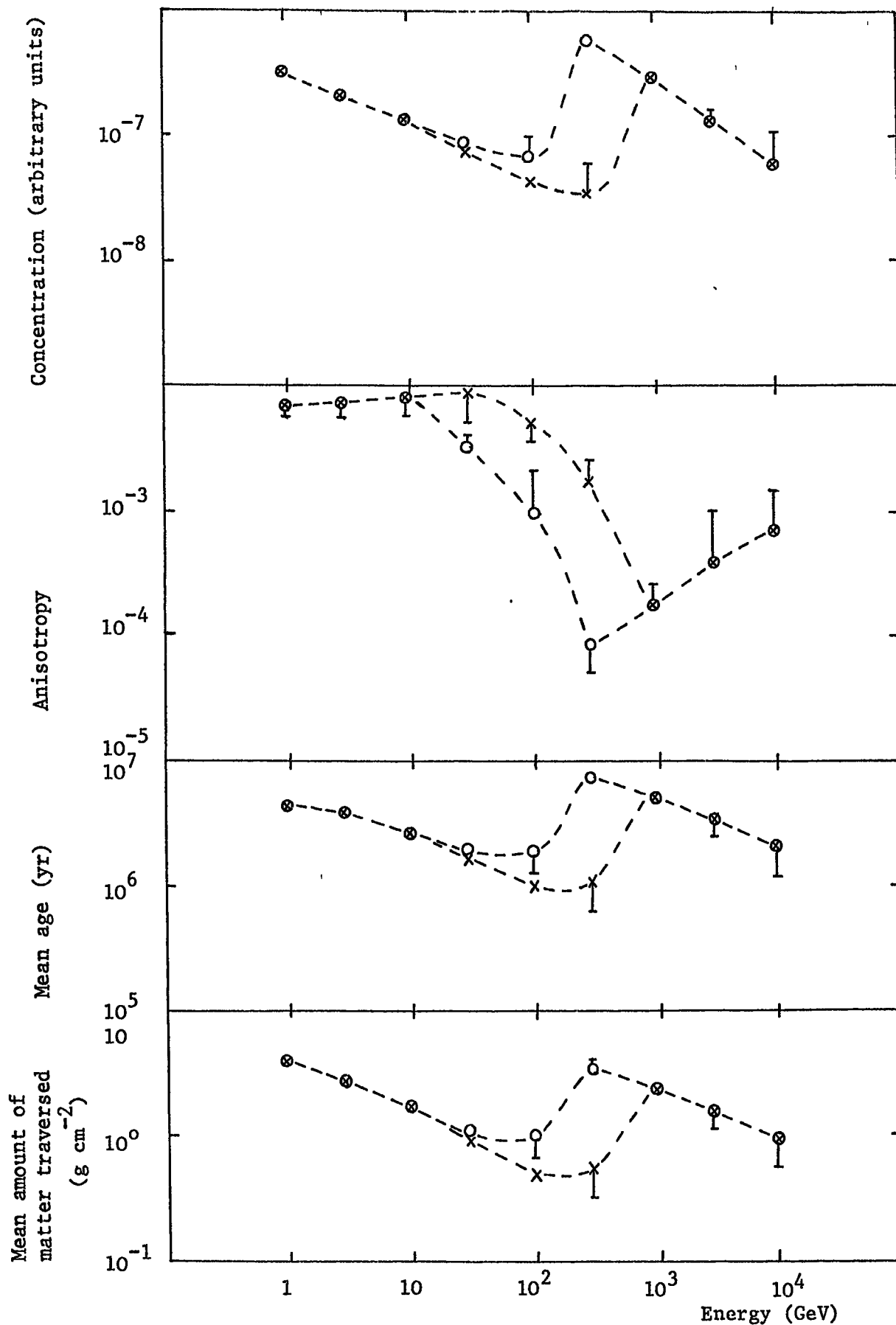
Figure 8.4: Calculated concentration, anisotropy, mean age and matter

traversed as a function of energy for Model B.

x   Model I)
                    calculated at t=0
0   Model II)

The error bars indicate the maximum and minimum values calculated

over a period of 10^6 years. The dotted lines are drawn to guide

the eye.

of propagation changes from confinement essentially due to the reflecting boundaries to confinement essentially due to the interstellar turbulence, a feature, which as later models show, is not easy to explain away.

The observed spectrum of cosmic rays found by Ryan et al (1972) in the region of 10^2 to 10^3 GeV as plotted in figure 2.3 shows only statistical errors. Ryan et al suggest that a systematic uncertainty in absolute intensity of $\pm$ 20% should be allowed for and that the estimate of the energy from their ionisation spectrometer at $\sim 10^3$ GeV is $\pm$ 25%. Given this present resolution any fine scale bump in the spectrum which enhances the concentration at some energy by a factor of ~ 2 would certainly be smeared out. The bump predicted in the calculations as shown in figures 8.3 and 8.4 is in the best case a factor of 2.5 and in the worst case a factor of 10. Bumps of this order of magnitude would be observed with our present resolution.

The calculated anisotropies are found to be smaller than the observed upper limits in the energy region where observations are possible. The high values at low energy, where the diffusion coefficient is large, are due to the earth being near the edge of the assumed source distribution. Barnden and McCracken (1973) have calculated that at 10^2 GeV the interplanetary magnetic field will dilute any Galactic anisotropy by a factor of ~ 2.5. The anisotropies predicted by model I calculations at 10^2 GeV when diluted by this factor would still be greater than the Elliot et al (1970) measurement (figure 2.5). However, the anisotropies predicted

by model II would be within the experimental limit when the diluting factor of the solar wind is allowed for. At lower energies the dilution by the solar wind will be even greater and the large anisotropies predicted at 10 GeV would not be observable.

The variation with energy of the mean age and matter traversed are in agreement with the cosmic ray observations in the energy regions where comparison is possible.

The concentration of cosmic rays of 1 GeV is enhanced by a factor of $\sim$2.5 at the Galactic Centre and depleted to a value $\sim$40% of that at the earth at a Galactic radius of 15 kpc. The variation with Galactic radius, in concentration of cosmic rays with energies up to 10 GeV, the energies which produce the Galactic γ-rays, will be similar to the 1 GeV cosmic rays as they have the same diffusion mean free path. This variation with Galactic radius would go part way to explaining the observations of γ-rays. However, such a variation in the cosmic ray density along with the observed neutral gas density variations would alter the geometry of the boundaries considerably.

8.5.2 Models C and D

Models A and B may be modified by considering the formation of a partially reflecting boundary at a Galactic radius of 15 kpc on the assumption that the gas density falls rapidly at such a radius. In models C and D the infinite disk of models A and B is replaced by a 30 kpc square to approximate the Galactic disk. A square is used instead of a disk in order to simplify the calculation. In order to

calculate the position of the reflecting boundary in the
Z-plane the same interstellar medium parameters are used
as in section 8.5.1. However, in models C and D the cosmic
ray spectrum used to calculate the boundary position is

$$N(p) = 3x10^{-3} (p/10)^{-2.7} cm^{-2} sr^{-1} s^{-1} GeV_C^{-1}$$

which gives a cosmic ray number density of 2π x10^{-10}
$p^{-2.7}$ cm^{-3} GeV_C^{-1}. Model C assumes a value for L of 2500 pc
and model D a value of 500 pc. The calculated boundary
positions above and below the Galactic plane and the cosmic
ray transmission coefficients as a function of energy for
models C and D are given in table 8.4. Models C and D use
the same source distribution as models A and B.

The solution to the diffusion equation is given by a
three dimensional version of the solution given in section
(i)-2(b) in the regime of cosmic ray energy where reflecting
boundaries are formed. For any given energy the transmission
coefficient for the boundary at the edge of the Galaxy is
the same as for the boundary above and below the Galactic
plane. The solution when no boundaries are formed is
found by setting the cosmic ray concentration to zero at
Z=±450 pc and at the edge of the Galaxy.

Figures 8.5 and 8.6 show the calculated cosmic ray con-
centration at the earth as a function of energy for models
C and D respectively. The matching between the low energy
propagation and the higher energy propagation is worse for
models C and D than for models A and B. The high energy
enhancement is reduced if the turbulence causing the dif-
fusion is effective over a smaller region of space e.g.

Table 8.4   Calculated Boundary positions above the Galactic Plane and cosmic ray transmission coefficients as a function of energy

Model	CI		CII		DI		DII	
Energy	Boundary Position (pc)	Transmission Coefficient	Boundary Position (pc)	Transmission Coefficient	Boundary Position (pc)	Transmission Coefficient	Boundary Position (pc)	Transmission Coefficient
1	211	5.283×10^{-4}	211	5.283×10^{-4}	211	5.77×10^{-4}	211	5.77×10^{-4}
3	277	7.423×10^{-4}	277	7.423×10^{-4}	277	8.527×10^{-4}	277	8.527×10^{-4}
10	332	1.132×10^{-3}	332	1.132×10^{-3}	332	1.407×10^{-3}	332	1.407×10^{-3}
30	374	1.745×10^{-3}	374	1.745×10^{-3}	374	2.365×10^{-3}	374	2.365×10^{-3}
100	413	2.988×10^{-3}	4.3	2.988×10^{-3}	413	4.519×10^{-3}	413	4.519×10^{-3}
300	446	5.211×10^{-3}	450	1.0	446	8.701×10^{-3}	450	1.0
10^3	450	1.0	450	1.0	450	1.0	450	1.0
$3 \ 10^3$	450	1.0	450	1.0	450	1.0	450	1.0
10^4	450	1.0	450	1.0	450	1.0	450	1.0

Figure 8.5: The calculated concentration as a function of energy for

Model C

x   Model I

0   Model II

+   Model III

The concentration has been calculated using Model III at

only one energy, 10^3 GeV. The Model III points at 300 GeV,

3×10^3 GeV and 10^4 GeV will lie below the Model II points by

a similar amount.
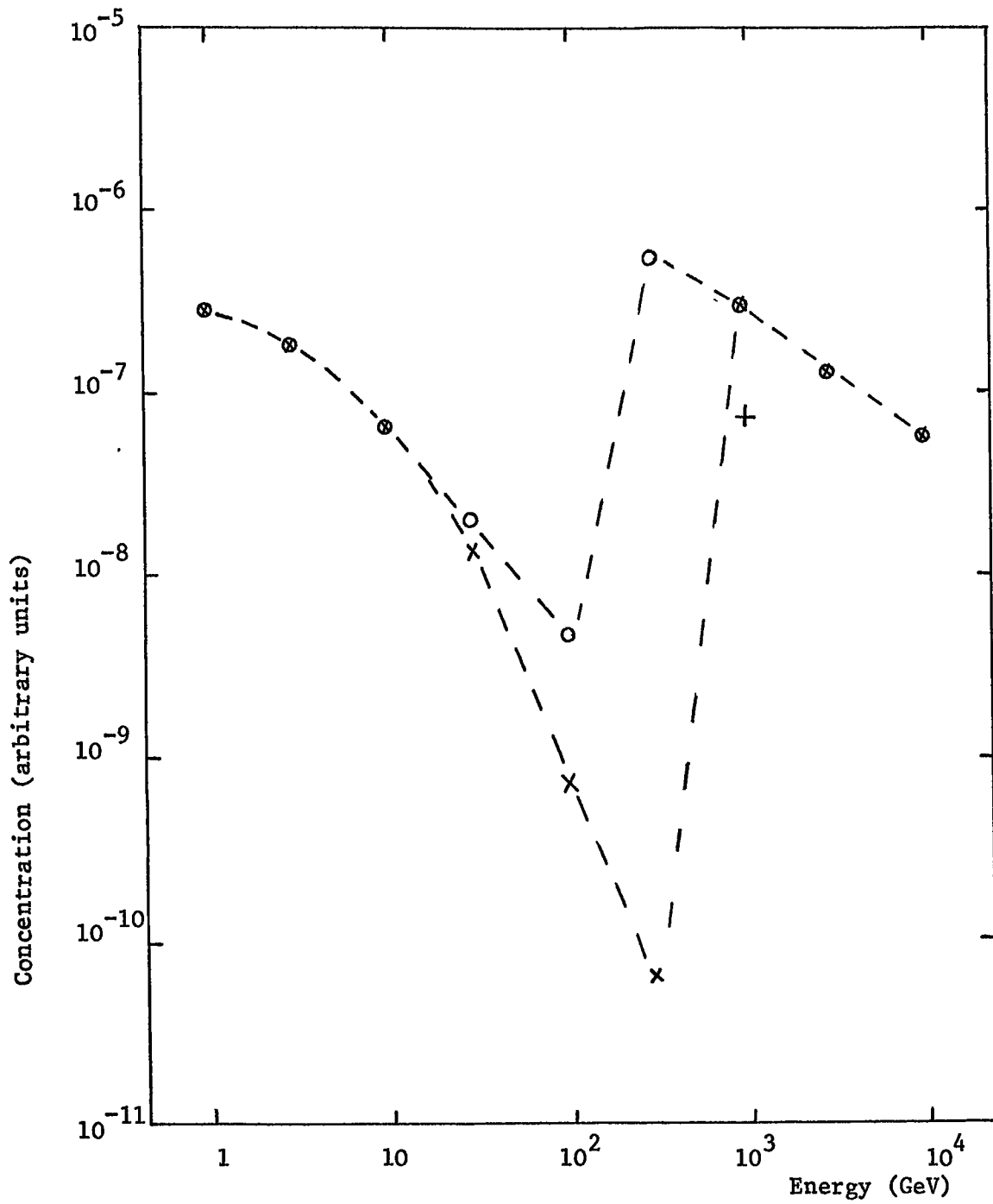
Figure 8.6: The calculated concentration as a function of energy for

Model D

x   Model I
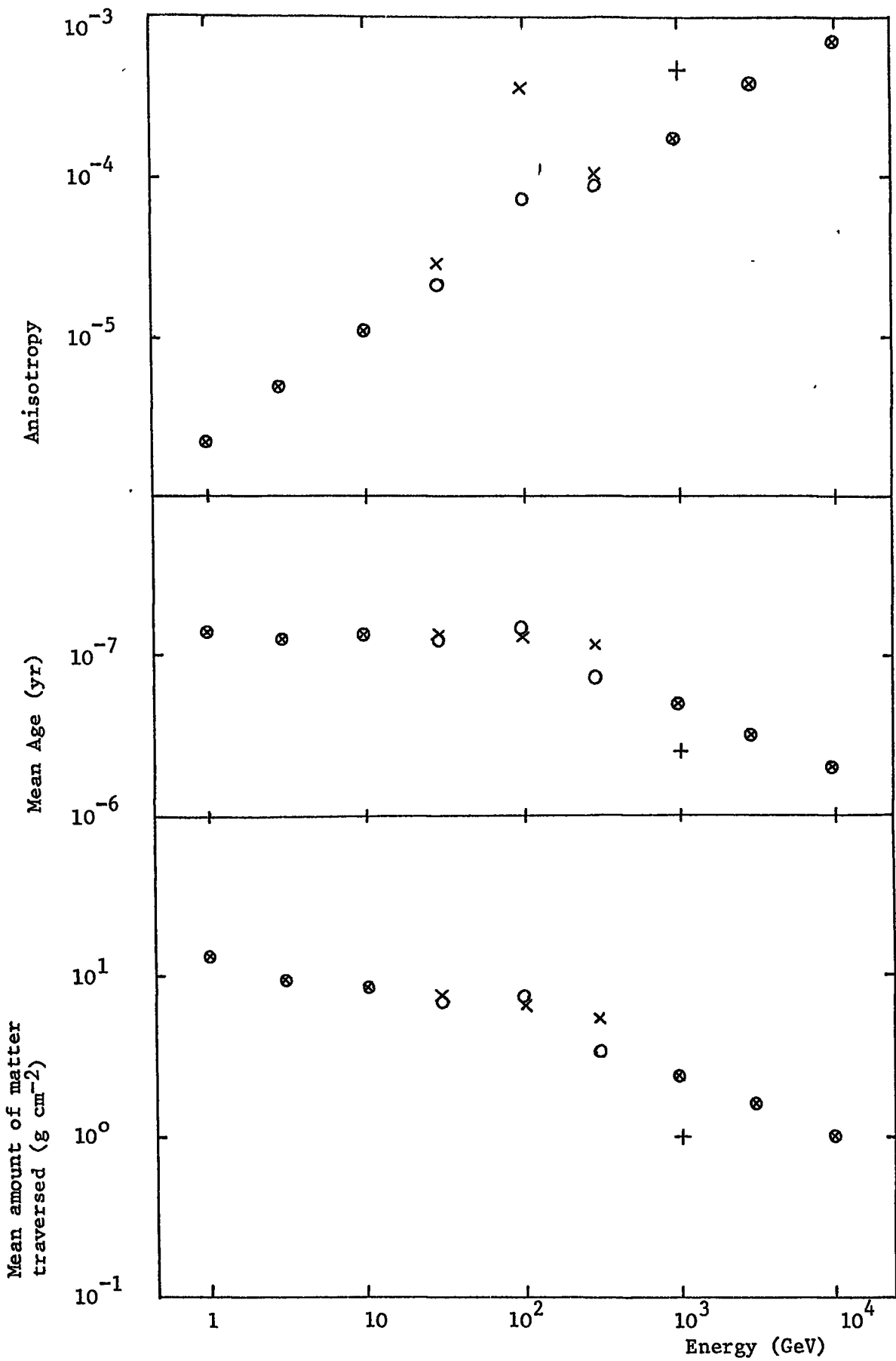
O   Model II

+   Model III

Figure 8.7: The calculated anisotropy, mean age and matter traversed
as a function of energy for Model D.

x Model I

O Model II

+ Model III

within only $\pm$ 250 pc of the Galactic Plane (Model III).
The variation of the cosmic ray anisotropy, mean age and
the mean amount of material traversed as a function of
energy for model D is plotted in figure 8.7. The anis-
otropy expected from this model is consistent with the
experimental observations. The mean age predicted for
the cosmic rays is approximately the upper limit of the
present day Be^{10} measurements (Webber et al, 1973). The
mean amount of matter traversed is higher by a factor ~ 2
than the value found from observations of the cosmic ray
composition. This discrepancy may be overcome if an
average interstellar gas density of 0.5 atoms cm^{-3}, as
suggested by figure 8.1 is adopted. This would make the
reflecting boundaries form slightly closer to the Galactic
plane since their position is $\propto [\ln(\text{gas density})]^{\frac{1}{2}}$. Although
the reflectivity of the boundaries would slightly increase,
the mean age of the cosmic rays would not be significantly
changed since the amount of time it would take to traverse
the Galaxy would be smaller and hence in a given time there
would be more interactions with the boundary. The mean
density of the material traversed in one crossing would
however be decreased by a factor of 2 hence reducing the
total mean amount of matter traversed during the cosmic
ray mean age by the same factor.

The variation of concentration of the cosmic rays at
energy 1 GeV with Galactic radius is very small, $<<1\%$ between
the Galactic centre and a radius of 12.5 kpc. This would

require the γ-ray excess towards the Galactic centre to
be entirely due to an enhanced gas density in that region.
(Dodds et al 1974, Solomon and Stecker 1974).

8.5.3 Model E

Model E differs from models C and D only in the cosmic
ray source distribution. In model E the source distribu-
tion is assumed to follow an exponential similar to that of
the radial distribution of stars. A source distribution
following an exp(-R/2.44 kpc) law is assumed, where R is
the distance from the Galactic Centre in kpc. The Galactic
distribution of supernovae in the Galaxy has been investi-
gated by Ilovaisky and Lequeux 1972. Their observed distri-
bution is flat out to 3 kpc from the Galactic centre and
then falls exponentially with Galactic radius, though there
are large uncertainties. The flat source distribution used
for models A, B, C and D and the exponential distribution
used in models E and F represent extremes to their observed
distribution. The expected cosmic ray concentration at the
earth as a function of energy is plotted in figure 8.8.
Also plotted on figure 8.8 are calculated points relating
to models III and IV for the turbulence. Comparison with
the observed energy dependence of the cosmic ray concentra-
tion is once again very poor in the energy region where the
propagation modes change over.

For the low energy, 1 GeV, cosmic rays, a 30% enhance-
ment of the cosmic rays is predicted at the Galactic centre,
compared to the concentration at the Earth.
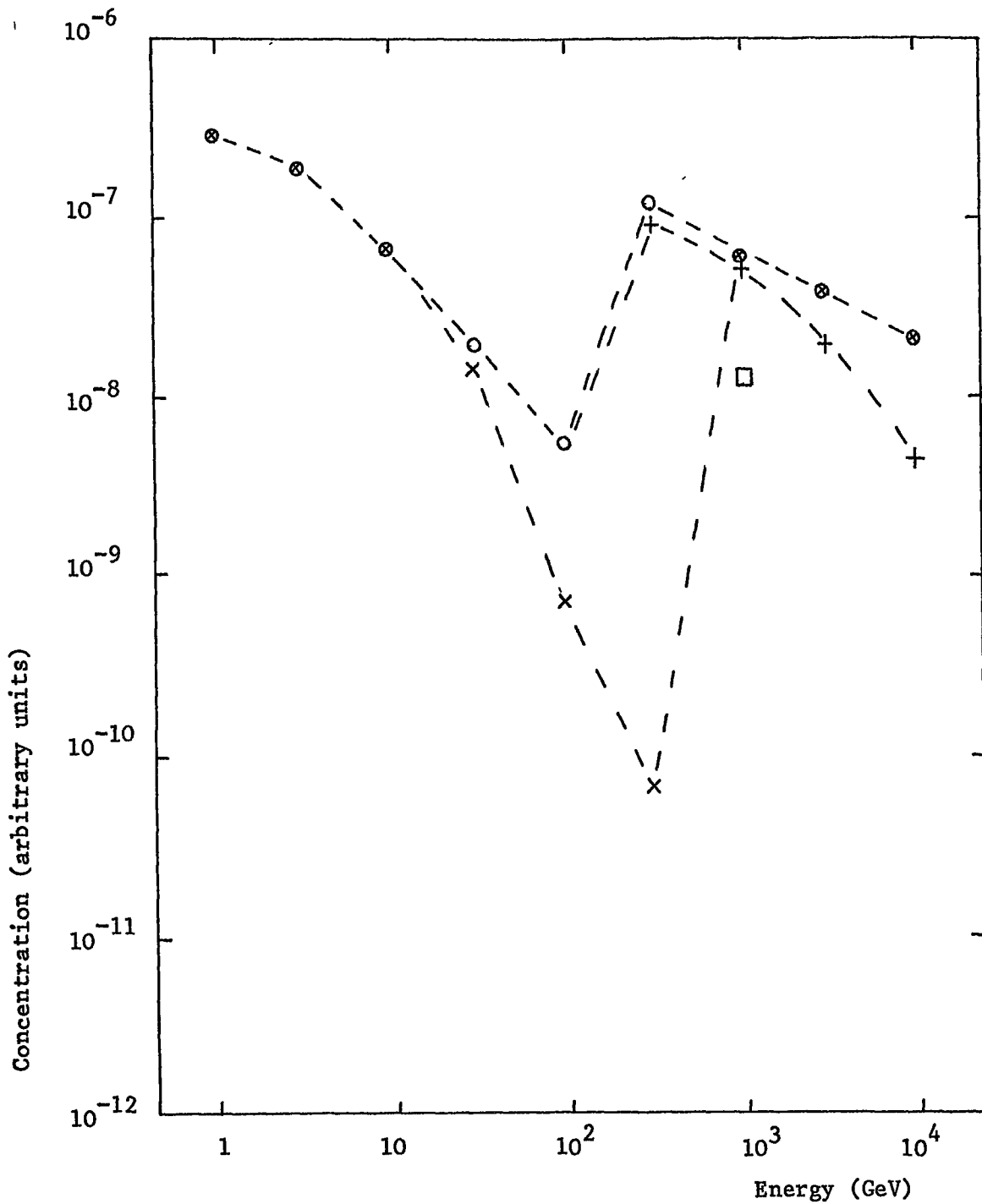
Figure 8.8: The calculated concentration as a function of energy for Model E.

x Model I   + Model III

O Model II   ▢ Model IV

The concentration has been calculated using model IV at only one energy, 10^3 GeV. The model IV points at 300 GeV, 3×10^3 GeV and 10^4 GeV will lie below the Model III points by a similar amount.

8.5.4 Model F

The density wave theory for spiral structure in our galaxy requires that the arm interarm gas density ratio is ~5 (Lin 1970). If the interarm gas density is very small compared to the gas density in the spiral arms, cosmic rays may be able to generate enough Alfvén waves to form a partially reflecting boundary at the edges of the spiral arms. In model F the assumption is made that cosmic rays are confined to the spiral arms by such boundaries. The boundaries above and below the Galactic plane and their transmission coefficients are the same as in model D. The transmission coefficients at the edges and ends of the spiral arms are taken to be the same as those above and below the Galactic plane for any given energy. The spiral structure of the Galaxy is approximated by the spiral calculated by Lin & Shu (1967) which is shown in figure 8.9. In the calculation the spiral is "unwound" and approximated by a rectangular tube 200 kpc long, 1 kpc wide and 2 Z_T high, where Z_T is the height of the boundary above the Galactic plane at energy T. Taking the X-direction as along the tube, the exponential distribution of sources used in Model E may be approximated by an exponential distribution following an exp(-X/15 kpc) law, where X is measured from the centre of the tube. On this model the earth is placed on the axis of the tube at a distance of 60 kpc from the centre of the tube.

The calculated concentration as a function of cosmic ray energy is plotted in figure 8.10 and again greatly disagrees with observation.
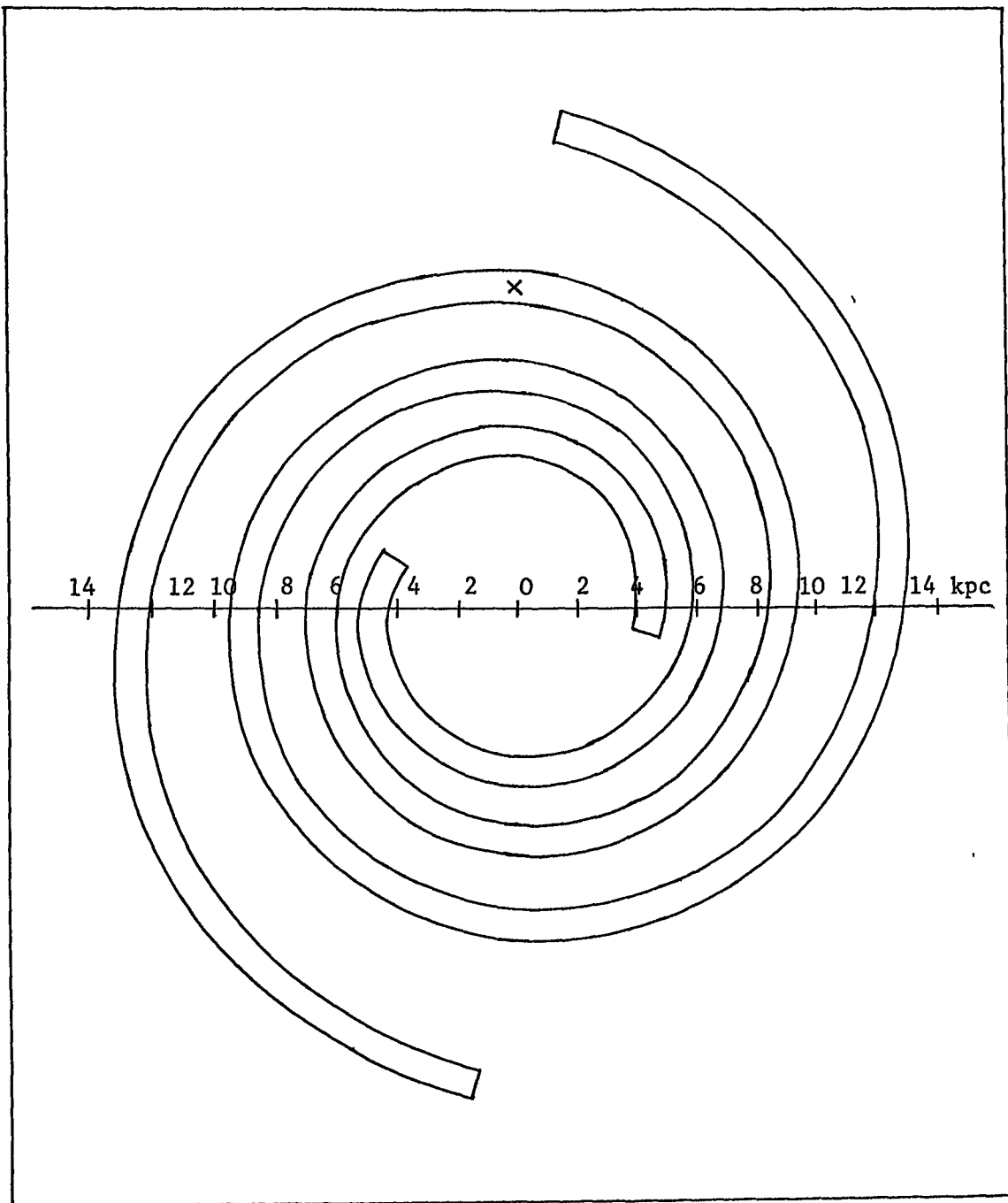
Figure 8.9: The Lin-Shu density wave pattern (Lin and Shu, 1967) which is used as the basis for Model F. The cross marks the position of the Earth as assumed in the calculation.
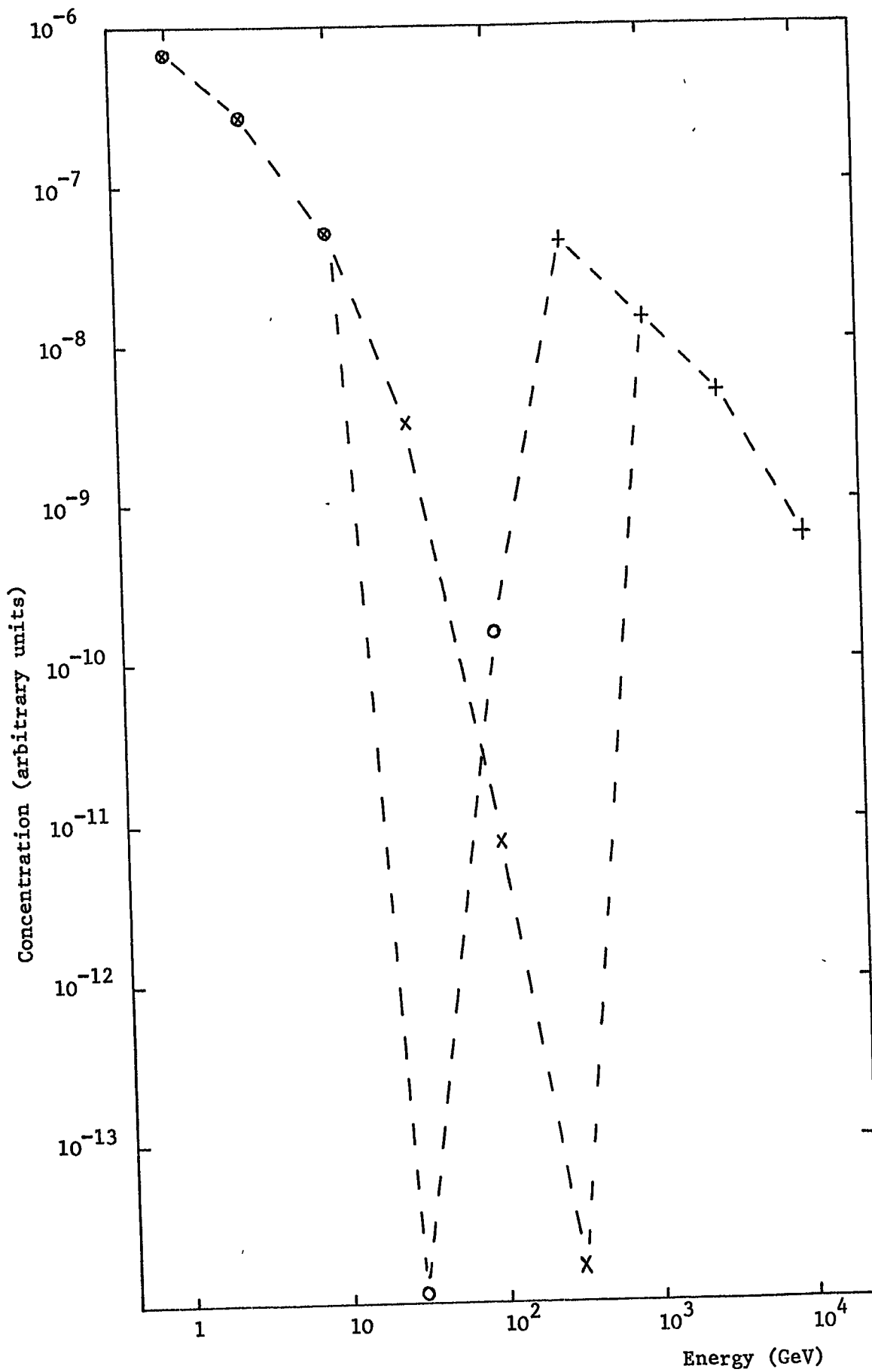
Figure 8.10: The calculated concentration as a function of energy for

Model F.

x   Model I

O   Model II

+   Model III

The concentration of 1 GeV cosmic rays at Galactic radii of 0, 5, 7, 10 and 14 kpc is also calculated as these are the Galactic radii at which the centres of the Lin & Shu spiral arms intersect the line from the Earth to the Galactic centre. There is, compared to the concentration at the Earth, a 15% enhancement in concentration at $R \lesssim 5$ kpc and a reduction in concentration of $\sim 15\%$ at a Galactic radius of 14 kpc.

8.5.5 Composite E/F Model

Further consideration of the reasoning behind model F, indicates that as the cosmic ray energy rises, there arrives an energy at which the gas density in the interarm region is not sufficiently low for cosmic rays to form Alfvén waves at the arm-interarm boundary in the Galactic plane. This may be the case at cosmic ray energies $\gtrsim 10$ GeV. For cosmic rays of energies $\gtrsim 10$ GeV, the confining region would be better approximated by model E than model F. When the mode of confinement changes the cosmic rays will be predominantly confined to the region where the diffusion coefficient is smallest, thus if the turbulence is mainly to be found in the spiral arms and not in the interarm regions, model F may be applicable at energies $\gtrsim 300$ GeV. This is the basis of the composite model; cosmic rays of energies < 10 GeV and > 300 GeV follow model F and cosmic rays in the intermediate energy range are better approximated by model E.

Figure 8.11 shows the concentration against energy plot expected from a composite model. At energies ≤ 10 GeV the points refer to model FII, at energies > 10 GeV and < 300 GeV
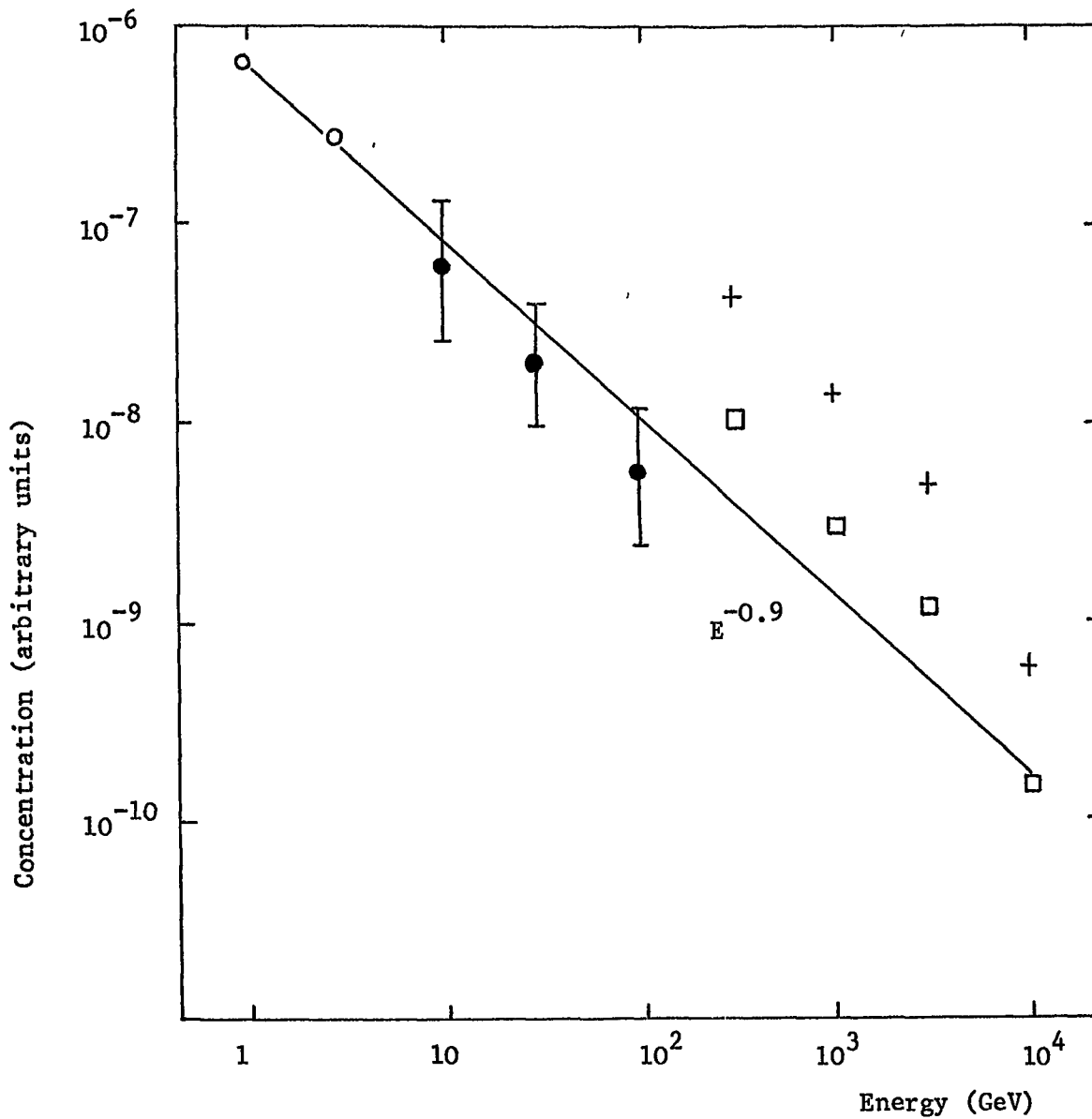
Figure 8.11: The calculated concentration as a function of energy for the composite E/F Model.

1 to 3 GeV : Model FII   o

10 to 10^2 GeV : Model EII   ●

>3x10^2 GeV : Model FIII   +

□ Model FIV, extrapolated from the relationship between the EIII and EIV calculation at 10^3 GeV.
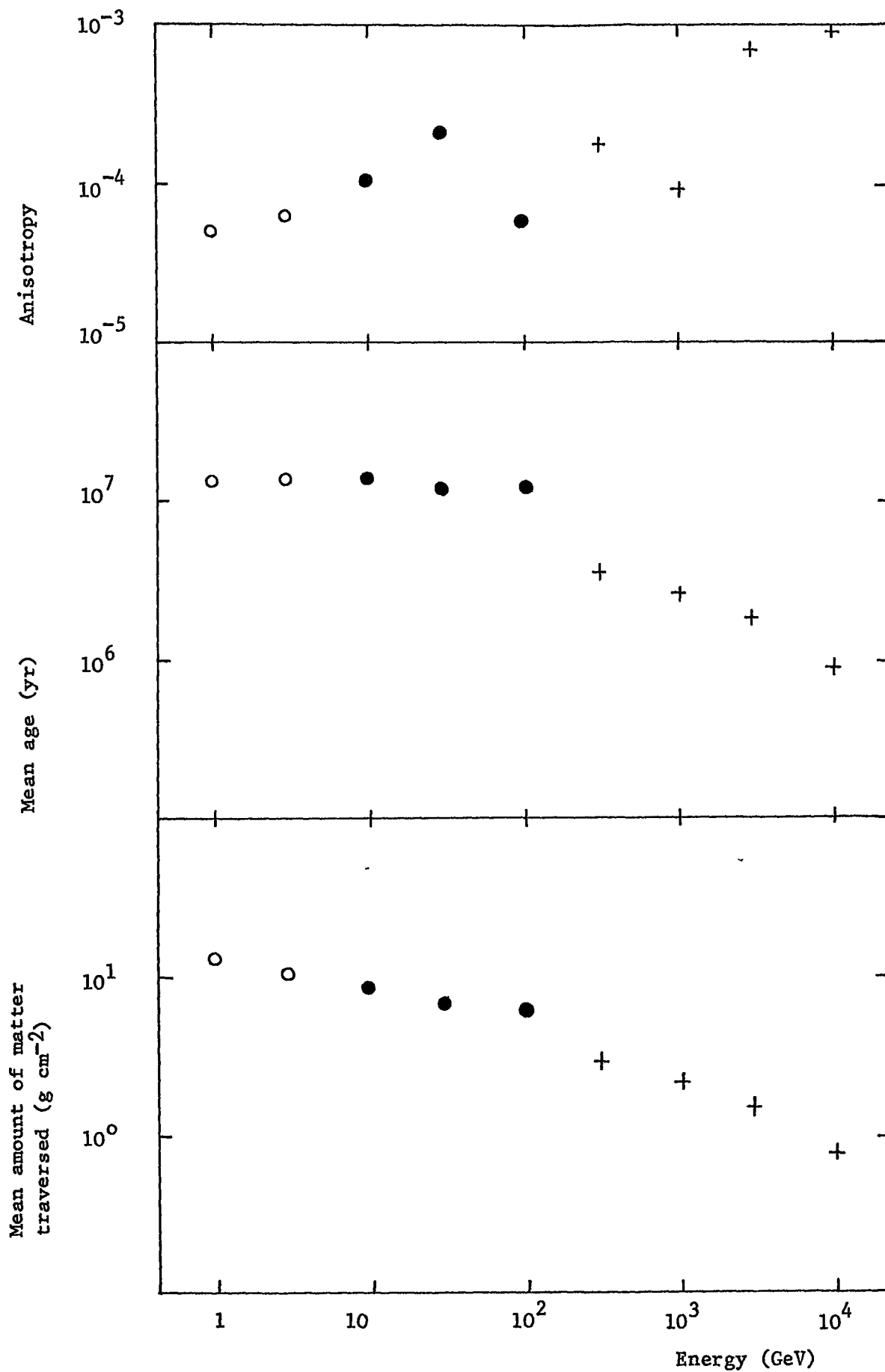
Figure 8.12: The calculated anisotropy, mean age and matter traversed

for the composite E/F model

1 to 3 GeV : Model FII   o

10 to 10^2 GeV : Model EII   ●

>3×10^2 GeV : Model FIII   +

the points refer to model EII and at energies >300 GeV the points refer to model FIII. The points from models E and F are not directly comparable since they are not calculated using exactly the same source distribution. Error bars of a factor $\pm$ 2 are shown on the model E points to indicate the order of magnitude error that the different source distribution may produce.

The points calculated using model FIII indicate a jump in the cosmic ray concentration of a factor of ~ 8 at ~ 300 GeV. Also plotted on figure 8.12 are points for model FIV, extrapolated from the variation in models EIII and EIV at 10^3 GeV. Considering the gross approximations and unknowns in the confining region geometry the behaviour of the concentration against energy plot for the composite model is quite encouraging when compared to the observed energy dependence. Though the prediction is by no means a perfect power law, the bump is reduced to a factor ~ 2 which is within the limits set by the observations of the energy spectrum in this energy range.

For the composite model the propagation modifies the source spectrum by a factor $E^{-0.9}$. Assuming the cosmic ray concentration at the earth is $2 \times 10^{-10} E^{-2.7}$ cm^{-3} GeV^{-1} where E is in GeV, the total number of particles from each source as a function of energy required by the model, which assumes one source in the Galaxy per 50 years, will be 3.3×10^{49} $E^{-1.8}$ GeV^{-1} where E is in GeV. If the sources accelerate all the cosmic rays with energy between 1 and 10^6 GeV each source is required to convert $\sim 4 \times 10^{48}$ ergs into relativistic particles in order to provide the observed cosmic ray concen-

tration. A typical supernova is expected to release $\sim 10^{50-51}$ ergs of energy, therefore the energy requirement of the model is favourable to the assumption of supernova explosions as sources of cosmic rays.

The behaviour of the cosmic ray anisotropy, mean age and mean amount of matter traversed by the cosmic rays as a function of energy from the composite model is plotted in figure 8.12.

The anisotropy behaves in a manner which is consistent with the present observed upper limits, cf figure 2.5. The mean age predicted at a few GeV is greater than the upper limit of the Be^{10} measured lifetime in the cosmic rays of $\sim 7 \times 10^6$ yr (Webber et al 1973), though Webber's measurement refers to an energy of ~ 200 MeV. The mean amount of matter traversed may be modified to a more realistic value in the way described in section 8.5.2. by using a lower value for the interstellar gas density.

8.6 Conclusions

The geometry of the confining region of the cosmic rays defined by cosmic ray generated Alfvén waves is very complex. Detailed knowledge about the parameters of the interstellar and cosmic rays is such that there are large uncertainties in the position of the boundaries of the confining region. The geometry of the boundaries must be grossly simplified in order to solve the diffusion equation analytically.

In regions where the neutral gas density is very low, non-linear wave-wave interactions are the predominant damping mechanism for the cosmic ray generated Alfvén waves.

Above energies ~100 GeV effective reflecting boundaries
are probably not formed by Alfvén waves and the cosmic rays
must be confined by some other mechanism.

At energies >few hundred GeV cosmic rays may be effect-
ively confined by the effects of interstellar turbulence,
though the extent and effectiveness of the turbulence is not
well known.

Idealised model calculations indicate that there is no
simple solution to the propagation problem given our present
day knowledge of the parameters of the interstellar medium.
The most reasonable solution to the problem suggested by the
model calculations is that cosmic rays with energy <10 GeV
are confined to spiral arms by self generated waves, cosmic
rays with energy in the range 10-300 GeV are confined in a
leaky box of Galactic proportions and that cosmic rays of
energy >300 GeV are confined by interstellar turbulence in
the spiral arms though the turbulence must not extend to
$\gtrsim 150$ pc from the Galactic Plane or the model for propagation
will break down.

An interesting prediction of the model is that cosmic
rays with energy >100 GeV will have passed through < 25% of
the matter that low energy cosmic rays pass through. The
composition of the cosmic rays in this region would there-
fore be expected to follow the source composition very
closely. The mean age of the cosmic rays is predicted to
be towards the upper limit of the present Be^{10} data.

The predicted variation in concentration of the 1 GeV
cosmic rays with Galactic radius, and consequently the

variation of cosmic rays of energy <10 GeV since they have
the same diffusion mean free paths, indicates that the
excess in Galactic γ-ray distribution in the region of
Galactic radius ~5 kpc can only be produced if there is
an excess of H_2 in that region.

* from page 118

$\langle V \rangle$ is the streaming velocity of the cosmic rays in the wave
zone, in a direction perpendicular to the boundary. For an
isotropic distribution of velocities in the free zone the
average component of the velocity of the particles in a
direction perpendicular to the boundary would be $c/2$ and not
c, hence the transmission probability across the boundary
would be $2\langle V \rangle/c$. Such a transmission probability would reduce
the mean age of the cosmic rays confined by the Alfvén wave
boundaries and their concentration by a factor ~2.

For low energy cosmic rays $\langle V \rangle$ is proportional to the
component of the Alfvén velocity in the z-direction, which
is in turn proportional to the magnitude of the z-component
of the magnetic field, B_z. The value of B_z used in these
calculations of 3 μgauss may be an overestimate of the true
value. If B_z is smaller than 3 μgauss the values for the
transmission probability given in the text may not be too
inaccurate.

References

Barnden, L. R. and McCracken, K. G., 1973 Proc. 13th
    Int. Conf. on Cosmic Rays, Denver, 2, 963.

Chin, Y. and Wentzel, D. G., 1972 Astrophys. Space. Sci.,
    16, 465.

Dodds, D., Strong, A. W., Wolfendale, A. W. and Wdowczyk, J.,
    1974 Nature, 250, 716.

Elliot, H., Thambyahpillai, T. and Peacock, D. S., 1970
    Acta. Phys. Acad. Sci. Hung., 29, suppl. 1, 491.

Ilovaisky, S. A. and Lequeux, J., 1972 Astron. Astrophys.,
    18, 169.

Lal. D., 1973 Proc. 13th Int. Conf. on Cosmic Rays, Denver,
    5, 3399.

Lin, C. C., 1970 'Spiral Structure of our Galaxy', I.A.U.
    Symp. 38, Ed. by W. Becker and G. Contopoulos (de Reidel).

Lin, C. C. and Shu, F. G., 1967 Radio Astronomy and the
    Galactic System, Ed. H. van Woerden, Academic Press,
    New York.

Puget, J. and Stecker, F. W., 1974 Goddard Space Flight
    Centre Preprint X-640-74-17.

Ryan, M. J., Ormes, J. F., Balasubrahmanyan, V. K., 1972
    Phys. Rev. Lett., 28, 985.

Skilling, J., 1975 Mon. Not. R. Astr. Soc. (to be published).

Solomon, P. M. and Stecker, F. W., Proc. VIIIth ESLAB
    Symposium on Gamma Ray Astronomy, Frascati, June 1974.

Webber, W. R., Lezniak, J. A., Kish, J. and Damle, S. V.,
    1973 Astrophys. Space Sci. 24, 17.

Wentzel, D. G., 1974 Ann. Rev. Astr. and Astrophys., 12.

Westerhout, G., 1970 Galactic Astronomy, Ed. H. Chiu
and A. Muriel, (Gordon and Breach, London) 1, 147.

Chapter 9   <u>On the propagation of cosmic rays in the Galaxy</u>

Discussion regarding the origin of the cosmic radiation has been taking place ever since its discovery over 60 years ago and is likely to continue for some while yet. This thesis has attempted to review and make comment on theories for the propagation of cosmic rays in the Galaxy on the assumption that the cosmic rays are galactic in origin, at least in the energy range 10^9 to 10^{14} eV, and most probably come from supernovae or their remnants. The possibility of the cosmic rays in this energy range being confined within a galactic halo has been considered improbable since at present there is no observational evidence for a large radio halo and the expected lifetimes for cosmic rays would be greater by at least an order of magnitude than the value the present day observations of the Be^{10} isotope indicate.

Over the years the problem for galactic disk confinement models has been to reconcile the isotropy of the cosmic rays with their lifetime and the mean amount of matter traversed. Theories based on a simple three dimensional diffusion model require a very small diffusion coefficient in order to explain the observations, but have not yet provided any physical argument for the magnitude of the diffusion coefficient or any definite dependence on energy. The compound diffusion model is able to predict small anisotropies with diffusion mean free paths of the order of observed magnetic field irregularities, by allowing individual field lines to wander through space in a stochastic manner and by postulating one dimensional diffusion along individual field lines. The

argument is invalidated when allowance is made for the fact
that the observations refer most probably only to one field
line. The one dimensional diffusion calculations presented
in chapter 5 indicate the improbability of the model. The
compound diffusion model also breaks down in the light of
recent ideas about the rate of separation of neighbouring
field lines due to interstellar turbulence. Calculations
of the rate of separation of neighbouring field lines in
space suggest that the motion of cosmic rays in interstellar
space is more likely to be an isotropic three dimensional
diffusion than a compound diffusion.

Observations of the composition of the cosmic rays at
a few GeV indicate an approximately exponential path distri-
bution. A confinement region which acts like a leaky box is
the best way of explaining this behaviour. Skilling (1971)
and Holmes (1974) propose that the partially reflecting walls
of such a "leaky box" may be formed by cosmic ray generated
Alfvén waves. Models based on this idea are able to predict
a low cosmic ray anisotropy since the "walls" have a high
reflectivity and also an energy dependent amount of material
the cosmic rays pass through since the "wall" position and
reflectivity are energy dependent. Wave damping mechanisms,
both linear and non-linear, for the Alfvén waves will prevent
the formation of effective reflecting boundaries to the con-
fining region at cosmic ray energies $\gtrsim 100$ GeV.

Cosmic rays will interact in a resonant manner with
turbulence with a length scale of the order of the cosmic
ray larmor radius. Given present day knowledge of the

spectrum of interstellar turbulence it is possible that interstellar turbulence may be effective in confining cosmic rays at energies $\gtrsim 300$ GeV to the Galactic disk.

Models combining confinement at low energy by Alfvén waves and confinement at high energy by interstellar turbulence have been constructed using very simplified geometry for the confining regions and generalised parameters for the interstellar medium. In the most promising of these models, cosmic rays with energy $\lesssim 10$ GeV are confined to spiral arms by self generated waves, cosmic rays with energy $\gtrsim 10$ GeV and $\lesssim 300$ GeV are confined in a "leaky box" as large as the Galactic disk again by self generated waves and cosmic rays with energy $\gtrsim 300$ GeV are confined to spiral arms by interstellar turbulence. This idea is consistent with the results of Price (1974) who analyses the electron synchrotron data in terms of relativistic electrons confined mainly to spiral arms. However, the uncertainties in some of the parameters used in the calculations are very large and a great amount of weight should not be attached to the result of one calculation with one particular set of parameters. For example the model would break down if; the interstellar turbulence was effective at distances $\gtrsim \pm 150$ pc of the Galactic plane; the cosmic ray lifetime as measured by the Be^{10} isotope is nearer the lower limit than the upper limit of the present day result.

Before further models are constructed greater understanding of the following points is really necessary.

(i)   The physics of the interaction between the cosmic rays

and the Alfvén wave zone, i.e. the boundary reflectivity,

position, possible energy loss by the cosmic rays, needs

further theoretical investigation. The scale height, L,

of the particles in the wave zone is a parameter which

needs special investigation, particularly as to any

possible energy dependence.

(ii) The physics of interstellar turbulence, particularly the

position of the viscous cut off in the turbulence spectrum,

requires better definition.

(iii)Knowledge of the parameters of the interstellar medium,

particularly the magnetic field strength, neutral and

ionised gas densities as a function of R and Z, and the

temperature needs improving so that the positions of any

reflecting boundaries may be calculated fairly accurately

and then if the geometry is too complex, more realistic

simplifications may be introduced.

As far as the observable properties of the cosmic rays

are concerned improvement in the resolution of the energy

spectrum in the energy range 10^2-10^3 GeV is necessary. All

the models predict some fine structure in the spectrum as

the mode of propagation changes from confinement by self

generated waves to confinement by interstellar turbulence.

The present generation of calorimeters and indirect methods

for determining the spectrum in this energy range do not

have the resolution to show any fine structure. The required

resolution may be achieved by the next generation of super-

conducting magnets.

Any improvement in the measurement of the cosmic ray anisotropy especially in the energy range 10^{12} to 10^{14} eV will be very welcome.

The composite model described in the previous chapter predicts that the already found decrease in the amount of material traversed by the cosmic rays as the energy increases will continue. Measurement of the cosmic ray composition at higher energy could confirm this prediction. The mean age of the cosmic rays predicted by the models is $\sim 10^{7}$ yrs. Present day observations of Be in the cosmic radiation are not able to confirm or reject 10^{7} yr as a probable cosmic ray lifetime. Improved resolution of the amount of the Be^{10} isotope in the cosmic radiation will be able to set more stringent limits to the cosmic ray lifetime in the Galaxy and hence support or refute the models of cosmic ray propagation described in chapter 8.

In conclusion, there are plausible ideas regarding the propagation of cosmic rays in the Galaxy which give encouraging results in terms of interpreting the observed properties of cosmic rays with energy between 10^{9} and 10^{14} eV in terms of a Galactic origin and confinement, although there are still large areas where lack of knowledge of the Physics and parameters of the interstellar medium allow plenty of scope for future work both from a theoretical and an experimental point of view.

References

Holmes, J. A., 1974 Mon. Not. R. Astr. Soc., <u>166</u>, 155.

Price, R. M., 1974 Astron. Astrophys., (to be published).

Skilling, J., 1971 Astrophys. J., <u>170</u>, 265.

Appendix (i)

Solutions to the Diffusion Equation under various boundary conditions

(i)-1   Diffusion along a line of infinite length

The equation governing diffusive motion of particles is:

$$\frac{\partial N}{\partial t} = D \nabla^2 N \qquad (i)-1$$

where N is the number of particles per unit volume and D is the diffusion coefficient (dimensions $L^2 T^{-1}$)

When only one dimension (in cartesian coordinates) is considered equation (i)-1 reduces to:

$$\frac{\partial N}{\partial t} = D \frac{\partial^2 N}{\partial x^2} \qquad (i)-2$$

The solution of equation (i)-2, assuming diffusion along a line of infinite length, for the concentration at a position x due to a source at position x_0 is given by:

$$N(x,t) = \frac{S}{\sqrt{4\pi D t}} \exp - \frac{(x-x_0)^2}{4Dt} \qquad (i)-3$$

where t is the time after the emission of S particles by the source.

(i)-2   Diffusion along a line of finite length, h

a)   N=0 at x=0 and at x=h

The concentration at (x,t) due to a source emitting S particles at (x_0, t=0) with boundary conditions, N=0 at x=0 and at x=h, is given by:

$$N(x,t) = \frac{2S}{h} \sum_{n=1}^{\infty} \exp \left[\frac{-n^2 \pi^2 Dt}{h^2} \right] \sin \frac{n\pi x_0}{h} \sin \frac{n\pi x}{h} \qquad (i)-4$$

This series converges rapidly for $t > h^2/4\pi D$.

For $t < h^2/4\pi D$ a solution to equation (i)-2 can be found by summing the contributions to the concentration of negative and positive reflections of the source at $x=x_0$ in the boundaries at $x=o$ and $x=h$, assuming each is diffusing along an infinite line. This is shown schematically in figure (i)-1.

The solution for $t < h^2/4\pi D$ is:

$$N(x,t) = \frac{S}{(4\pi Dt)^{\frac{1}{2}}} \left\{ \exp\left(\frac{-(x_0-x)^2}{4Dt}\right) - \left[\exp\left(\frac{-(-x_0-x)^2}{4Dt}\right) + \exp\left(\frac{-(2h-x_0-x)^2}{4Dt}\right)\right] + \left[\exp\left(\frac{-(2h+x_0-x)^2}{4Dt}\right) + \exp\left(\frac{-(-2h+x_0-x)^2}{4Dt}\right)\right] - \ldots\ldots \right\}$$

(i)-5

b) At $x=o$ and $x=h$ there is a probability r of a particle being reflected.

The concentration, $N(x,t)$ due to a source emitting S particles at $(x_0, t=o)$, with reflecting boundaries at $x=o$ and $x=h$, is given by:

$$N(x,t) = \sum_{n=1}^{\infty} \frac{S \left\{ \sin\frac{\lambda_n x_0}{h} + \frac{\lambda_n}{hK} \cos\frac{\lambda_n x_0}{h} \right\}}{\int_0^h \left\{\sin\frac{\lambda_n x}{h} + \frac{\lambda_n}{hK} \cos\frac{\lambda_n x}{h} \right\}^2 dx} \left\{\sin\frac{\lambda_n x}{h} + \frac{\lambda_n}{hK} \cos\frac{\lambda_n x}{h} \right\} \exp-\left(\frac{\lambda_n^2 Dt}{h^2}\right)$$

(i)-6

where $K = \frac{1}{\lambda_{mfp}} \left\{ \frac{1-r}{1+r} \right\}$, λ_{mfp} is the diffusion mean free path and the λ_n are given by solutions to:

$$\tan \lambda = \frac{2\lambda Kh}{\lambda^2 - (Kh)^2}$$

(i)-7
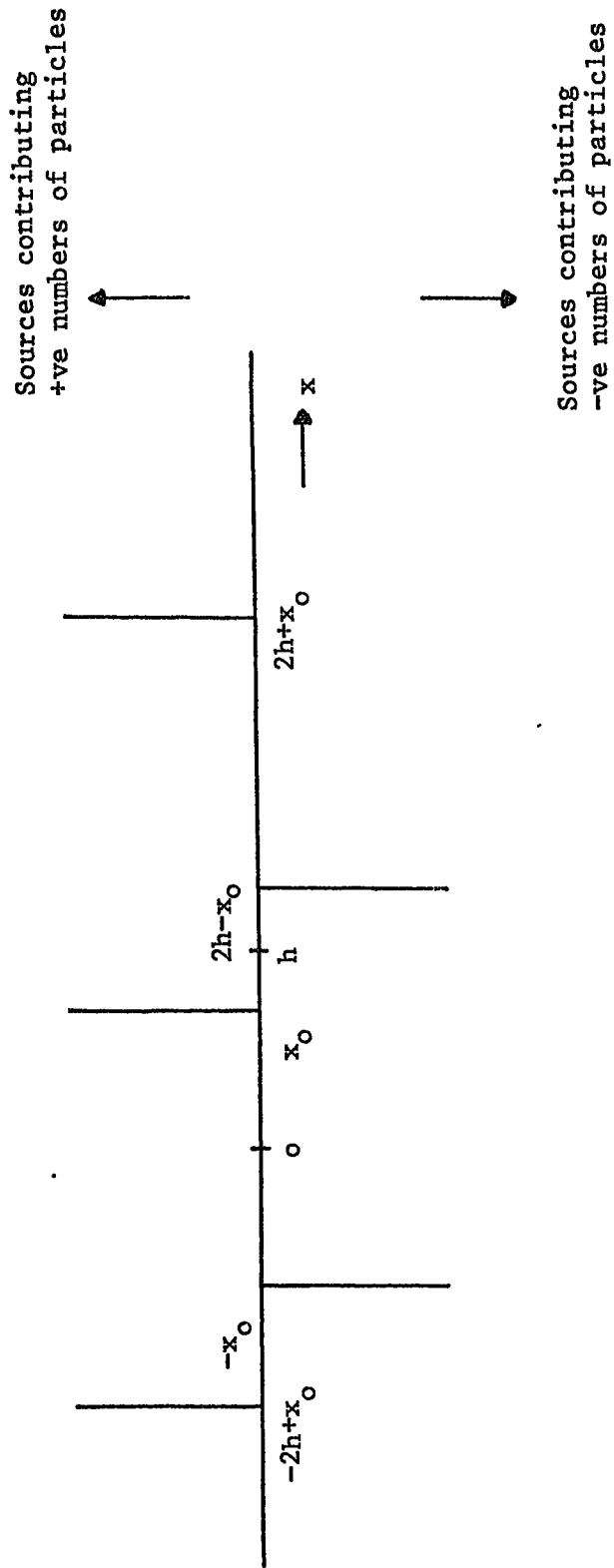
Figure (i)-1: Sources contributing to the short time solution of the diffusion equation with boundary conditions N=o at x=o and x=h.

(i)-3   <u>Isotropic Diffusion in 3-dimensions (cartesian</u>
<u>coordinates</u>)

a)   Diffusion in an infinite medium

The solution to equation (i)-1 for the concentration at a point (x,y,z,t) due to a source at $(x_0,y_0,z_0,t=o)$ emitting S particles into an infinite medium is given by

$$N(x,y,z,t) = \frac{S}{(4\pi Dt)^{3/2}} \exp - \left(\frac{(x-x_0)^2 + (y-y_0)^2 + (z-z_0)^2}{4Dt} \right)$$

$$(i)-8$$

b)   Diffusion in a medium, with infinite dimensions in the x and y planes and a reflecting boundary at z=o and z=h.

The solution to equation (i)-1 for the concentration at (x,y,z,t) due to a source emitting S particles at $(x_0,y_0,z_0,t=o)$, in a medium extending to ∞ in the x and y directions and a reflecting boundary at z=o and z=h is given by:

$$N(x,y,z,t) = S \left(\frac{3}{4\pi \lambda_{mfp} c t} \right) \exp \left[\frac{-3(x-x_0)^2 + 3(y-y_0)^2}{4\lambda_{mfp} c t} \right]$$

$$\sum_{n=1}^{\infty} \frac{\left\{ \frac{\sin \lambda_n z_0}{h} + \frac{\lambda_n}{hK} \cos \frac{\lambda_n z_0}{h} \right\}}{\int_0^h \left\{ \frac{\sin \lambda_n z}{h} + \frac{\lambda_n}{hK} \cos \frac{\lambda_n z}{h} \right\}^2 dz} \left\{ \frac{\sin \lambda_n z}{h} + \frac{\lambda_n}{hK} \cos \frac{\lambda_n z}{h} \right\}$$

$$\exp - \left(\frac{\lambda_n^2 Dt}{h^2} \right) \qquad\qquad (i)-9$$

Where λ_{mfp}, K and the λ_n are as defined in section (i)-2b and c is the velocity of light.

ACKNOWLEDGEMENTS